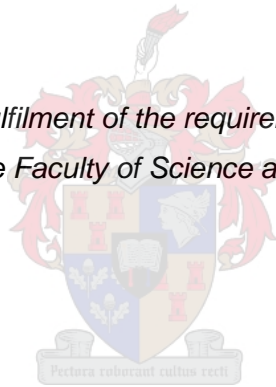


The volatile tale of *Arabidopsis thaliana*: Enhancing plant growth and salinity stress tolerance by overexpressing α -acetolactate decarboxylase to produce acetoin *in planta*

by

Catharina Magdalena (Carlien) Rust

*Thesis presented in fulfilment of the requirements for the degree of
Master of Science in the Faculty of Science at Stellenbosch University*



Supervisors: Dr Paul N Hills and Dr Christell van der Vyver

March 2021

Declaration

By submitting this thesis electronically, I declare that the entirety of the work contained therein is my own, original work, that I am the sole author thereof (save to the extent explicitly otherwise stated), that reproduction and publication thereof by Stellenbosch University will not infringe any third party rights and that I have not previously in its entirety or in part submitted it for obtaining any qualification.

CM Rust

December 2021

Copyright © 2021 Stellenbosch University

All rights reserved

Abstract

The greater need for food security, along with increased abiotic stress (salinity and drought) associated with climate changes, has intensified pressure on agriculture to develop effective and eco-friendly methods to continuously increase crop yields. Moreover, particularly salinity affects an estimated 20% of irrigated land and increased salt concentrations in the soil can cause the death of vegetation and negatively affect crop production. Plant growth promoting rhizobacteria (PGPR) that live in symbiosis with plant roots were suggested as a potential source of new alternative methods to enhance plant growth and induce tolerance to stress. In particular, volatile compounds, such as acetoin produced by certain PGPR, have been shown to enhance plant growth and induce salinity stress tolerance in different plant species. The aim of this study was to investigate the effect of acetoin on plant growth and salinity stress tolerance via the application of the pure compound, and, as a volatile organic compound, produced by transgenic *Escherichia coli* bacteria and transgenic *Arabidopsis thaliana* plants. Both transgenic bacteria and plants were generated by transforming the *ALDC* gene encoding α -acetolactate decarboxylase, responsible for converting α -acetolactate to acetoin, into the respective genome.

A transformed *E. coli* BL21-CodonPlus(DE3)-RIPL strain that can produce the volatile acetoin was successfully generated. Although the *ALDC* protein could not be detected in transformed *E. coli* cells through protein analysis, including immunoblotting, acetoin was detected via GC-MS analysis. *Arabidopsis* plants were further exposed to transgenic *E. coli* in growth and salinity tolerance experiments to determine the effect of bacterially-produced acetoin. A significant increase of fresh mass of plants exposed to the transgenic bacteria producing acetoin was found in both growth and salinity tolerance experiments when compared to plants exposed to non-engineered *E. coli*. No significant increase was found for dry mass between plants exposed to the different treatments, indicating a probable link between growth enhancement and relative water content.

Two independent homozygous T₃ acetoin-producing plants were further characterized. The expression of the *ALDC* transgene was demonstrated via RT-sqPCR *in planta*, and as a major novel achievement, the production of acetoin in both independent homozygous A-line *Arabidopsis* plants via GC-MS analysis was also shown. The presence of the transgene enhanced plant growth in one transgenic line (A6.8 line) grown *ex vitro* when compared to wild-type *Arabidopsis* plants, while neither of the two transgenic *Arabidopsis* lines had *in vitro* enhanced growth or salinity tolerance.

The exposure of plants to the transgenic acetoin-producing bacteria was further *in vitro* more successful regarding increase of plant growth and eliciting salinity tolerance when compared to *in planta* acetoin production. The *in vitro* studies with transgenic *Arabidopsis* were not highly successful to demonstrate better plant growth and salt tolerance due to acetoin production. However, the

transgenic bacteria and transgenic plants might have a greater potential to enhance plant growth and salinity stress tolerance *ex vitro*. This view is supported by the significant increase in average fresh and dry mass for the *ex vitro* grown A6.8 plants.

Samevatting

Die groter behoefte aan voedselsekuriteit, tesame met verhoogde abiotiese stres (soutstres en droogte) wat verband hou met klimaatsverandering, het die druk op die landbou sektor verhoog om doeltreffende en omgewingsvriendelike metodes te ontwikkel om oesopbrengse deurlopend te bevorder. Boonop beïnvloed soutstres ongeveer 20% van land onder besproeiing, en die verhoogde soutkonsentrasies in grond kan die dood van vegetasie veroorsaak en oesopbrengs negatief affekteer. Plantegroei-bevorderende rhizobakterieë (PGPR) wat in simbiose met plantwortels leef, is voorgestel as moontlike bron van nuwe alternatiewe metodes om plantegroei te bevorder en stresverdraagsaamheid te induseer. In die besonder is getoon dat vlugtige verbindings soos asetoëne wat deur sekere PGPR geproduseer word, die groei van plante en die soutverdraagsaamheid by verskillende plantsoorte bevorder. Die doel van hierdie studie was om die effek van asetoëne op die groei van plante en soutverdraagsaamheid deur die gebruik van die suiwer verbinding te ondersoek, en as 'n vlugtige organiese verbinding wat geproduseer word deur transgeniese *Escherichia coli* bakterieë en transgeniese *Arabidopsis thaliana* plante. Beide transgeniese bakterieë en plante is gegenereer deur die *ALDC*-geen wat α -asetolaktaat dekarboksilase kodeer, verantwoordelik vir die omskakeling van α -asetolaktaat na asetoëne, in die onderskeie genoomkonteks in te voeg.

'n Getransformeerde *E. coli* BL21-CodonPlus (DE3)-RIPL-stam wat die vlugtige asetoëne kan produseer, is suksesvol gegenereer. Alhoewel die *ALDC*-proteïene nie deur proteïen-uitdrukkingsanalise, insluitend immunoklad-analise, opgespoor kon word in transgeniese *E. coli* nie, is asetoëne deur GC-MS-ontleding opgespoor. *Arabidopsis* plante is blootgestel aan die transgeniese bakterieë in groei- en soutverdraagsaamheidsproewe om die effek van bakteriële geproduseerde asetoëne te bepaal. 'n Beduidende toename in gemiddelde vars plantmassa vir plante wat blootgestel is aan die transgeniese bakterieë wat asetoëne produseer, in vergelyking met plante wat blootgestel is aan wilde-tipe *E. coli*, is waargeneem vir beide groei- en soutverdraagsaamheidsproewe. Daar is egter geen noemenswaardige toename in droë massametinge tussen die plante van die verskillende behandelings gesien nie, wat dui op moontlike verband tussen die bevordering van plantegroei en relatiewe waterinhoud.

Twee onafhanklike homosigotiese T_3 asetoëne-produserende plante is verder gevestig. Daarbenewens is die uitdrukking van die *ALDC*-transgeen via RT-sqPCR en, as 'n beduidende nuwe resultaat, is *in planta* produksie van asetoëne in *Arabidopsis* in beide onafhanklike homosigotiese A-lyn plante getoon via GC-MS-analise. Die aanwesigheid van die transgeen het die groei van plante in een transgeniese lyn (A6.8-lyn) verhoog wat *ex vitro* gegroei is, in vergelyking met die wilde-tipe

Arabidopsis-plante, maar nie een van die twee transgeniese A-lyn *Arabidopsis* het egter groei of soutverdraagsaamheid *in vitro* verbeter nie.

Die blootstelling van plante aan die transgeniese asetoïen-produiserende bakterieë was verder *in vitro* meer suksesvol met betrekking tot toename in plantegroei en die verkryging van soutverdraagsaamheid in vergelyking met die produksie van asetoïen *in planta*. Die *in vitro*-studies met transgeniese *Arabidopsis* was oor die algemeen nie baie suksesvol om beter plantegroei en soutverdraagsaamheid as gevolg van asetoïen produksie te toon nie. Alhoewel, die transgeniese bakterieë en transgeniese plante 'n groter potensiaal kan hê om die plantegroei en soutverdraagsaamheid *ex vitro* te verbeter. Hierdie siening word ondersteun deur die beduidende toename in die gemiddelde vars en droë massa vir die *ex vitro* gekweekte A6.8 plante.

Acknowledgements

I would like to extend my thanks to Dr Paul Hills and Dr Christell van der Vyver for their guidance and support throughout this project.

I hereby acknowledge the financial assistance from the Institute for Plant Biotechnology (IPB), the National Research Foundation (NRF) and Stellenbosch University towards this research. Opinions expressed and conclusions arrived at, are those of the author and are not necessarily to be attributed to the NRF.

Sincerest thanks to Dr Shaun Peters for taking the time to assist me with Gateway cloning.

I hereby acknowledge the assistance with GC-MS analysis from Mr Lucky Mokwena at Mass Spectrometry, CAF.

Furthermore, I would like to thank Mr Rafael Keret, for taking the time to aid me in determining the most appropriate data analysis to be implemented for the experimental data.

I would also like to thank Ms Casey Gabriel, Mr Desren Jacobs, and Mr Jonathan Jewell for all the assistance with my protein work.

Lastly, but certainly not least, to my family and friends, I thank you immensely for always being supportive through this journey.

Table of Contents

Abstract	ii
Summary	iv
Acknowledgements	vi
List of Figures	xi
List of Tables	xxiii
List of Abbreviations and non-SI units	xxiv
Chapter 1	1
Literature Review.....	1
1.1 Rhizobacteria and plant growth	1
1.2 Rhizobacteria and stress	3
1.3 Rhizobacteria, plants and salinity stress	4
1.4 Rhizobacteria and phytohormones	11
1.5 <i>Bacillus</i> spp: Abundant rhizobacteria with potential to enhance plant growth.....	14
1.6 Volatile organic compounds and plant growth.....	16
1.7 Volatile organic compounds and abiotic stress	18
1.8 An alternative approach to VOC research	20
1.9 <i>ALDC</i> and <i>BDH</i> genes	20
1.10 Previous research on VOCs at the Institute for Plant Biotechnology	22
1.11 Aims and objectives.....	24
Chapter 2	26
Trials with synthetic volatile compounds.....	26
2.1 Introduction	26
2.1.1 Dose-dependent curve.....	26
2.1.2 Circadian clock and photoperiod	26

2.1.3	Aim of chapter	28
2.2	Materials and methods.....	29
2.2.1	Plant material.....	29
2.2.2	Growth trials with synthetic volatiles exposure.....	29
2.2.3	Salinity trials with synthetic volatiles exposure.....	29
2.2.4	Statistical analysis.....	30
2.3	Results.....	31
2.3.1	Growth trials with synthetic volatiles exposure.....	31
2.3.2	Salinity trials with synthetic volatiles exposure.....	35
2.4	Discussion.....	38
2.4.1	Growth trials with exposure to synthetic volatiles	38
2.4.2	Salinity trials with exposure to synthetic volatiles	39
2.5	Conclusion	42
Chapter 3	43
Acetoin-production in <i>Escherichia coli</i>	43
3.1	Introduction	43
3.1.1	Volatile production by PGPR.....	43
3.1.2	Deficiencies in bacterial and synthetic volatile studies	43
3.1.3	<i>Escherichia coli</i> BL21	44
3.1.4	Aim of chapter	44
3.2	Materials and methods.....	45
3.2.1	DNA and RNA isolations.....	45
3.2.2	Polymerase chain reaction (PCR)	45
3.2.3	Restriction enzymes	46
3.2.4	Competent cells of <i>Escherichia coli</i>	46
3.2.5	Bacterial growth.....	47

3.2.6	Construction of a protein expression vector	47
3.2.7	Semi-quantitative analysis of <i>ALDC</i> expression in transformed bacteria	47
3.2.8	Analysis of <i>ALDC</i> protein expression	48
3.2.9	Protein immunoblots.....	49
3.2.10	Detection of acetoin production	50
3.2.11	Growth trials with bacterial exposure.....	50
3.2.12	Salinity trials with bacterial exposure.....	51
3.2.13	GC-MS analysis of acetoin production in transgenic bacteria	51
3.2.14	Statistical analysis.....	52
3.3	Results.....	53
3.3.1	Construction of a protein expression vector	53
3.3.2	Analysis of <i>ALDC</i> protein expression	55
3.3.3	GC-MS analysis of acetoin production in transgenic bacteria	59
3.3.4	<i>Arabidopsis</i> growth trials with transgenic <i>E. coli</i> exposure.....	60
3.3.5	<i>Arabidopsis</i> salinity trials with transgenic <i>E. coli</i> exposure	63
3.4	Discussion.....	66
3.4.1	Protein expression and detection	66
3.4.2	<i>Arabidopsis</i> growth trials with transgenic <i>E. coli</i> exposure.....	67
3.4.3	<i>Arabidopsis</i> salinity trials with transgenic <i>E. coli</i> exposure	68
3.5	Conclusion	70
Chapter 4	71
Acetoin-production in <i>Arabidopsis thaliana</i>	71
4.1	Introduction	71
4.1.1	<i>Agrobacterium</i> transformation method	71
4.1.2	Vector construct	71
4.1.3	Transgenic plants.....	72

4.1.4	Chloroplast transit peptides.....	72
4.1.5	Aim of chapter	73
4.2	Materials and methods.....	74
4.2.1	Cloning of recombinant vector	74
4.2.2	Competent cells for <i>Agrobacterium</i>	75
4.2.3	Transformation of plants	75
4.2.4	Establishing homozygous transgenic lines	76
4.2.5	Transgenic versus wild-type plant trials	78
4.2.6	Trials with transgenic plants as an acetoin source	78
4.2.7	Gas chromatography-mass spectrometry analysis to detect acetoin	79
4.2.8	Statistical analysis.....	80
4.3	Results.....	81
4.3.1	Establishing homozygous transgenic plants.....	81
4.3.2	Detection of acetoin production <i>in planta</i>	86
4.3.3	Transgenic plant growth versus wild-type plant growth	90
4.3.4	Trials with transgenic plant as acetoin source.....	95
4.4	Discussion.....	98
4.4.1	Detection of acetoin production <i>in planta</i>	98
4.4.2	Transgenic plant growth versus wild-type plant growth	99
4.4.3	Trials with transgenic plants as acetoin source.....	101
4.5	Conclusion	102
	Conclusion	104
	Literature cited.....	107
	Addendum 1	117
	Addendum 2	120

List of Figures

Name	Page
Figure 1.1: A representation of salinity sensitive (glycophyte) vs salinity tolerant (halophyte) plants during salinity stress. Salinity stress inhibits growth significantly in salinity sensitive plants, especially in aerial parts. The decrease in potassium is a key reflection of nutrient imbalance caused by the accumulation of sodium in leaves. Salinity stress also affects relative water content and the photosynthetic rate by decreasing chlorophyll content, regulating stomatal closure and starch accumulation. Due to senescence favoured in salinity stressed leaves, ethylene, and ABA increases while auxin and cytokinin decreases (Modified from Acosta-Motos <i>et al.</i> , 2017; picture obtained from Amtmann, 2008).	7
Figure 1.2: Representation of the effects on plants due to salinity stress showing changes between the presence and absence of PGPR. The accumulation of sodium ions causing ion imbalance and accumulation of ROS can be countered by the presence of PGPR that can assist in the restoration of water balance, photosynthesis, and regulation of salinity tolerance mechanisms (PGPR: Plant growth promoting rhizobacteria, modified from Bakka and Challabathula, 2020).	11
Figure 1.3: Mechanisms of PGPR. Direct and indirect mechanisms to promote growth through interactions between PGPR and plant cells. The rhizobacteria can directly assist plant growth by supplying bacterial forms of plant hormones or enhancing nutrient uptake of phosphorus and iron. The root exudates excreted from plant cell in turn fuels rhizobacterial metabolism to produce antibiosis, lytic enzymes and volatile compounds that can defend the plant against pathogenic attack (Modified from Kashyap <i>et al.</i> , 2019).	14
Figure 1.4: Chemical structures. A) 2,3-butanediol and B) acetoin.	21
Figure 1.5: Biosynthesis of acetoin and 2,3-butanediol in bacteria and fungi. The biosynthesis of acetoin is similar in bacteria and fungi for the exception of an additional route found in fungal species indicated in red. A) pyruvate decarboxylase B) α -acetolactate synthase C) acetolactate decarboxylase D) diacetyl synthetase E) diacetyl reductase F) acetaldehyde condensation G)	21

oxidative decarboxylation H) 2,3-butanediol dehydrogenase (BCAA: branched chain amino acids; NAD(P): nicotinamide adenine dinucleotide (phosphate); NAD(P)H: reduced nicotinamide adenine dinucleotide (phosphate); CO₂: carbon dioxide, CoA: coenzyme A; modified from Xu et al., 2011).

Figure 2.1: Setup of cultures for *in vitro* trial to expose plants to synthetic volatiles. A small petri dish was placed onto the medium surrounded by 8 plants, containing a specific concentration of synthetic volatiles diluted in sterile water. 30

Figure 2.2: Growth trials to determine the effect of synthetic acetoin and 2,3-butanediol exposure on seedling growth. Identically-sized 13 d old seedlings were used to set up the experiment. After two weeks of exposure to the respective volatiles, the plates were photographed, and fresh and dry mass of plants were measured. Growth trials were conducted under both **A)** short-day-length (10 h:14 h photoperiod) and **B)** long-day-length (14 h:10 h photoperiod) conditions. Indicated are the different concentrations used for each respective synthetic volatile compound to which plants were exposed. 32

Figure 2.3: Analysis of effect of synthetic acetoin and 2,3-butanediol exposure on seedling growth at short-day-length photoperiod. Fresh mass (mg) and dry mass (mg) of 13 d old *Arabidopsis thaliana* Col-0 seedlings exposed for 14 d to synthetic acetoin (indicated by A before concentration tested) or 2,3-butanediol (indicated by B before concentration tested) grown under a 10 h:14 h light:dark photoperiod *in vitro*. Values represent the mean \pm SE (n = 48). Different letters indicate significantly different values ($p \leq 0.05$) as determined by Kruskal-Wallis and Dunn's multiple comparisons test. 33

Figure 2.4: Analysis of untreated plants of each individual repeat for long-day-length synthetic volatile growth trials. Fresh mass (mg) and dry mass (mg) of 13 d old *Arabidopsis thaliana* Col-0 seedlings grown for 14 d grown under a 14 h:10 h light:dark photoperiod *in vitro*. Values represent the mean \pm SE (n = 24). Different letters indicate significantly different values ($p \leq 0.05$) as determined by one-way ANOVA and Tukey's multiple comparisons test. 33

Figure 2.5: Analysis of effect of synthetic acetoin and 2,3-butanediol exposure on seedling growth during long-day-length photoperiods. Experimental repeats are indicated by numbers 1 to 3 to show the different outcomes under the same treatment conditions. Fresh mass (mg) and dry mass 34

(mg) of 13 d old *in vitro* *Arabidopsis thaliana* Col-0 seedlings exposed for 14 d to synthetic acetoin (indicated by A before concentration tested) or 2,3-butanediol (indicated by B before concentration tested) grown under a 14 h:10 h light:dark photoperiod *in vitro*. Values represent the mean \pm SE ($n = 24$). Different letters indicate significantly different values ($p \leq 0.05$) as determined by one-way ANOVA and Tukey's multiple comparisons test.

Figure 2.6: *In vitro* growth trials to determine the effect of salinity stress and exposure to synthetic volatiles on seedling growth and survival. 36
Identically-sized 13 d old seedlings were used to set up the experiment. After two weeks of exposure to the respective volatiles (200 ng), the seedlings grown on medium with **A)** 50 mM NaCl or **B)** 100 mM NaCl were photographed, and fresh and dry mass of plants were measured of plants that survived. The 50 mM NaCl treatment had a visibly higher survival (indicated by red circle) rate for plants than the 100 mM NaCl treatment.

Figure 2.7: Analysis of volatile effects on seedling growth during salinity stress. 37
The growth parameters of 13 d old *Arabidopsis thaliana* Col-0 seedlings exposed for 14 d to 100 mM NaCl and synthetic acetoin (indicated by A before concentration tested) or 2,3-butanediol (indicated by B before concentration tested) grown under a 14 h:10 h light:dark photoperiod *in vitro*, was measured. Values represent the mean \pm SE (n varied based on survival rate, n for untreated = 96). Different letters indicate significantly different values ($p \leq 0.05$) as determined by one-way ANOVA and Tukey's multiple comparisons test. All plants per treatment were combined to determine the average dry mass (mg) per plant for each repeat of experiment.

Figure 3.1: Setup of cultures for *in vitro* trial to expose plants to transgenic bacteria. 51
A small petri dish containing bacteria was placed in the middle of a large culture container containing $\frac{1}{2}$ MS media onto which 8 *Arabidopsis* plants were evenly spaced. The small petri dish contains semi-solid LB-media with overnight culture of *E. coli* BL21-CodonPlus(DE3)-RIPL bacteria with pRSETA vector (with and without *ALDC* gene). The untreated plates lacked the small petri dish in the centre.

Figure 3.2: PCR analysis confirming the cloning of the *ALDC* gene into the pRSETA vector using gene-specific primers. 53
The recombinant vector was

additionally sequenced and the integrity of the transgene in relation to the 6xHis-tag confirmed. The following primer sets were used **A)** pRSET_ALDC F/pRSET_ALDC R and **B)** AF2 /AR1. Indicated are base pairs (bp); the pUbi510:ALDC plasmid as positive control (+); and a negative non-template control (NTC); and lanes 1 and 2 individual clones.

Figure 3.3: Colony PCR to confirm transformation of the recombinant pRSETA:ALDC vector into *E. coli* BL21-CodonPlus (DE3)-RIPL using gene-specific primer set. Four of the colonies obtained were confirmed for incorporation of the transgene by colony PCR using transgene specific primers (AF2/AR1). All the colonies yielded positive results for the transformation. Indicated are base pairs (bp); a negative non-template control (NTC); and lane 1, 2, 3, and 4 individual colonies.

Figure 3.4: Semi quantitative PCR analysis confirming the expression of ALDC in *E. coli* BL21-CodonPlus(DE3)-RIPL. PCR analysis was performed with the primer pairs specific for the **A)** 16S rDNA reference gene (U968/L1401) and **B)** a transgene specific (AF2/AR1). Indicated are base pairs (bp); the non-template control (NTC); wild-type strain without modifications (WT); bacteria transformed with empty pRSETA vector (EV) and bacteria transformed with pRSETA::ALDC vector (AA).

Figure 3.5: SDS-PAGE gel analysis of induction ALDC-encoded protein (39 kDa) expressed by transgenic *E. coli* BL21-CodonPlus(DE3)-RIPL. Different conditions were tested for protein expression namely, **A)** induction at 37°C; or **B)** at 20°C; or **C)** at 20°C with 5% sugar added to growth medium. Boxes represent the area in which protein would be expected. Also indicated are the molecular weight marker (MW); the wild-type BL21 bacteria (WT); empty pRSETA vector (EV); empty pRSETA vector induced (EVI); pRSETA::ALDC (AA); and pRSETA::ALDC vector induced (AAI).

Figure 3.6: Western blot to analyse ALDC protein expression in transgenic *E. coli* BL21-CodonPlus(DE3)-RIPL using a His-tag antibody. Western blot was performed on *E. coli* BL21-CodonPlus(DE3)-RIPL pRSETA::ALDC induced with IPTG to identify the ALDC-encoded protein (39 kDa) linked to a His-tag. 6x-His tag monoclonal (HIS.H8), DyLight 550 Mouse/IgG2b host was used with anti-mouse as secondary antibody. Different conditions were tested: **A)** Induction at

37°C, **B1**) Induction at 20°C, **B2**) Induction of different strain at 20°C (Rosette Origami (DE3) 2), **C**) Induction at 20°C with 5% sugar added to medium. Boxes represent area where protein would be expected. Also indicated are the molecular weight marker (MW); the wild-type BL21 bacteria (WT); empty pRSETA vector (EV); empty pRSETA vector induced (EVI); pRSETA::ALDC (AA); and pRSETA::ALDC vector induced (AAI).

Figure 3.7: Voges-Proskauer test to detect acetoin in transgenic *E. coli* BL21-CodonPlus(DE3)-RIPL transformed with the pRSETA:ALDC recombinant vector. The Voges-Proskauer test was performed on cultures grown for **A**) 4 h or **B**) overnight in MR-VP media. Synthetic pure acetoin was used as a positive control and developed a red-pinkish colour. As a negative control the BL21-CodonPlus(DE3)-RIPL transformed with an empty pRSETA vector (EV) appear yellowish. The *E. coli* BL21 strain transformed with the transgene exhibited a pale pink colour (AA) indicating low levels of acetoin

Figure 3.8: Gas chromatography-mass spectrometric analysis of transgenic bacteria to detect the presence of acetoin. *E. coli* BL21-CodonPlus(DE3)-RIPL was grown in SPME headspace vials containing 2 mL LB medium for 6 d. **A**) EV detected no acetoin and **B**) AA detected acetoin at 14,66 min indicated by red arrow.

Figure 3.9: Growth performance of *Arabidopsis* seedlings exposure to the transgenic *E. coli* expressing the ALDC gene. Identically-sized 13 d old seedlings were used to set up the experiment. After two weeks of exposure to the respective *E. coli* BL21-CodonPlus (DE3)-RIPL strains, the plates were photographed, and fresh and dry mass of plants were measured. Growth trial was conducted *in vitro* at long-day-length (14 h:10 h photoperiod) conditions. Indicated are the wild-type *E. coli* BL21-CodonPlus (DE3)-RIPL (WT); empty pRSETA vector (EV); and pRSETA::ALDC (AA) to which plants were exposed.

Figure 3.10: Analysis of plant growth in response to exposure to transgenic *E. coli* expressing the ALDC gene. Fresh mass (mg), dry mass (mg), and rosette diameter (mm) of 13 d old *Arabidopsis thaliana* Col-0 seedlings, grown under a 14 h:10 h light:dark photoperiod *in vitro*, exposed for 14 d to *E. coli* BL21 bacteria with and without ALDC gene. Values represent the mean \pm SE (n = 48). For the dry mass, three plants were measured together for greater accuracy of

measurement. Each different letter indicates a value that was determined to be significantly different ($p \leq 0.05$) by one-way ANOVA and Tukey's multiple comparisons test. Indicated are the wild-type *E. coli* BL21-CodonPlus (DE3)-RIPL (WT); empty pRSETA vector (EV); and pRSETA::ALDC (AA) to which plants were exposed.

Figure 3.11: Salinity stress tolerance of *Arabidopsis* seedlings exposure to the transgenic *E. coli* expressing the ALDC gene. Identically-sized 13 d old seedlings were used to set up the experiment. After two weeks of exposure to the respective *E. coli* BL21-CodonPlus (DE3)-RIPL strains, the plates were photographed, and fresh and dry mass of plants were measured. Salinity stress tolerance trial was conducted *in vitro* at long-day-length (14 h:10 h photoperiod) conditions. Indicated are the wild-type *E. coli* BL21-CodonPlus (DE3)-RIPL (WT); empty pRSETA vector (EV); and pRSETA::ALDC (AA) to which plants were exposed.

Figure 3.12: Analysis of plant growth under saline conditions (100 mM NaCl) in response to exposure to transgenic *E. coli* expressing ALDC. Fresh mass (mg), dry mass (mg), and rosette diameter (mm) of 13 d old *Arabidopsis thaliana* Col-0 seedlings, grown under a 14 h:10 h light:dark photoperiod *in vitro* on medium containing 100 mM NaCl, exposed for 14 d to *E. coli* BL21 bacteria with and without ALDC gene. Values represent the mean \pm SE ($n = 48$). For the dry mass, three plants were measured together for greater accuracy of measurement. Each different letter indicates a value that was determined to be significantly different ($p \leq 0.05$) by one-way ANOVA and Tukey's multiple comparisons test. Indicated are the wild-type *E. coli* BL21-CodonPlus (DE3)-RIPL (WT); empty pRSETA vector (EV); and pRSETA::ALDC (AA) to which plants were exposed.

Figure 4.1: Layout for growth trials with transgenic plants. A) Control eight WT seedlings placed on $\frac{1}{2}$ MS media with or without 100 mM NaCl. **B)** Eight WT seedlings surrounding one transgenic plant in the centre of the container.

Figure 4.2: PCR confirmation of the transformation of the ALDC gene into the pMDC32 and the BDH1 gene into the pCAMBIA2300 vector. The transformation of ALDC into pMDC32 vector was confirmed using the AF2/AR1 primer set, whereas BF1/BR1 primer set was used to confirm successful insertion of BDH1 into pCAMBIA2300. Indicated are *base pairs (bp)*; the non-template

control (NTC); positive control pUBI510::ALDC (+); plasmid DNA of the pMDC32 vector containing *ALDC* (A); plasmid DNA of pCAMBIA2300 vector containing *BDH1* (B); and positive control pUBI510::BDH1 (+).

Figure 4.3: Screening T₁ putative transgenic *Arabidopsis* seedlings. Seeds 82
obtained from plants inoculated with *Agrobacterium* to transform with **A)** *ALDC* only (A line) or **B)** a combination of *ALDC* and *BDH1* (AB line) were screened by making use of media containing the appropriate antibiotics, namely hygromycin for A-lines and hygromycin and kanamycin for the AB-lines. Germination and growth were allowed for 2-4 weeks depending on the growth rate and clear distinction between seedlings.

**Figure 4.4: PCR analysis using genomic DNA extracted from putative T₁ 82
plants as template to determine the insertion of the *ALDC* gene into the plant genome using gene-specific primers.** Sixteen of the 33 putative A-line plants (A1 – A33) tested for the presence of the *ALDC* was positive for the transgene, while 8 of the plants yielded very faint bands. The plants showing clear bands for the transgene(s) were grown for T₂ seed collection. Indicated are *base pairs (bp)*; *Arabidopsis thaliana* Col-0 (WT); positive control of pUBI50::ALDC plasmid DNA (+); single *ALDC* transformant (A); and arrows for faint bands.

**Figure 4.5: PCR analysis using genomic DNA extracted from putative 83
transgenic T₂ plants as template to determine the insertion of the *ALDC* gene into the plant genome using gene-specific primers.** All T₂ generation plants from each line that was tested yielded an amplicon corresponding to the transgene the AF3/AR3 primer set. Indicated are *base pairs (bp)*; *Arabidopsis thaliana* Col-0 (WT); positive control of pUBI50 plasmid DNA (+); single *ALDC* transformant (A).

**Figure 4.6: Semi-quantitative PCR analysis of the expression of *ALDC* in T₂ 84
generation A-line transgenic plants.** The expression levels of the *ALDC* gene were determined using a **A)** gene-specific primer set (AF3 /AR1) in comparison with the expression of the **B)** EF-1α reference gene (EF-1α F/ EF-1α R). Indicated are *base pairs (bp)*; *Arabidopsis thaliana* Col-0 (WT); positive control of pUBI50::ALDC plasmid DNA (+); single *ALDC* transformant (A); and arrows for faint bands.

Figure 4.7: Screening T_3 putative seedlings for homozygous line. Seeds 85
obtained from T_2 A-line plants were screened for homozygosity by sowing a small batch of seed on media containing 15 µg/mL hygromycin. Germination and growth were allowed for 16 days, whereafter the germination percentage was determined, taking into consideration seed viability which was calculated by sowing seeds on non-selective plates. Lines showing 90-95% germination were considered homozygous and used in further experiments. Homozygous lines identified were **A)** A8.5 and **B)** A6.8 which are shown on non-selective and selective media.

Figure 4.8: Expression level of *ALDC* in T_3 generation A-line plants.. The 85
expression level of the *ALDC* gene was determined using **A)** gene-specific primer set (AF3/AR1) and **B)** EF-1α as reference gene (EF-1α F/ EF-1α R). Indicated are base pairs (bp); non-template control (NTC); positive control of pUBI50::ALDC plasmid DNA (+); *Arabidopsis thaliana* Col-0 (WT); homozygous T_3 A-line 6.8 (A6.8); homozygous T_3 A-line 8.5 (A8.5); and 1 and 2 indicate individual plants.

**Figure 4.9: Gas chromatography-mass spectrometric analysis of transgenic 87
 T_3 plants.** Whole 30 d old T_3 transgenic *Arabidopsis* plants were placed in a SPME headspace vials with 2 ml ½ MS media for 6 days to determine if plants produced the volatile compound, acetoin. **A)** Wild-type *Arabidopsis* Col-0 leaf (WT) and **B)** WT leaf spiked with synthetic acetoin were used as controls. Acetoin was detected in the WT leaf spiked with acetoin at a retention time of 14.83 min. Acetoin was detected in the two transgenic A-line plants, **C)** A8.7 at 14.57 min and **D)** A10.6 at 14.59 min. (A8.7: T_3 A-line transgenic *Arabidopsis* plant; A10.6: T_3 A-line transgenic *Arabidopsis* plant; Red arrow: Indicates acetoin peak).

**Figure 4.10: Gas chromatography-mass spectrometric analysis at different 88
growth stage of transgenic T_3 A6.8 plants.** Whole T_3 A6.8 *Arabidopsis* plants at different age and leaf stage were placed in a SPME headspace vials with 2 ml ½ MS media for 6 days to estimate the amount of acetoin produced. Acetoin was detected in the **A)** whole 13 d old plant (4 leaves) at 14.52 min and in the **B)** whole 21 d old plant (8 leaves) at retention time of 14.57 min. Acetoin peak is indicated by red arrow.

**Figure 4.11: Gas chromatography-mass spectrometric analysis at different 89
growth stage of transgenic T_3 A8.5 plants.** The T_3 A8.5 *Arabidopsis* plants at

different growth were placed in a SPME headspace vials for 6 days to estimate the amount of volatile compound, acetoin produced. Acetoin was detected in the **A)** whole 13 d old plant with 4 leaves at 14.86 min in trace amounts, **B)** whole 21 d old plant with 8 leaves at 14.58 min, **C)** whole 30 d old plant with 10 leaves at 14.58 min, and **D)** single leaf of 52 d old plant with 14 leaves at start of reproductive stage at retention time of 14.52 min. Acetoin peak is indicated by red arrow.

Figure 4.12: Growth and salinity stress trials to compare WT *Arabidopsis* to transgenic *Arabidopsis* plants. The growth parameters were compared between wild-type *Arabidopsis thaliana* Col-0 (WT) and T₃ homozygous A-lines (A6.8 and A8.5) through **A)** growth and **B)** salinity stress trials. After two weeks at long-day-length (14 h:10 h photoperiod) conditions, the plates were photographed, and fresh mass, rosette diameter, and dry mass of plants were measured.

Figure 4.13: Analysis of *in vitro* plant growth of wild-type *Arabidopsis* compared to transgenic *Arabidopsis* possessing the *ALDC* gene. The fresh mass (mg), rosette diameter (mm) and dry mass (mg) of 13 d old wild-type *Arabidopsis thaliana* Col-0 (WT) and two T₃ homozygous transgenic *Arabidopsis thaliana* lines (A6.8 and A8.5), grown under a 14 h:10 h light:dark photoperiod *in vitro* for 14 d was compared. Values represent the mean \pm SE (n = 48). For the dry mass, three plants were measured together for greater accuracy of measurement. Different letters indicate a value that was determined to be significantly different ($p \leq 0.05$) by one-way ANOVA and Fisher's LSD multiple comparisons test.

Figure 4.14: Analysis of *in vitro* salinity stress tolerance of wild-type *Arabidopsis* compared to transgenic *Arabidopsis* possessing *ALDC* gene. The fresh mass (mg), rosette diameter (mm) and dry mass (mg) of 13 d old wild-type *Arabidopsis thaliana* Col-0 (WT) and two transgenic *Arabidopsis thaliana* lines (A6.8 and A8.5), grown under a 14 h:10 h light:dark photoperiod *in vitro* for 14 d was compared. Values represent the mean \pm SE (n = 24). For the dry mass, three plants were measured together for greater accuracy of measurement. Different letters indicate a value that was determined to be significantly different ($p \leq 0.05$) by one-way ANOVA and Fisher's LSD multiple comparisons test.

Figure 4.15: *Ex vitro* growth trials to compare wild-type *Arabidopsis* to transgenic *Arabidopsis* plants. Seeds of wild-type *Arabidopsis* (WT) and two transgenic *Arabidopsis thaliana* lines (A6.8 and A8.5), were sown in water saturated peat, respectively and allowed to germinate. After 30 days at long-day-length (14 h:10 h photoperiod) conditions, the plants were photographed, and fresh mass, rosette diameter, and dry mass of plants were measured.

93

Figure 4.16: Analysis of *ex vitro* plant growth of wild-type *Arabidopsis* compared to transgenic *Arabidopsis* possessing *ALDC* gene. The fresh mass (mg), rosette diameter (mm) and dry mass (mg) of 30 d old wild-type *Arabidopsis thaliana* Col-0 (WT) and two transgenic *Arabidopsis thaliana* lines (A6.8 and A8.5), grown in peat under a 14 h:10 h light:dark photoperiod was compared. Values represent the mean \pm SE ($n = 5$). For the dry mass, each plant was measured separately. Different letters indicate a value that was determined to be significantly different ($p \leq 0.05$) by one-way ANOVA and Fisher's LSD multiple comparisons test.

94

Figure 4.17: *In vitro* growth trials to study effect of transgenic *Arabidopsis* plants as acetoin source on neighbouring wild-type *Arabidopsis* plants. Identically-sized 13 d old WT seedlings surrounding a 16 d old transgenic plant (A6.8 and A8.5) were used to set up the experiment. After two weeks of exposure to the respective transgenic A-line plants, the plates were photographed, and fresh mass, rosette diameter, and dry mass of plants were measured. Growth trials were conducted at long-day-length (14 h:10 h photoperiod) conditions.

95

Figure 4.18: Analysis of *in vitro* plant growth of wild-type *Arabidopsis* exposed to transgenic *Arabidopsis* possessing *ALDC* gene. The fresh mass (mg), rosette diameter (mm) and dry mass (mg) of 13 d old *Arabidopsis thaliana* Col-0 exposed to 16 d old transgenic *Arabidopsis thaliana* plants (A6.8 and A8.5), grown under a 14 h:10 h light:dark photoperiod *in vitro* for 14 d was compared. Values represent the mean \pm SE ($n = 48$). For the dry mass, three plants were measured together for greater accuracy of measurement. Different letters indicate a value that was determined to be significantly different ($p \leq 0.05$) by one-way ANOVA and Fisher's LSD multiple comparisons test.

96

Figure 4.19: Gas chromatography-mass spectrometric analysis of 16 d old transgenic T₃ plants allowed to accumulate acetoin for 11 days. Whole 16 d

97

old T₃ *Arabidopsis* plants of A6.8 and A8.5, respectively were placed in a SPME headspace vials (SU86009, 10 ml, Merck) with 2ml ½ MS media for 11 days to estimate the amount of acetoin accumulated in containers during TGAS trial. Acetoin was detected in the **A)** A6.8 plants at 14.55 min and in the **B)** A8.5 plant at retention time of 14.56 min. (TGAS: Transgenic plant as acetoin source, Red arrow: Indicates acetoin spike)

Figure 5.1: Alignment of transgene ALDC with Xpress tag in pRSETA vector. 117

α-Acetolactate decarboxylase was transformed into pRSETA in frame with Xpress tag to ensure expression of protein with His-tag. The alignment shows that the gene in frame with the 6 × His-tag, T7 tag and enterokinase site, as well as the T7 terminator.

Figure 5.2: Protein expression vector construct for ALDC. 118

α-Acetolactate decarboxylase was transformed into pRSETA via ligation with T4 DNA Ligase in frame with Xpress tag to ensure expression of protein with His-tag.

Figure 5.3: Vector constructs for ALDC and BDH1. 119

α-Acetolactate decarboxylase was transformed into pMDC32 via Gateway cloning, while acetoin reductase/2,3-butanediol dehydrogenase was transformed into pCAMBIA2300 through ligation with T4 DNA Ligase. Both genes were inserted in frame with a CaMV 35S promotor and flanked by a ferredoxin-NADP⁺ reductase (FNR) chloroplastic transit peptide.

Figure 5.4: BSA standard curve at 595 nm. 120

Standard curve was determined using a range of BSA from 0,0625 mg/mL to 1 mg/mL. The absorbance (10 mm) was measured at 595 nm and the standard curve obtained had a regression (R²) of 0.953.

Figure 5.5: Identification of acetoin in gas chromatography-mass 121

spectrometric analysis. Compounds were tentatively identified by comparison of retention times (T_R) and, by comparison with NIST11 mass spectral library. In order to identify the compound at specific peak on the chromatogram (Relative abundance vs retention time), **A)** the mass-to-charge (m/z) ratio for the peak at specific retention time is used (Relative abundance vs m/z). In this specific case, acetoin was detected in the sample at a retention time of 14,58 min with a m/z of 45,02. **B)** The m/z value is used to identify the compound in the NIST11 mass

spectral library, and acetoin is known to have a m/z of 45. Indicated by red arrow is the retention time for sample; and black arrow indicates mass-to-charge ratio for acetoin.

Figure 5.6: Roots of plants exposed to bacterial strains. Identically-sized 13 d old seedlings were used to set up the experiment. After two weeks of exposure to the respective *E. coli* BL21-CodonPlus (DE3)-RIPL strains, the plants were photographed. Growth trials were conducted at long-day-length (14 h:10 h photoperiod) conditions. Indicated are *E. coli* BL21 wild-type strain (WT); *E. coli* BL21 strain with pRSETA empty vector (EV); *E. coli* BL21 strain with pRSETA vector containing ALDC gene (AA). 122

Figure 5.7: Roots of plants exposed to bacterial strains and salinity. Identically-sized 13 d old seedlings were used to set up the experiment. After two weeks of exposure to the respective *E. coli* BL21-CodonPlus (DE3)-RIPL strains and 100 mM NaCl, the plants were photographed. Growth trials were conducted at long-day-length (14 h:10 h photoperiod) conditions. Indicated are *E. coli* BL21 wild-type strain (WT); *E. coli* BL21 strain with pRSETA empty vector (EV); *E. coli* BL21 strain with pRSETA vector containing ALDC gene (AA). 122

Figure 5.8: Gas chromatography-mass spectrometric analysis of *Escherichia coli* bacteria and wild-type *Arabidopsis thaliana*. The volatile profile of WT *Arabidopsis thaliana* and both *E. coli* BL21-CodonPlus(DE3)-RIPL strains containing the ALDC gene and empty vector were compared. All three volatile profiles showed the presence of ethylene glycerol isomers (at T_R of ± 23.39 , 26.77, 30.31 and, 31.3 min). Indicated are **A)** WT *Arabidopsis thaliana*, **B)** *E. coli* BL21-CodonPlus(DE3)-RIPL strain containing the ALDC gene, **C)** *E. coli* BL21-CodonPlus(DE3)-RIPL strain containing empty vector, acetoin by red arrow, and indole by black star. 123

List of Tables

Name	Page
Table 1.1: Summary of effects caused by salinity stress on cellular level in plants at different time periods (Modified from Munns, 2002b).	8
Table 1.2: Genes affected by volatiles. The exposure to acetoin and 2,3-butanediol can induce or suppress genes related to the biosynthesis or signalling response of phytohormones.	17
Table 2.1: Effect of synthetic volatiles at different photoperiods on growth traits of <i>Arabidopsis thaliana</i>.	41
Table 3.1: Standard PCR cycling protocol for GoTaq DNA Polymerase	45
Table 3.2: Primer pairs and sequences used in this study	46
Table 3.3: RT-sqPCR conditions	48
Table 4.1: PCR cycling protocol for Q5® High-Fidelity DNA Polymerase	75
Table 4.2: A-tailing protocol for blunt PCR fragments	75
Table 4.3: RT-sqPCR conditions	77
Table 4.4: Growth stages of two transgenic lines analysed by GC-MS to determine the effect of age on acetoin production	88

List of Abbreviations and non-SI units

Abbreviation	Expansion
µF	Microfarad
µg	Microgram
µg/mL	Microgram per millilitre
µL	Microliter
µm	Micrometer
µM	Micromolar
µmol photons/m ² /s ¹	Micromole photons per square meter per second
A or A-line	Transgenic plants containing the <i>ALDC</i> gene
AA	<i>E. coli</i> BL21-CodonPlus(DE3)-RIPL with <i>ALDC</i> gene
AB or AB-line	Transgenic plants containing both the <i>ALDC</i> and <i>BDH1</i> genes
ABA	Absciscic acid
ACC	1-Aminocyclopropane-1-carboxylate
ACO2	Aconitate hydratase 2
ACS4	1-Aminocyclopropane-1-carboxylate synthase 4
ACSI2	Acetyl-CoA synthetase 2
ACT2	Actin 2
AHK	<i>Arabidopsis</i> histidine kinase genes
AHP	<i>Arabidopsis</i> histidine phosphotransferase genes
AKT1	K ⁺ transporter
ALDC	α-Acetolactate decarboxylase
ANOVA	Analysis of variance
AP2	Apetala2
ARR	<i>Arabidopsis</i> response regulator
ASA1	Anthranilate synthase

ATP	Adenosine 5'-triphosphate
B or B-line	Transgenic plants containing the <i>BDH1</i> gene
BCAA	Branched chain amino acids
BDH1	Acetoin reductase/2,3-butanediol dehydrogenase
BGT	Bacterial growth trial
bp	Base pairs
BSA	Bovine serum albumin
BST	Bacterial salinity trial
bZIP	Basic leucine zipper
°C	Degrees Celsius
Ca ⁺ /Ca ²⁺	Calcium ion
CaMV	Cauliflower mosaic virus
cDNA	Complementary deoxyribonucleic acid
CHIB	Chitinase B
C ₂ H ₂	Cys2His2-like fold
CO ₂	Carbon dioxide
CoA	Coenzyme A
<i>cre1</i>	Cytokinin receptor-deficient mutant
CTAB	Cetyltrimethylammonium bromide
d	Day(s)
DAG	Days after germination
DAS	Days after sowing
DNA	Deoxyribonucleic acid
dNTP	Deoxynucleotide triphosphate
DREB	Dehydration-responsive element binding
<i>E. coli</i>	<i>Escherichia coli</i>
EDTA	Ethylenediaminetetraacetic acid

EF-1 α	Elongation-factor-1- α
<i>ein2</i>	Ethylene insensitive 2 mutant
EV	<i>E. coli</i> BL21-CodonPlus(DE3)-RIPL with empty vector
ERF1	Eukaryotic translation termination factor 1
EXP	Expansin genes
FIT1	Fe-deficiency-inducing transcription factor 1
FMO1	Flavin containing monooxygenase 1
FNR	Ferredoxin-NADP ⁺ reductase
g/L	Grams per litre
GC-MS	Gas chromatography-mass spectrometry
gDNA	Genomic deoxyribonucleic acid
GORK	Gated outwardly-rectifying K ⁺ channel
GRAS	Generally regarded as safe
GST2	Glutathione S-transferase 2
h	Hour(s)
H ⁺	Hydrogen ion
<i>HAK5</i>	High-affinity K ⁺ transporter 5
HE-TPP	Hydroxyethyl-thiamine pyrophosphate
HCl	Hydrochloric acid
HPLC	High-performance liquid chromatography
HKT1	High-affinity K ⁺ transporter 1
HS-SPME	Head space solid phase microextraction
HXK1	Hexose sensor kinase 1
IAA	Indole-3-acetic acid
IPS1	Myo-inositol-1-phosphate synthase
IPTG	Isopropyl- β -D-thiogalactoside
IRT1	Iron-regulated transporter 1

ISR	Induced systemic resistance
IST	Induced systemic tolerance
JAR1	Jasmonic response 1
JIN1	Jasmonate insensitive 1
K ⁺	Potassium ion
kDa	Kilodalton
KCl	Potassium chloride
KH ₂ PO ₄	Dipotassium phosphate
kPa	Kilopascal
LB	Luria Bertani or Lysogeny broth
MAT3	Methionine adenosyltransferase 3
Mg ⁺	Magnesium ion
mg/mL	Milligram per millilitre
min	Minute(s)
mL	Millilitre
mL/min	Millilitre per minute
mM	Millimolar
mm	Millimeter
Mn ⁺	Manganese ion
MR-VP	Methyl-Red Voges-Proskauer
½ MS	Murashige and Skoog
MS	Mass spectrometry
m/v	Mass per volume
m/z	Mass-to-charge ratio
MYB	Myeloblastosis
MYB75	Myb-related protein 75
Na ⁺	Sodium ion

NaCl	Sodium chloride
NAD ⁺ /NADH	Nicotinamide adenine dinucleotide (oxidized/reduced forms)
Na ₂ HPO ₄	Disodium phosphate
ng	Nanogram
NHX	Na ⁺ /H ⁺ exchanger
NIT	Nitrilase genes
nm	Nanometer
NPR1	Non-expressor of pathogenesis-related protein 1
NSCC	Non-selective cation channels
<i>ocs</i>	<i>Octopine synthase</i>
P5CS	Δ-1-pyrroline-5-carboxylate synthase
P5CR	Δ-1-pyrroline-5-carboxylate reductase
PBS	Phosphate-buffered saline
PCR	Polymerase chain reaction
PDF1.2	Plant defensin 1.2
PDF1.3	Plant defensin 1.3
<i>PDH1</i>	Proline dehydrogenase
PEG	Polyethylene glycerol
pg	Picogram
PGPR	Plant growth promoting rhizobacteria
PGPV	Plant growth promoting volatile
PHO2	Phosphate transporter
PHR1	Phosphate starvation response 1
PR	Pathogenesis-related protein
<i>PSII</i>	Second photosystem
RNA	Ribonucleic acid
RPM	Rotations per minute

ROS	Reactive oxygen species
RT	Room temperature
SAM2	S-Adenosylmethionine synthase 2
SAR	Systemic acquired resistance
SDS	Sodium dodecyl sulfate
SDS-PAGE	Sodium dodecyl sulfate polyacrylamide gel electrophoresis
SE	Standard error
SOS	Salt overly sensitive
SPME	Solid phase microextraction
RT-sqPCR	Reverse Transcriptase semi-quantitative PCR
T _R	Retention time
TE	Tris-EDTA buffer
TGAS	Transgenic plant as acetoin source
TPP	Thiamine pyrophosphate
Tris	Tris(hydroxymethyl)aminomethane
TSB2	Tryptophan synthase
V	Volt
v/v	Volume per volume
VSP2	Vegetative storage protein 2
WT	Wild-type
xg	Relative centrifugal force or <i>g</i> -force
Ω	Ohm

Chapter 1

Literature Review

The ever-growing world population requires a significant increase in present agricultural production to meet the demand for food. However, the yield of crops that are considered the main source of nutrition is already deliberated to have reached its plateau of biomass enhancement (Brilli *et al.*, 2019). In addition, the increased population also increases levels of pollution that evidently affect the world climate. In recent decades, climates over the world have been changing, with increased drought and infrequent rainfall seasons in several regions (Brilli *et al.*, 2019). This result in a greater effect of abiotic stress (drought, salinity etc.) on crop production further limiting increase in biomass at a time when food security is a major concern. One of the most significant abiotic stresses is salinity, which affects an estimated 20% of irrigated land, responsible for a third of world food production (Nadeem *et al.*, 2013). Increased salt concentrations in the soil can cause the death of vegetation and other organisms, leaving fertile land barren (Fouda *et al.*, 2019). Salinity affects different periods in the plant life cycle, from synthesis of phytohormones to growth of roots and stems of plants, consequently affecting crop yield, reducing flowering and seed production (Numan *et al.*, 2018). Thus far these issues have been addressed through the input of agrochemicals to increase crop production (Zhang *et al.*, 2017). These agrochemicals, however, can be expensive, ecologically damaging, and unsustainable in the long term (Mauchline and Malone, 2017). This has led to an urgent need to develop agricultural methods that are eco-friendly, effective, and sustainable to ensure food security, such as methods utilizing the soil microbiome to address both the increase in biomass needed and alleviating stress in plants.

1.1 Rhizobacteria and plant growth

In natural environments, plant growth is reliant on interactions with bacterial and fungal species (Sasse *et al.*, 2017). Several studies suggest that plant productivity can be improved by the microorganisms living in the rhizosphere, which is the region of soil envrioning plant roots. This rhizosphere is vital to the plant due to interactions occurring in this area, which affect growth and nutrient exchanges (Hassan *et al.*, 2019). The rhizosphere is defined as the volume of soil extending up to 2 mm from roots and includes the rhizoplane, which refers to the root surface itself (Dotaniya and Meena, 2015).

The rhizosphere is the location for intricate interactions between plant roots, microorganisms, and soil. Rhizosphere carbon sequestration, nutrient cycling and ecosystem functioning rely

on plant-microbe interactions which are vital for plant growth, nutrition, and crop quality (Hassan *et al.*, 2019). Root-soil interactions have active involvement from rhizosphere microorganisms, while roots in turn are responsible for mediation of microbe-microbe and microbe-soil interactions in the rhizosphere through root secretions (Zhang *et al.*, 2017). Secretion of cutin monomers, flavonoids, organic acids, phenolic acids, strigolactones and various volatile compounds by roots can act as signals to regulate colonization of plant roots by beneficial, harmful, or neutral microorganisms (Nadeem *et al.*, 2013; Zhang *et al.*, 2017; Hassan *et al.*, 2019). One such example is the ability of root secretions to interfere with quorum sensing, used by bacteria to detect cell population density (Zhang *et al.*, 2017). Quorum sensing is important for colonization of the rhizosphere by root-associated bacteria. By mimicking or interfering with this process, the plant can cause quorum quenching in an attempt to control pathogenic microbes (Zhang *et al.*, 2017). However, quorum quenching can also prevent beneficial microbes from performing their own quorum sensing regulated functions, which benefit plant health and fitness (Olanrewaju *et al.*, 2017). Thus, finding the optimal balance at which the plant can control pathogenic organisms through quorum quenching while still benefitting from beneficial bacteria performing quorum sensing would be ideal. Colonizing rhizosphere microorganisms, in turn, release diverse signalling components that affect plant growth, either directly or indirectly (Nadeem *et al.*, 2013).

One of the main mechanisms by which rhizosphere microorganisms directly promote plant growth involves assisting plant roots in acquiring nutrients through fixation of nitrogen or solubilization of minerals such as phosphorus or iron, and releasing micronutrients such as potassium (Zhang *et al.*, 2017). Nitrogen is one of the most essential nutrients for crop growth and soil deficiency has led to the application of large amounts of fertilizers to meet plant requirements to achieve maximum yield (Dotaniya and Meena, 2015). Despite being in plentiful supply, nitrogen is not freely accessible and requires conversion to ammonia to be suitable for plant assimilation (Olanrewaju *et al.*, 2017). Nitrogen-fixing bacteria are responsible for fixing atmospheric nitrogen (N_2) in soil to ammonia (NH_4) for plant assimilation (Dotaniya and Meena, 2015). Nitrogen-fixing rhizobacteria are well known for their mutualistic relationships with legumes and certain cereal crops, in which the bacteria exist in a root nodule as bacteroids without a cell wall to fix N_2 via a nitrogenase enzyme. In turn, the plant provides organic acids as fixed carbon from photosynthesis to support bacterial growth (Olanrewaju *et al.*, 2017).

Certain rhizobacteria can also directly affect plant growth by either supplying bacterial compounds, such as phytohormone analogues, to aid growth or by regulating the biosynthesis of plant phytohormones (Beneduzi *et al.*, 2012). Various phytohormone-producing genes can be activated via organic signalling compounds from either rhizobacteria, which activate genes

in plants, or plant roots, which activate genes in the bacteria (Hashem *et al.*, 2019; Hassan *et al.*, 2019). This allows rhizobacteria to influence physiological processes and facilitate plant development by altering the hormonal balance (Nadeem *et al.*, 2013). These phytohormones include, but are not limited to, auxins, cytokinins, abscisic acid (ABA) and ethylene (further discussion on the role of these phytohormones in plant growth is presented in Section 1.4).

1.2 Rhizobacteria and stress

The ability of some rhizobacteria to control pathogens indirectly affects plant growth by reducing or even preventing effects of pathogen attacks on the plant. When plants are under attack from pathogens, they alter root exudate profiles to select for plant-protective microorganisms and activities in soil to aid their immune response (Bakker *et al.*, 2018). Alteration in root exudate profiles is most likely due to hormones linked to systemic defence responses in plants (Hassan *et al.*, 2019). The key hormones in immune response in plants are jasmonic acid and salicylic acid. These hormones can determine which hormone-dependent secondary metabolites are excreted to allow for communication with microorganisms (Bakker *et al.*, 2018). Salicylic acid is generally linked to defence responses against biotrophic pathogens that complete their life cycle dependent on living host cells, whereas jasmonic acid plays a vital role in the response to insects, herbivores and necrotrophic pathogens that kill host cells (Coolen *et al.*, 2016; Bakker *et al.*, 2018). Both jasmonic and salicylic acids alter the root microbiome composition and root exudate profiles to assemble a microbiome to assist in fulfilling the needs of the plant (Bakker *et al.*, 2018).

The composition of the root microbiome can also be altered by abiotic stress situations. It has been suggested that the plant's responses to abiotic stress cross-communicate with its biotic responses (including salicylic acid and jasmonic acid) to shape the rhizosphere microbiome to assist plant growth and help to overcome stress situations such as disease and abiotic stress (Bakker *et al.*, 2018). Phosphate starvation is one example of a nutritional stress response in plants, which is coordinated with the immune response to alter the root microbiome. The major transcriptional regulator, phosphate starvation response 1 (PHR1), that is activated during phosphate starvation can bind to promoters of salicylic acid and jasmonic acid responsive genes to negatively regulate the immune response and prioritize nutrient uptake over immunity (Bakker *et al.*, 2018). The altered composition of excretion from plant roots changes the availability of nutrients that rhizobacteria can obtain from the plant, which can affect which bacteria are favoured to colonize the surface of roots.

Other mechanisms utilized by rhizobacteria to protect plants from environmental stresses include lowering stress-induced ethylene levels, production of exopolysaccharides, regulation of nutrient uptake to assist photosynthesis, enhancing antioxidant activity and improving plant

tolerance against heavy metals (Nadeem *et al.*, 2013; Forni *et al.*, 2017). Production of exopolysaccharides can assist plants suffering from water-deficit stress by forming a protective layer in the soil to prevent desiccation and, moreover, improve colonization of beneficial microorganisms and aid transport of water and nutrients to plant roots (Nadeem *et al.*, 2013). During water-deficit stress, leaf osmotic sensitivity leading to wilting can be beneficial, as the transpiration rate will be reduced by the smaller, wilted leaf surface area (Forni *et al.*, 2017). However, this also reduces photosynthetic rates, which in turn decreases plant growth. In mature plants subjected to abiotic stress, accelerated leaf senescence and abscission are frequently observed, whilst roots generally elongate to reach deeper water supplies (Forni *et al.*, 2017). One factor suggested to assist plants to enhance photosynthetic activity under these conditions is a higher accumulation of nitrogen and iron, aided by rhizobacteria.

1.3 Rhizobacteria, plants and salinity stress

Salinity is a severe environmental stress and soil with a salt concentration of 40 mM or more is regarded as saline (Shrivastava and Kumar, 2015; Forni *et al.*, 2017). The major salt contributing to salinity is considered to be sodium chloride (NaCl). Salinity stress affects a wide range of plant processes on the physiological, biochemical, and molecular levels, inhibiting growth or even causing plant death (Ashraf, 2004). Traditionally, artificial selection and conventional breeding based on agronomic characteristics (genetics and environmental effects on plant growth) are used to improve tolerance to salinity stress; however, these traditional methods are complicated by epistasis (genotype-environment interactions) and the multitude of genes involved in conveying salinity tolerance (Ashraf, 2004; Assaha *et al.*, 2017).

Plants are generally divided into two groups based on their ability to tolerate salinity, namely glycophytes and halophytes (Figure 1.1). Most crops fall within the glycophyte category, which can hardly tolerate salinity stress (100 mM NaCl or higher) and display signs of necrosis or plant death when subjected to high concentrations of salt (Acosta-Motos *et al.*, 2017; Assaha *et al.*, 2017). *Arabidopsis*, for example, is able to adapt to 50 mM NaCl at the reproductive stage and grow relatively normally but exhibits significant growth retardation at concentrations of 75 mM NaCl or higher (Sanders, 2000; Tassoni *et al.*, 2008).

The effects of salinity stress on plant growth are imposed over a period of time and the outcome depends on the developmental stage of the plant, severity of the salinity stress, and the stress exposure period (Table 1.1). The effect of salinity stress might not be clear in a short exposure period and differences in effect of salinity on growth between species or within same species often only become clear during a longer exposure time to salinity (Munns, 2002a). Promptly after the onset of salinity stress exposure, both plant leaves and roots

experience growth rate changes due to the sudden presence of salinity conditions, however, this is likely due to changes in water relations and not excess amounts of sodium. Depending on the salinity concentration, these changes in overall growth rate can recover to a new steady adjusted growth rate due to the stress conditions (Munns, 2002b).

After days of salinity exposure, it is suggested that hormonal signals rather than water relations control plant growth. If a plant has a poor ability to exclude NaCl, the older leaves will start to exhibit necrosis. Once the vacuole is saturated with sodium ions, the sodium will start to build up in the cytoplasm or cell wall, leading to cell death within a matter of days (Munns, 2002b). The rate of accumulation in the cytoplasm or cell wall depends on temperature, humidity, and the available nutrient solutions (Munns, 2002a). Cell dimensions change, resulting in smaller, thicker leaves with a higher chloroplast density (Munns and Tester, 2008). This reduces the overall photosynthetic rate in plants as the leaf surface area is reduced (Munns and Tester, 2008). Within weeks, necrosis occurs, and the plant starts to die. The rate at which the older leaves die due to salinity stress and new leaves grow determines whether the plant survives (Munns, 2002b). If the older leaves die faster than new leaves are produced, the ability to photosynthesise will decrease and eventually result in plant death (Munns, 2002b).

Plants have developed strategies to overcome salinity stress including ion homeostasis, antioxidant biosynthesis and activation, osmoprotectants (such as proline and trehalose), nitric oxide generation, hormone modulation and transport of ions (Numan *et al.*, 2018; Bakka and Challabathula, 2020). Certain rhizobacteria can provide the plant with the necessary support to execute salinity prevention strategies, as discussed below, to ensure salinity stress alleviation.

All major processes are affected during salinity stress, including lipid metabolism, photosynthesis, and enzyme synthesis, as a consequence of two factors, namely osmotic and ionic imbalance (Assaha *et al.*, 2017). A high ionic concentration decreases the porosity of the soil, leading to reduced water availability, consequently decreasing the availability of nutrients usually obtained from water, which leads to an osmotic imbalance (Rasool *et al.*, 2013; Kaushal *et al.*, 2016). Failure to balance osmotic levels can cause loss of turgidity, dehydration of cells and ultimately to cell death (Ashraf, 2004). Ionic or nutrient imbalance occurs due to an accumulation of sodium ions in the plant inducing cytosolic potassium ion efflux, the consequence being imbalanced cellular homeostasis, oxidative stress, nutrient deficiency, and inhibition of plant growth (Assaha *et al.*, 2017). The higher concentration of NaCl in soil causes roots to absorb sodium ions because of their abundance compared to magnesium, potassium, phosphorus, and nitrogen ions (Numan *et al.*, 2018). Furthermore, accumulation of sodium ions enhances the formation of reactive oxygen species (ROS), causing further

imbalance in the cell homeostasis (Kaushal *et al.*, 2016). Additionally, chloride ions are considered toxic to plants and detrimental to biochemical pathways, leading to growth retardation (Numan *et al.*, 2018).

Photosynthetic rate is decreased due to several factors such as leaf area and gas exchange being reduced, and unused photosynthates causing feedback inhibition (Ilangumaran and Smith, 2017). Photosynthesis is further affected by reductions in stomatal conductance, efficiency of photosystem II, transpiration rate and chlorophyll content during salinity stress (Ashraf, 2004; Fouda *et al.*, 2019). Stomatal closure at the onset of salinity stress can contribute to the delay of ion accumulation and flow in the transpiration system, allowing plants additional time to respond to salinity stress (Acosta-Motos *et al.*, 2017). Several changes are observed in the chloroplast, including in the number and size of chloroplasts, membrane organization, and the number and size of plastoglobuli (Acosta-Motos *et al.*, 2017). Accumulation of sodium ions in photosynthetic tissue causes stacking of adjacent membranes in the grana and thylakoid shrinkage, changing the organization of the chloroplast (Ashraf, 2004). Furthermore, a reduction in potassium levels can contribute to the disintegration of the second photosystem (PSII) while accumulation of chloride ions can cause the degradation of chlorophyll and consequently impairs efficiency of photosynthesis (Ashraf, 2004; Forni *et al.*, 2017).

During salinity stress, the homeostasis of sodium and potassium ions is essential for survival. A positive correlation has been shown between the ability to retain potassium and salinity tolerance (Sun *et al.*, 2015). Potassium ions act as co-factors for several enzymes and high concentrations are required during synthesis of proteins (Fouda *et al.*, 2019). A high concentration of sodium ions can lead to sodium ions replacing potassium ions as co-factors in biochemical reactions, causing conformational changes to proteins (Fouda *et al.*, 2019). Furthermore, potassium is involved in growth development and physiological processes such as osmoregulation, enzyme activation, stomatal regulation, and protein transport, to name a few (Assaha *et al.*, 2017).

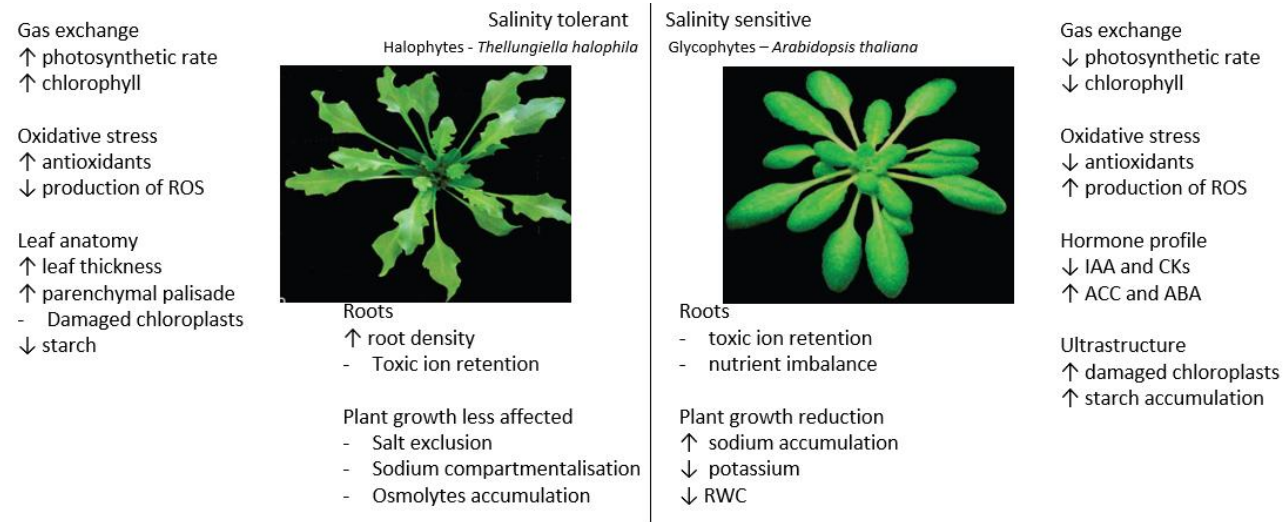


Figure 1.1: A representation of salinity sensitive (glycophyte) vs salinity tolerant (halophyte) plants during salinity stress. Salinity stress inhibits growth significantly in salinity sensitive plants, especially in aerial parts. The decrease in potassium is a key reflection of nutrient imbalance caused by the accumulation of sodium in leaves. Salinity stress also affects relative water content and the photosynthetic rate by decreasing chlorophyll content, regulating stomatal closure and starch accumulation. Due to senescence favoured in salinity stressed leaves, ethylene, and ABA increases while auxin and cytokinin decreases (Modified from Acosta-Motos *et al.*, 2017; picture obtained from Amtmann, 2008).

Table 1.1: Summary of effects caused by salinity stress on cellular level in plants at different time periods (Modified from Munns, 2002b).

Time period	Growth observation	Cellular level	State or regulatory signal	Cause
Minutes	↓ Growth rate (instantaneous) Rapid partial recovery of growth rate	↓ Cell volume Restoration – turgor regain	Hydraulic	Water stress
Hours	Steady reducing of growth rate	Rheology of cell wall changes	Hormone	Water stress Ca ²⁺ deficiency
Days	↓ leaf emergence rate ↑ root: shoot ratio	↓ Cell production rate ↓ Primordia development	Hormone/sugar	Water stress Ca ²⁺ deficiency
Weeks	Old leaves die ↓ branch/tiller formation	↑ Na ⁺ accumulation in cells Apical development altered	Ion toxicity Hormone/sugar	Ion toxicity Water stress

Several genes encoding different channels, transporters and exchangers are regulated during salinity stress to ensure plant survival. Non-selective cation channels (NSCC), AKT1 potassium channels and HAK5 high-affinity potassium transporters are some of the ion transporters suggested to mediate sodium ion uptake by a symplastic route in roots (Zhao *et al.*, 2020). Certain plants can use the SOS (salt overly sensitive) pathway to reduce sodium ion imbalances (Liu *et al.*, 2015). The Na^+/H^+ exchanger (SOS1/NHX7) is the most prominent exchanger to counterbalance uptake of sodium ions. At the cellular level, SOS1 encodes a Na^+/H^+ antiporter to regulate sodium ion efflux in the plasma membrane. Transport activity of SOS1 is enhanced through phosphorylation due to the interaction of a threonine kinase/serine kinase with a FISL motif at the C-terminal (encoded by SOS2) with a SOS3 (myristoylated Ca^{2+} -binding) protein. The loading of the SOS3-SOS2 complex occurs when SOS1 is phosphorylated to create sodium ion influx to reduce the ion imbalance (Numan *et al.*, 2018). Plants lacking the ability to tolerate salinity stress transport excess salt to the vacuole or to older tissues that are sacrificed for survival (Numan *et al.*, 2018). The tonoplast-based Na^+/H^+ exchangers (NHX family) are traditionally viewed as being responsible for vacuolar Na^+ sequestration but are suggested to represent only part of the system (Zhao *et al.*, 2020). Recent reports on the relationship between vacuolar sequestration and Na^+/H^+ antiporters (NHX family) showed that they have high affinity to potassium, thus additional mechanisms must be involved in depositing sodium ions in vacuoles (Zhao *et al.*, 2020). High-affinity sodium transporters (HKT1) are highly selective for sodium ions over potassium and are responsible for the retrieval of sodium from the xylem. HKT1 is also considered to play a major role in recirculating sodium back to plant roots via the phloem (Zhao *et al.*, 2020). In roots, HKT1 functions to assist sodium concentration regulation in xylem by transporting sodium ions to xylem parenchymal cells (Assaha *et al.*, 2017). Salinity-induced potassium loss is mediated by GORK (gated outwardly-rectifying K^+) channels and is highly sensitive to membrane potential changes. To use GORK channels to prevent potassium leakage, plants must pay a significant ATP cost that compromises plant growth to allow for more active H^+ pumping (Zhao *et al.*, 2020). ROS produced in the apoplast by AtRboD and AtRboF (plasma-membrane-localized respiratory burst oxidative homologs) can aid in the reduction of the Na^+/K^+ ratio by promoting potassium transport into the cytosol and reducing delivery of sodium ions from roots to shoots through restriction of sodium distribution in the xylem (Zhao *et al.*, 2020). Although ROS can assist plants initially, an excessive accumulation during salinity stress has detrimental effects on key cellular structures and leads to osmotic stress. ROS-scavenging machinery is key to help prevent additional stress (Zhao *et al.*, 2020).

Proline is an osmoprotectant that acts as a ROS scavenger and molecular chaperone to protect the integrity of proteins (Rasool *et al.*, 2013; Zhao *et al.*, 2020). During salinity stress, proline accumulates at much higher levels in comparison with other amino acids (Ashraf, 2004). Accumulation of proline is achieved by the activation of the biosynthesis pathway and deactivation of the catabolic pathway of proline. Genes encoding P5C synthase (P5CS, Δ -1-pyrroline-5-carboxylate synthase, EC 2.7.2.11/1.2.1.41) and P5C reductase (P5CR, Δ -1-pyrroline-5-carboxylate reductase, EC 1.5.1.2) in the biosynthesis pathway are

upregulated during salinity stress, while PDH1 (proline dehydrogenase, EC 1.5.99.8) is downregulated in the catabolic pathway (Per *et al.*, 2017; Zhao *et al.*, 2020). The exogenous application of different phytohormones is suggested to have an additive effect on proline accumulation to aid salinity tolerance (Per *et al.*, 2017). Absciscic acid accumulation can aid tolerance of salinity in plants by mitigating inhibitory effects on growth, and together with proline, calcium (Ca^{2+}) and potassium (K^+), neutralizes the effect of sodium ion imbalance (Numan *et al.*, 2018). Calcium and nitric oxide act as signals for ABA accumulation (Fouda *et al.*, 2019). Absciscic acid is suggested to be involved in regulation of P5CS and P5CR to influence accumulation of proline under salinity stress (Per *et al.*, 2017). Furthermore, ethylene, salicylic acid and gibberellic acid have also been suggested to have positive relationships with proline accumulation, acting as signal molecules and inducers (Per *et al.*, 2017).

Certain rhizobacteria, mostly of which are referred to as PGPR can alleviate salinity stress by reducing the uptake of toxic sodium ions from NaCl and providing the plant with the necessary support to execute these salinity prevention strategies (Figure 1.2). Some rhizobacteria produce exopolysaccharides that can form a hydrophilic biofilm around roots to prevent desiccation. Sodium ions bind to the biofilm, which restricts the influx of the ions into roots (Kaushal *et al.*, 2016). Other rhizobacteria can induce osmolyte accumulation, phytohormone signalling, and stimulate carbohydrate metabolism and transport to aid growth rate and photosynthesis. Several rhizobacteria have also been shown to enhance stomatal conductance without affecting chlorophyll concentrations or PSII efficiency (Ilangumaran and Smith, 2017). The beneficial rhizobacteria can increase auxin (IAA) and cytokinin levels, while decreasing ABA and ethylene levels to prevent premature senescence of leaves. Bacterial IAA can counteract ABA levels in plants while still having a positive effect on the Na^+/K^+ ratio and increasing chlorophyll levels. Certain rhizobacteria are also suggested to influence expression of genes responsible for SOS1, HKT1 and certain members of the NHX family proteins (Ilangumaran and Smith, 2017).

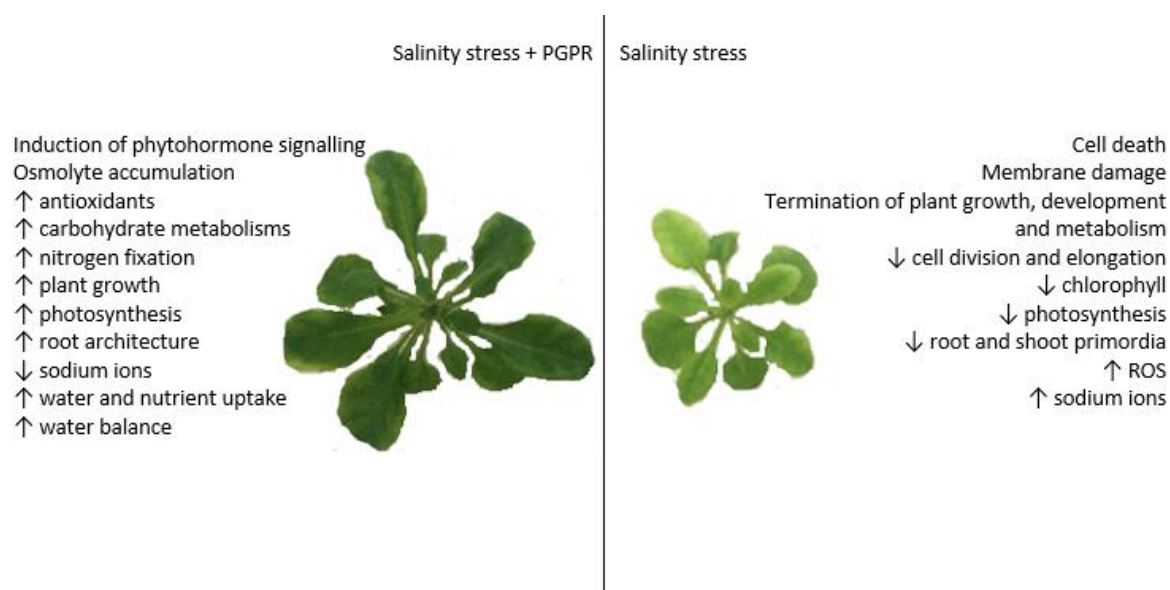


Figure 1.2: Representation of the effects on plants due to salinity stress showing changes between the presence and absence of PGPR. The accumulation of sodium ions causing ion imbalance and accumulation of ROS can be countered by the presence of PGPR that can assist in the restoration of water balance, photosynthesis, and regulation of salinity tolerance mechanisms (PGPR: Plant growth promoting rhizobacteria; modified from Bakka and Challabathula, 2020).

1.4 Rhizobacteria and phytohormones

Different phytohormones are involved in different processes of plant development and, depending on environmental stimuli, rhizobacteria can regulate these processes by supplying the compound or affecting biosynthesis of the hormone. This can directly or indirectly benefit the plant through growth promotion or heightening responses to stress.

Auxins are well known for their role in development of plant roots and their antagonistic relationship with cytokinins (Hwang *et al.*, 2012). The ability of auxins to improve root structure can aid in better nutrient exchange, which is important for plant growth processes (Kashyap *et al.*, 2019). The main natural auxin in plants is indole-3-acetic acid (IAA), which is involved in most growth processes including cell cycle progression, and shoot and root meristems (Tsukanova *et al.*, 2017; Sharifi and Ryu, 2018). Levels of auxin in plants can be altered by certain rhizobacteria via activity of influx and efflux carriers, degrading endogenous auxin or supplying exogenous auxins to the plant (Tsukanova *et al.*, 2017). The rhizobacteria achieve this by altering expression of genes responsible for proteins involved in auxin synthesis, transport, and signalling (Tsukanova *et al.*, 2017). Thus, by supplying the plant with additional IAA, rhizobacteria can support growth processes that require IAA to operate efficiently when plant hormone levels are sub-optimal or inhibit growth if auxin levels are supra-optimal (Olanrewaju *et al.*, 2017). Furthermore, auxins are also important role players in the maintenance of plant-microorganism relationships. The changes in auxin

availability increase root surface area, allowing more opportunity for colonization of the root and uptake of root exudates (Olanrewaju *et al.*, 2017). Moreover, certain rhizobacteria can aid a higher proline content and antioxidant activity (such as peroxidase and ascorbate peroxidase) to enhance salinity tolerance by providing IAA (Forni *et al.*, 2017).

As mentioned, cytokinins are antagonistic to auxins and are involved to a greater extent in the development of shoots rather than roots (Hwang *et al.*, 2012). The relationship between cytokinins and auxins plays an important role during embryogenesis to ensure normal development. The cytokinin sensing system in the transit zone of plants regulates auxin carrier proteins to control the release of auxin. Beyond embryogenesis, cytokinin sensing is alleviated to allow the release of auxin by negatively regulating carrier proteins. The efflux of auxin allows initiation of differentiation in the plant cell (Olanrewaju *et al.*, 2017). Cytokinins are also involved in cell cycle progression, regulation of chlorophyll biosynthesis and chloroplast biogenesis (Tsukanova *et al.*, 2017). Under salinity stress, lower levels of cytokinin can assist the adaption to decreased water availability by working antagonistically to ABA resulting in ABA-mediated stomatal closure and giving preference to allocating carbon for root growth (Forni *et al.*, 2017). Cytokinins can further protect the biochemical pathways associated with photosynthesis and delay senescence to overcome growth inhibition due to ABA-mediated processes during alleviation of abiotic stress (Forni *et al.*, 2017). Furthermore, cytokinin levels are mostly enhanced in roots during abiotic stress conditions to modify shoot hormonal and ion status.

Absciscic acid is a major role player in alleviation of abiotic stress as it is responsible for stomatal closure to reduce water loss through transpiration and contributes to salinity tolerance. Absciscic acid is antagonistic to cytokinins with regards to stomatal opening, photosynthesis, and transpiration. The presence of ABA further contributes to drought stress alleviation through the degradation of auxin transporters that negatively regulate root hair elongation. Some rhizobacteria can synthesize ABA to increase internal plant ABA levels that will aid plant drought resistance, while other rhizobacteria break down ABA to decrease levels in plant shoots, which will reduce the negative feedback of ABA on sugar accumulation (Tsukanova *et al.*, 2017; Sharifi and Ryu, 2018). This does suggest that based on the plant's need for ABA and the antagonistic relationship with cytokinins and gibberellins, different rhizobacteria might be of importance in certain conditions.

Another phytohormone, ethylene, is involved in inhibition of root elongation, promotion of fruit ripening and promotion of leaf abscission (Forni *et al.*, 2017). Ethylene is also responsible for limiting root and shoot growth to maintain plant homeostasis (Hashem *et al.*, 2019). Furthermore, ethylene has been repeatedly reported as being involved in regulation of primary resistance responses alongside key hormone-dependent secondary metabolites in the plant's immune response (Hase *et al.*, 2003). Depending on the concentration, ethylene can stimulate or inhibit plant growth (Tsukanova *et al.*, 2017). Ethylene, together with cytokinin signalling, is also known to activate a two-component regulatory system found in prokaryotes

and eukaryotes that mediates a wide range of responses to environmental stimuli, in which these two phytohormones are negative regulators of each other (Taiz *et al.*, 2015). Therefore, the regulation of ethylene biosynthesis by rhizobacteria can influence plant systemic resistance response relying on ethylene. Certain rhizobacteria can reduce ethylene in plants by cleaving plant-derived 1-aminocyclopropane-1-carboxylate (ACC; precursor of ethylene) with ACC deaminase (Forni *et al.*, 2017). Furthermore, ethylene levels increase under stress conditions and initial low levels of ethylene activate defence and protective proteins to aid stress tolerance. A second peak of ethylene, resulting from continued stress, retards growth and initiates processes such as chlorosis, senescence, and leaf abscission. Thus, the plant would benefit from the initial peak in ethylene production but not the second. To address this issue, ACC deaminase or auxin can regulate ACC synthase, which is responsible for conversion of ACC to ethylene, to alleviate the impact of salinity stress and maintain normal growth (Hashem *et al.*, 2019).

Gibberellins are key regulators of plant reproductive organ formation and play a role in ripening of fruit and production of viable seeds (Olanrewaju *et al.*, 2017; Tsukanova *et al.*, 2017). Gibberellins are also responsible for seed germination and suppressing germination at high temperatures when seedlings would not survive (Olanrewaju *et al.*, 2017). Certain rhizobacteria can synthesize gibberellins resembling those of plants and can increase endogenous level of gibberellins in plant shoots or stimulate gibberellin synthesis system of the plant (Tsukanova *et al.*, 2017). Exogenous gibberellins have been shown to stimulate shoot growth, xylem development and inhibition of root growth (Olanrewaju *et al.*, 2017).

1.5 *Bacillus* spp: Abundant rhizobacteria with potential to enhance plant growth

It is clear that microorganisms that form part of the rhizosphere microbiome can extend the plant's functionality through enhancement of nutrient uptake, improved root architecture, and increased defence against abiotic and biotic stress (Bakker *et al.*, 2018; Figure 1.3). The different mechanisms rhizobacteria can utilize to extend the plant's functionality are difficult to isolate or single out. Most of these processes are closely related and use the same machinery for a range of outcomes. Thus, it can be said that mechanisms and outcomes are dependent on environmental conditions, since this can influence the organisms present and their ability to colonize the plant roots. Plants are thus in a symbiotic relationship with these root-colonizing microorganisms, including those species known as plant growth-promoting rhizobacteria (PGPR). The predominant PGPR in the rhizosphere are certain members of the *Bacillus* and *Pseudomonas* spp. (Beneduzi *et al.*, 2012).

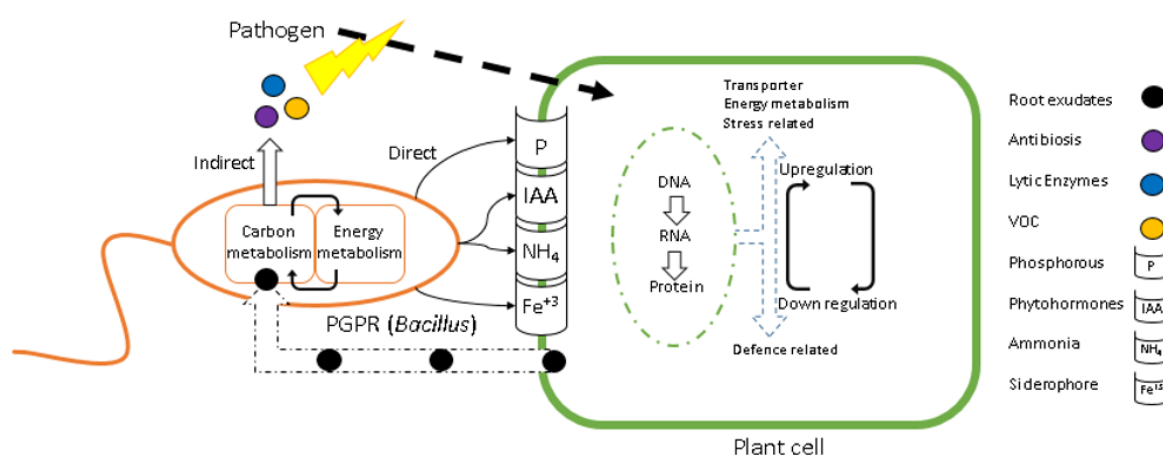


Figure 1.3: Mechanisms of PGPR. Direct and indirect mechanisms to promote growth through interactions between PGPR and plant cells. The rhizobacteria can directly assist plant growth by supplying bacterial forms of plant hormones or enhancing nutrient uptake of phosphorus and iron. The root exudates excreted from plant cell in turn fuels rhizobacterial metabolism to produce antibiosis, lytic enzymes and volatile compounds that can defend the plant against pathogenic attack (Modified from Kashyap *et al.*, 2019).

Bacillus spp. make up 95% of Gram-negative bacteria in the rhizosphere (Rosier *et al.*, 2018). *Bacillus* spp. are known to replicate rapidly, produce hard, resistant endospores and have resistance to adverse environmental conditions; moreover, *Bacillus* has GRAS (generally regarded/recognized as safe) status, which makes it suitable to investigate as an alternative to agrochemicals (Shafi *et al.*, 2017). *Bacillus* spp. have been reported as plant growth promoters, systemic resistance inducers and producers of a broad range of antimicrobial properties such as antibiotics, enzymes and lipopeptides (Shafi *et al.*, 2017). *Bacillus* spp. can alter a plant's global gene expression to promote plant growth (Kashyap *et al.*, 2019). Several genes found to be upregulated in plants in response to *Bacillus*-derived signals include genes related to

auxin, metabolism, stress response and certain plant defence systems, whereas genes related to the modification of the cell wall and other plant defence systems are downregulated (Kashyap *et al.*, 2019). In turn, genes related to oxidative reduction, transmembrane transport and organic substance metabolism in *Bacillus* can also be altered during interactions with plants (Kashyap *et al.*, 2019). *Bacillus subtilis* can activate induced systemic resistance (ISR) in plants by inducing the synthesis of jasmonic acid, ethylene and the *non-expressor of PR1 (NPR1)*-regulatory gene. Furthermore, ISR activation is associated with the production of glucanases, chitinases and phytoalexins (Hashem *et al.*, 2019). *Bacillus* spp. produce a range of lipopeptides depending on secondary metabolites produced by the plant, which allows specific activity to be triggered in the bacteria against plant pathogens, especially fungi. This includes blockage, distraction and pore formation in cell walls and cell membranes, and cellular changes (Shafi *et al.*, 2017). *Bacillus* spp. are also silicate mineral-solubilizing bacteria that can enhance the availability of potassium ions in soil for plants (Nadeem *et al.*, 2013).

The plant growth promoting ability of *Bacillus* is a result of several mechanisms, including production of lipophilic, low molecular weight compounds that are eco-friendly and effective at promoting plant growth (Fincheira and Quiroz, 2018). These compounds are better known as volatile compounds and can act as signal molecules over various distances. Volatile compounds can communicate with the plant in order to regulate biosynthesis of plant hormones, in particular gibberellic acid and IAA (Shafi *et al.*, 2017). In addition to plant growth promotion, these volatile compounds also play a role in inducing plant resistance to biotic and abiotic stresses via cross-protection by taking advantage of natural cross-talk between stress-response pathways (Shafi *et al.*, 2017; Rosier *et al.*, 2018). The effects of volatile compounds can be seen on the genetic, metabolic, and proteomic levels, relating to phytohormones, nutrition and metabolic pathways (Fincheira and Quiroz, 2018).

The first plant growth promoting volatiles (PGPVs) identified to promote plant growth were acetoin and 2,3-butanediol, emitted by two *Bacillus* strains (Ryu *et al.*, 2003). *Arabidopsis thaliana* plants were exposed to seven different PGPR *in vitro* using I-plates (centre-partitioned petri dishes) to allow exposure of plants only to airborne compounds produced by the bacteria (Ryu *et al.*, 2003). Only *Bacillus amyloliquefaciens* GB03 (previously *Bacillus subtilis* GB03; Choi *et al.*, 2014) and *Bacillus amyloliquefaciens* IN937a enhanced total leaf area of exposed plants (Ryu *et al.*, 2003). The volatile emissions of these two *Bacillus* strains were analysed via GC-MS (gas chromatography-mass spectrometry) and showed high levels of acetoin and 2,3-butanediol that were absent in the other PGPR tested, suggesting that bioactive PGPV synthesis is strain-specific (Ryu *et al.*, 2003; Farag *et al.*, 2006). Mutants of these two strains that lacked the ability to produce acetoin and 2,3-butanediol did not enhance plant growth (Ryu *et al.*, 2003). Furthermore, exposure of plants to synthetic 2,3-butanediol also enhanced plant growth in a dose-dependent manner (Ryu *et al.*, 2003).

Although the exact manner in which these PGPVs can alter and regulate plant processes to affect growth is still unknown, several affected processes have been identified, including photosynthesis, mineral uptake, plant hormones and alleviation of biotic and abiotic stress (Sharifi and Ryu, 2018). The increase in shoot mass and leaf surface area after exposure to acetoin and 2,3-butanediol in *Arabidopsis* is likely due to the regulation of the plant hormones auxin, ABA, ethylene and cytokinin, which are involved in different processes within the plant to directly or indirectly enhance growth (Ryu *et al.*, 2003; Lee *et al.*, 2012).

1.6 Volatile organic compounds and plant growth

The presence of acetoin and 2,3-butanediol can affect expression of genes related to phytohormone-responsive proteins and enzymes involved in the biosynthesis of several phytohormones (Table 1.2). The regulation of genes related to several phytohormones is needed to elicit plant growth promotion in plants, suggesting the importance of hormonal crosstalk (Zhang *et al.*, 2007).

The presence of 2,3-butanediol and acetoin downregulate *ARR5* (*Arabidopsis response regulator 5*), a cytokinin responsive gene involved in signal transduction due to the presence of cytokinins, ethylene and light (Zhang *et al.*, 2007). The importance of this functional cytokinin and ethylene signalling system for PGPV regulation was further supported via the use of a *cytokinin receptor-deficient* (*cre1*) mutant and an *ethylene insensitive 2* (*ein2*) mutant. Neither showed enhanced growth in response to acetoin and 2,3-butanediol, although increased photosynthesis and flower production associated with cytokinin and ethylene was found in WT *Arabidopsis* exposed to the volatiles (Lee *et al.*, 2012; Sharifi and Ryu, 2018). Furthermore, after *Arabidopsis* plants were exposed to a bacterial strain producing acetoin and 2,3-butanediol, transcriptomic results showed a decrease in expression level of genes for ethylene synthesis and upregulation of genes linked to cytokinin, jasmonic acid signalling, and salicylic acid signalling of (Kwon *et al.*, 2010; Forni *et al.*, 2017; Tahir *et al.*, 2017a; Tahir *et al.*, 2017b; Sharifi and Ryu, 2018).

Table 1.2: Genes affected by volatiles. The exposure to acetoin and 2,3-butanediol can induce or suppress genes related to the biosynthesis or signalling response of phytohormones.

Host plant	Strain	Volatile	Genes	Function	Effect	Reference
<i>Arabidopsis thaliana</i>	<i>Bacillus subtilis</i> GB03	2,3-butanediol Acetoin	↑ <i>EXPB1</i> , <i>EXPB3</i> , <i>EXP4</i> , <i>EXP5</i>	Up-regulation promotes cell expansion	Plant growth promotion	Bailly and Weisskopf, 2012
	<i>Bacillus subtilis</i> GB03	2,3-butanediol Acetoin	↑ <i>IRT1</i> ↑ <i>EXP5</i> ↑ <i>IPS1</i> ↑ <i>NIT1</i> , <i>NIT2</i> ↑ <i>TBS2</i> , <i>ASA1</i> ↓ <i>ARR5</i>	Iron-responsive transporter Up-regulation promotes cell expansion Myo-inositol biosynthesis Trp-dependent IAA pathway Tryptophan biosynthesis Cytokinin primary response	Plant growth promotion	Zhang et al., 2007
	<i>Bacillus subtilis</i> GB03	2,3-butanediol Acetoin	↑ <i>MAT3</i> , <i>SAM2</i> , <i>ACS4</i> , <i>ACS12</i> , <i>ACO2</i> ↑ <i>ERF1</i> , <i>GST2</i> , <i>CHIB</i> ↑ <i>PDF1.2</i> , <i>VSP2</i> ↑ <i>PR1</i> , <i>FMO1</i>	Ethylene biosynthesis Ethylene response Jasmonic response Salicylic response	ISR priming against <i>Erwinia carotovora</i> subsp. <i>carotovora</i>	Kwon et al., 2010
	<i>Bacillus subtilis</i> FB17	Acetoin	↑ <i>PDF1.2</i> ↑ <i>PR1</i>	Jasmonic response Salicylic response	ISR priming against <i>Pseudomonas syringae</i> pv. tomato DC3000	Rudrappa et al., 2010
	<i>Bacillus</i> sp. LZR216	Not specified	↑ <i>AHK3/AHK4</i> , <i>AHP1/AHP3</i> , <i>ARR4/5/7/10/12/15</i> (roots) ↓ <i>AHK3/AHK4</i> , <i>AHP1</i> , <i>ARR4/5/7/10/12/15</i> (shoots)	Cytokinin primary response	Plant growth promotion	Wang et al., 2018
<i>Nicotiana benthamiana</i>		2,3-butanediol	↑ <i>PRb-1b</i> , <i>PR-2</i> , <i>PR-5</i>	Pathogenesis-related	ISR priming against <i>Collectotrichum orbiculare</i>	Chung et al., 2016

In addition to enhancing plant growth through hormone regulation, acetoin and 2,3-butanediol can indirectly enhance photosynthesis and carbohydrate accumulation to increase chlorophyll content and photosynthetic efficiency. The PGPVs reduce biosynthesis of ABA, which in turn represses hexose sensor kinase 1 (HXK 1) signalling, alleviating negative feedback from sugar accumulation to increase photosynthetic efficiency (Sharifi and Ryu, 2018). Furthermore, chlorophyll production requires high uptake of iron by the plant. The presence of PGPVs can enhance iron uptake by utilizing the plant's own FIT1 (Fe-deficiency-inducing transcription factor 1)-dependent iron acquisition (Rosier *et al.*, 2018). FIT1 is responsible for increased expression of the iron transporter IRT1 (iron-regulated transporter 1) that transports iron to the plant cytosol (Sharifi and Ryu, 2018).

This indirectly leads to acidification of soil by reducing insoluble iron to favour iron solubility (Kwon *et al.*, 2010; Xie *et al.*, 2014; Rosier *et al.*, 2018; Sharifi and Ryu, 2018). The increase in photosynthetic rate due to increased iron uptake also delays leaf senescence (Rosier *et al.*, 2018). In addition to increasing iron uptake, the presence of PGPVs can also enhance uptake of copper, selenium and sulfur by plant roots (Kwon *et al.*, 2010; Sharifi and Ryu, 2018).

1.7 Volatile organic compounds and abiotic stress

The presence of PGPVs such as acetoin and 2,3-butanediol can assist in the alleviation of abiotic stress via induced systemic tolerance (IST) by means of regulating hormonal signalling, antioxidant production, proline production and sodium accumulation (Sharifi and Ryu, 2018). White clover (*Puccinellia tenuiflora*) subjected to salinity stress showed an increase in growth parameters when exposed to *B. amyloliquefaciens* GB03 (Niu *et al.*, 2016). The white clover had increased chlorophyll content, improved cell membrane integrity, decreased leaf osmotic potential and reduced sodium ion accumulation after being exposed to the bacteria (Niu *et al.*, 2016). Growth parameters and phytohormone levels (ABA, salicylic acid and jasmonic acid) were analysed in *Mentha piperita* (peppermint) plants exposed to salinity stress (75 and 100 mM NaCl), *B. amyloliquefaciens* GB03, or both (Cappellari and Banchio, 2020). Plants exposed to only salinity stress showed a decrease in all growth parameters and increases in levels of ABA, salicylic acid and jasmonic acid (Cappellari and Banchio, 2020). Peppermint plants exposed to only *B. amyloliquefaciens* GB03 had a slight increase in ABA and decrease in jasmonic acid, while salicylic acid level was unaltered compared to controls. Exposure to *B. amyloliquefaciens* GB03 also increased growth of peppermint plants (Cappellari and Banchio, 2020). The growth of plants exposed to both salinity stress and *B. amyloliquefaciens* GB03 was significantly increased compared to plants subjected to salinity stress only. Furthermore, they had salicylic acid levels similar to salinity-stressed plants; however, jasmonic acid and ABA levels were decreased (Cappellari and Banchio, 2020). It was also observed that *B. amyloliquefaciens* GB03 produced more acetoin in combination with salinity stress, suggesting that during abiotic stress PGPR can increase volatile production to aid stressed plants. This was further supported by the observation that 10 mM synthetic acetoin provided to the plant instead of *B. amyloliquefaciens* GB03,

resulted in effects similar to the bacterial treatment. However, this fixed concentration of the synthetic volatile treatment had a reduced effect on plant fresh mass compared to the bacterial treatment when plants were exposed to a higher stress level of 100 mM NaCl (Cappellari and Banchio, 2020).

The increased ABA levels due to salinity stress reduced water loss and increased shoot weight and ABA-mediated stomatal closure (Rosier *et al.*, 2018). However, research studying the effect of volatiles from *Bacillus amyloliquefaciens* GB03 (acetoin and 2,3-butanediol) found that genes related to ABA were unaffected (Cappellari and Banchio, 2020; Lee and Seo, 2014). The ABA levels were increased compared to control plants in salinity-stressed plants without acetoin present, but similar to controls in salinity-stressed plants exposed to acetoin (Cappellari and Banchio, 2020). This suggests that acetoin IST is ABA-independent. However, an increase in salicylic acid levels was observed for salinity-stressed plants exposed to acetoin, assisting restoration of dry mass, leaf area, photosynthetic rate, and pigment levels (Cappellari and Banchio, 2020). The presence of 2,3-butanediol can induce plant production of nitric oxide, which can act as a signal for ABA accumulation, thus indirect involvement of ABA cannot be ruled out since there is complex cross communication between nitric oxide, salicylic acid, and ABA (Liu *et al.*, 2015).

The volatile 2,3-butanediol released from *Pseudomonas chlororaphis* O6 induced salinity-tolerance in *Arabidopsis*, resulting in reduced water loss and 30% higher levels of stomatal closure (Cho *et al.*, 2008). Under salinity stress conditions, levels of ABA were found to be increased in plants, whereas plants exposed to 2,3-butanediol did not display the increased levels of ABA (Cho *et al.*, 2008). However, mutants for kinases (ABA-activated open stomatal 1 kinase, OST1) in the ABA-activated stomatal pathway lacked IST when exposed to salinity stress, indicating that although IST might be ABA-independent, it still requires a functional ABA pathway to regulate stomatal closure and water loss (Cho *et al.*, 2008). OST1 also acts upstream of the production of ROS, suggesting possible involvement of ROS in IST of 2,3-butanediol (Cho *et al.*, 2008).

The presence of acetoin and 2,3-butanediol induces sodium tolerance through HKT1, which is involved in sodium transport into roots of the plant (Numan *et al.*, 2018). HKT1 is a xylem parenchyma-expressed Na⁺ transporter responsible for removing sodium from xylem sap to exclude it from leaves (Liu *et al.*, 2015). The *HKT1* gene was downregulated in roots and upregulated in *Arabidopsis thaliana* shoots, resulting in an overall reduced uptake of sodium as sodium is transported from roots to shoots, assisting in the continued uptake of water. However, overexpression of the *HKT1* gene in *Arabidopsis* did not increase salt tolerance and the presence of the volatiles did not restore salt tolerance in *htk1* mutants, indicating that additional factors are contributing towards the observed salt tolerance, such as the SOS (Salt Overly Sensitive) pathway (Rosier *et al.*, 2018). Exposure to the volatiles reduced the concentration of sodium ions in *Arabidopsis* by approximately 50%, compared to only a 15% reduction in a *sos3* mutant, indicating the importance of the activation of SOS1 (Na⁺/H⁺) antiporter in the SOS pathway for reduction of sodium ion imbalance (Liu *et al.*, 2015). Gene expression analyses of white clover exposed to *B. amyloliquefaciens*

GB03 showed that genes related to the reduction of sodium transport from roots to shoots (*PtHKT1;5* and *PtSOS1*) were upregulated, whereas a gene linked to sodium uptake (*PtHKT2;1*) was downregulated (Niu *et al.*, 2016).

1.8 An alternative approach to VOC research

All previous research into the effects of acetoin and 2,3-butanediol on plant growth was conducted either through exposure of plants to bacteria producing these volatiles (i.e. *Bacillus subtilis* FB17 strain, or *Bacillus amyloliquefaciens* GB03 and IN937a strains) or to the synthetic volatile compounds. The importance of continual or constant exposure to volatile emissions, whether from bacteria or synthetic, was highlighted by the observation that early withdrawal resulted in a loss of growth enhancement (Xie *et al.*, 2009). During exposure to the volatiles, photosynthetic capabilities and iron levels of plants were elevated, but after withdrawal of the volatiles these returned to levels equal to those of WT plants. Similarly, effects on differential transcriptional expression of genes relating to iron regulation and cell wall functions were only observed during exposure to these PGPVs (Xie *et al.*, 2009). This observation indicates that experiments using the synthetic compounds would require multiple applications to allow constant exposure, which would be hard to regulate and control. Thus, exposure to PGPR would be more reproducible; however, this would only be plausible in an *in vitro* environment and difficult to implement in an agricultural environment. Engineering a plant to produce these PGPVs *in planta* would address several of these limitations and would possibly result in transgenic plants with enhanced growth and abiotic stress tolerance.

1.9 ALDC and BDH genes

Engineering plants to produce PGPVs such as acetoin and 2,3-butanediol (Figure 1.4) requires genes encoding the enzymes necessary to produce these volatiles. The volatile alcohols acetoin and 2,3-butanediol are produced by certain bacteria, yeast, and fungi. Although the pathways of synthesis of acetoin in bacteria and yeast may differ (Figure 1.5), acetoin can be converted to 2,3-butanediol by the same acetoin reductase/2,3-butanediol dehydrogenase (BDH1; EC 1.1.1.4) enzyme in both yeast and bacteria.

In bacteria, the intermediate product between pyruvate and acetoin is α -acetolactate, which can be converted to acetoin or diacetyl via the catabolic pathway, or leucine and valine via the anabolic pathway (Figure 1.5; Xu *et al.*, 2011). Pyruvate is converted to α -acetolactate by acetolactate synthase and further converted to acetoin by means of α -acetolactate decarboxylase (ALDC; EC 4.1.1.5). Under anaerobic conditions, the cytoplasm can become acidified, utilizing the catabolic pathway to produce acetoin to aid in neutralizing the pH (Xu *et al.*, 2011). Acetoin can be excreted or further converted to 2,3-butanediol to regulate the NAD⁺/NADH ratio (Forlani, 1998; Xu *et al.*, 2011).

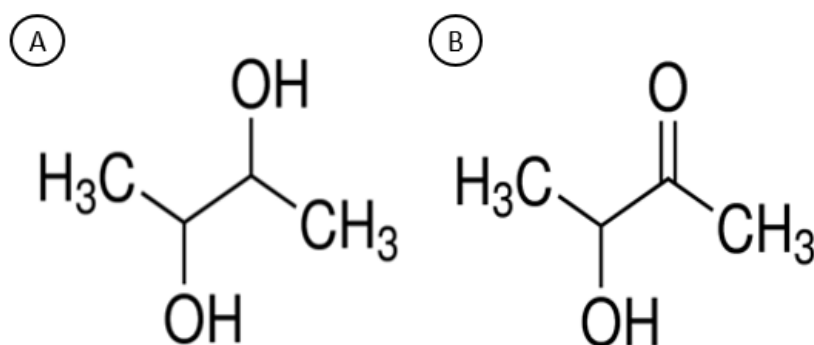


Figure 1.4: Chemical structures. A) 2,3-butanediol and B) acetoin.

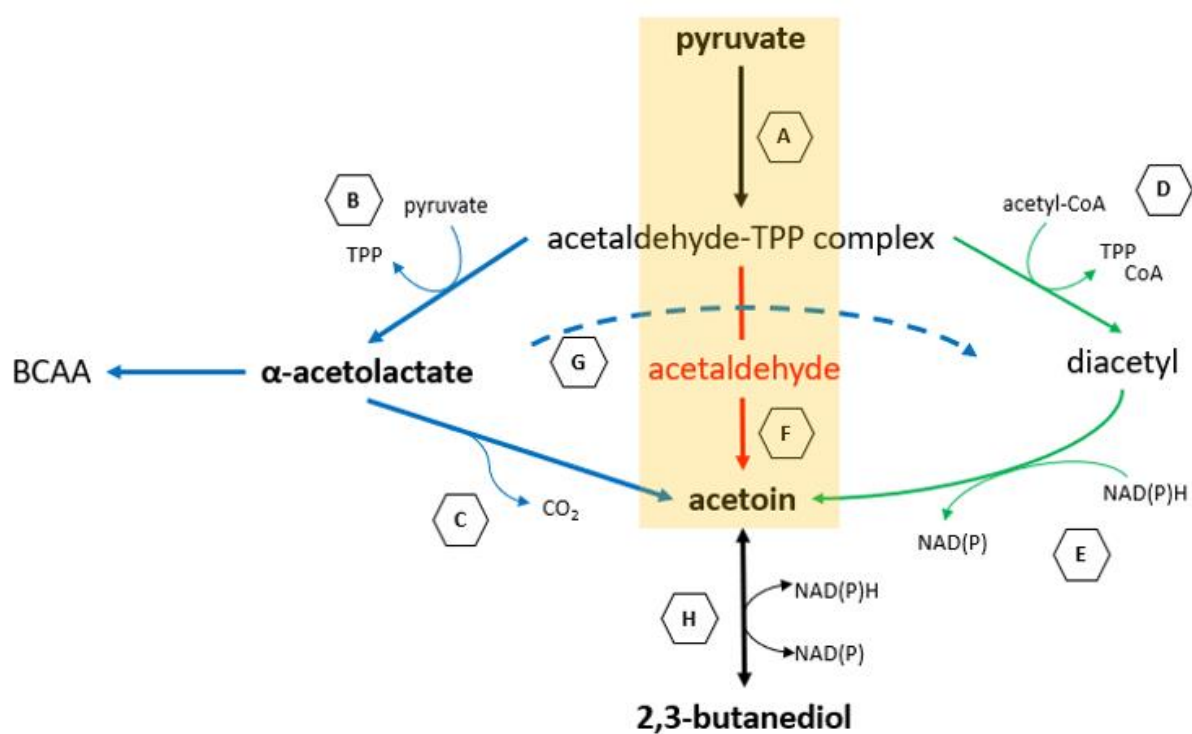


Figure 1.5: Biosynthesis of acetoin and 2,3-butanediol in bacteria and fungi. The biosynthesis of acetoin is similar in bacteria and fungi for the exception of an additional route found in fungal species indicated in red. A) pyruvate decarboxylase B) α-acetolactate synthase C) acetolactate decarboxylase D) diacetyl synthetase E) diacetyl reductase F) acetaldehyde condensation G) oxidative decarboxylation H) 2,3-butanediol dehydrogenase. (BCAA: branched chain amino acids; NAD(P): nicotinamide adenine dinucleotide (phosphate); NAD(P)H: reduced nicotinamide adenine dinucleotide (phosphate); CO₂: carbon dioxide, CoA: coenzyme A; modified from Xu *et al.*, 2011).

In yeast, either acetaldehyde or pyruvate is converted to acetoin by pyruvate decarboxylase (PDC; EC 4.1.1.1) or, alternatively, acetoin is produced from diacetyl by means of diacetyl reductase (EC 1.1.1.303; Figure 1.5). The production of acetoin has been detected in cell cultures of carrot, maize, rice, and tobacco (Forlani *et al.*, 1999), wheat germ and ripening pea seed tissue (Singer and Pensky, 1952; Davies, 1964). This acetoin is produced by a side reaction of PDC and pyruvate carboligase by means of direct condensation of hydroxyethyl-thiamine pyrophosphate (HE-TPP) bound as intermediate to an acetaldehyde moiety (Chen and Jordan, 1984; Forlani *et al.*, 1999). The presence of acetoin in plant tissues has only been detected with pyruvate or acetaldehyde as substrates and in the presence of thiamine pyrophosphate (TPP) and divalent cations (Mg^{2+} and Mn^{2+} ; Forlani *et al.*, 1999).

1.10 Previous research on VOCs at the Institute for Plant Biotechnology

This study represents a continuation of previous research conducted at the Institute for Plant Biotechnology (IPB), Stellenbosch University, which investigated the effects of the overexpression of α -acetolactate decarboxylase (*ALDC*) and acetoin reductase/2,3-butanediol dehydrogenase (*BDH1*) genes *in planta* (Dempers, 2015; Van der Merwe, 2016; Rosmarin, 2020). The previous research aimed to enhance plant growth of *Arabidopsis thaliana* and sugarcane by overexpressing genes from fungal and yeast strains known to produce acetoin and 2,3-butanediol, as well as to test the transgenic plants for enhanced growth and resistance to stress (biotic and drought).

The α -acetolactate decarboxylase (*ALDC*) gene was isolated from *Aspergillus niger* ATCC and acetoin reductase/2,3-butanediol dehydrogenase (*BDH1*) from *Saccharomyces cerevisiae* W303, as most bacterial species possessing the desired genes are either Gram-positive with different codon usage from eukaryotic organisms or are potentially pathogenic species. Isolation of genes from eukaryotic origins also prevent reduced transgene expression associated with the use of bacterial genes in eukaryotic species (Iglesias *et al.*, 1997). The *ALDC* (A) and *BDH1* (B) genes were transformed into separate pCambia vectors (1300 and 2300) before transforming *Arabidopsis* with the respective vectors to establish single (A or B) and double transgenic (AB) lines (Dempers, 2015). The expression levels for different lines were tested and three plant lines showing high expression were selected. After establishing T₃ generations, it was found that some of the single lines and all AB lines exhibited gene silencing (Dempers, 2015). A possible explanation of silencing seen in the A lines was hypothesized to be an effort by the plant to survive as requirements to produce acetoin from acetolactate might have been too much to support. The transgene silencing may also have been due to gene copy number or integration position and methylation patterns in the chromosome. Furthermore, GC content and methylation sites in the transgene may possibly also have affected compatibility with the genome of the host organism (Dempers, 2015). Growth of single successful T₃ generation A and B lines was tested against the WT *Arabidopsis* and results indicated that only A lines had promoted growth parameters compared to WT, as expected due to B line plants lacking the gene to produce acetoin, the precursor for 2,3-butanediol. Mixed results were obtained for non-

homozygous T₂ AB lines, since the T₃ generation exhibited gene silencing and trials had to be conducted under selective pressure as the T₂ lines were not homozygous, influencing the ability to determine if transgenic plants showed enhanced growth compared to the WT plants which did not experience this selective pressure (Dempers, 2015). Due to time constraints, the experiment could not be repeated (Dempers, 2015).

Attempts were made to detect the presence of the volatile compounds, acetoin and 2,3-butanediol, in the transgenic plants via GC-MS, HPLC (high-performance liquid chromatography) and enzymatic assays, but all were unsuccessful (Dempers, 2015). Suggested explanations for this lack of detection were that the volatiles were produced by the transgenic plants at extremely low quantities that were below the experimental detection limit, or that the plant system immediately used the compounds as they were produced. It was also considered that the significant increase in growth of the transgenic plants may have been due to positional effects of transgene insertions, although this latter possibility was highly unlikely since multiple independent lines were tested (Dempers, 2015).

Three lines (A₃, B₈ and AB₂) were investigated in the second study to test the effect of *Botrytis cinerea* infection on the transgenic *Arabidopsis thaliana* plants (Van der Merwe, 2016). The infection trials were designed to determine the direct effect of the 2,3-butanediol and acetoin volatiles on ISR, whether these were produced *in planta* or where WT plants were exposed to the synthetic compounds. Eight gene markers for ISR; *JAR1* (jasmonic acid signalling), *PR2* (salicylic signalling), *NPR1* (ISR and SAR marker), *VSP2* (jasmonic acid pathway), *MYB75* (phenylpropanoid pathway), *ERF1* (ethylene signalling), *MYC2* (jasmonic acid signalling) and *PDF1.3* (ethylene/jasmonic acid signalling), were also analysed to confirm the direct effects of the volatiles on disease-resistance (Van der Merwe, 2016). Only plants exposed to synthetic acetoin showed an increase in resistance. Further analysis of gene markers indicated that genes related to jasmonic acid signalling were up-regulated during exposure to the pathogen and acetoin (Van der Merwe, 2016). These results are in accordance with previous research that found that acetoin triggered priming of jasmonic acid related genes (Ryu *et al.*, 2004; Glazebrook, 2005; Kwon *et al.*, 2010). Similarly to the abovementioned observation, the A line showed the most resistance while the B line showed no resistance increase compared to WT plants. Although none of the results were significant, most probably due to low levels of the volatiles *in planta*, results showed similar trends to the trial which studied synthetic compounds (Van der Merwe, 2016). It was further supported by analysing transcription levels of eight marker genes mentioned above. It was thus concluded that elicitation of the ISR in plants is most probably due to acetoin and not 2,3-butanediol (Van der Merwe, 2016).

Subsequent research aimed to study effects of the overexpression of *ALDC* and *BDH1* genes on drought resistance in *Saccharum officinarum* (sugarcane; Rosmarin, 2020). The effect on growth of transgenic sugarcane was tested *in vitro* and *ex vitro*, thereafter drought tolerance was tested in an *ex vitro* pot trial. No significant increase in growth or drought tolerance was observed, most likely due to difficulties in

selecting uniform plants, leading to high variance in data and inconsistent results. Furthermore, the study hypothesized that volatiles might have different effects on C₄ plants, and their photosynthesis compared to C₃ plants such as *Arabidopsis*. Overall, the study was inconclusive.

1.11 Aims and objectives

This particular study will focus on the effect on plant growth and as novel addition, salinity stress tolerance in *Arabidopsis thaliana*. Previous research summarized above only showed enhance growth in a single homozygous A-line *Arabidopsis* as some lines exhibited gene silencing of transgenes and was unable to confirm the production of acetoin *in planta* (Dempers, 2015). The current study aimed to generate new recombinant vector systems (with previously isolated genes) and new transgenic plant material to determine if gene silencing would be observed once more and to attempt to detect the production of acetoin *in planta*. Furthermore, salinity stress tolerance (IST) has of yet not been studied in previous research in the research group on transgenic *Arabidopsis* producing acetoin *in planta* and was added as novel addition to the research.

As mentioned in Section 1.8, engineering a plant to produce acetoin *in planta* would address several of the limitations of exposing the plant to an acetoin-producing bacteria or synthetic compound. Furthermore, it would possibly result in transgenic plants with enhanced growth and abiotic stress tolerance. The main aim of this study was to enhance *Arabidopsis thaliana* growth by overexpressing the genes isolated from fungi and yeast responsible for the production of acetoin and 2,3-butanediol *in planta*. The objectives in order to achieve this, involved firstly to construct two separate recombinant vectors (pMDC32 and pCAMBIA2300). These vectors contained the α -acetolactate decarboxylase or acetoin reductase/2,3-butanediol dehydrogenase genes, respectively, under control of the constitutive CaMV35S promoter, in combination with a ferredoxin-NADP⁺ reductase (FNR) chloroplastic transit peptide sequence and octopine synthase (*ocs*) terminator. Secondly, to independently transform *Arabidopsis thaliana* by means of the *Agrobacterium*-mediated floral dipping method with the pMDC32 (*ALDC*) and pCAMBIA2300 (*BDH1*) vectors. Lastly, to confirm overexpression of the transgenes in *Arabidopsis* and functionally analyse the transformants in regard to plant growth and salinity stress tolerance. It is hypothesized that acetoin-producing *Arabidopsis thaliana* plants would display increased growth and salinity stress tolerance compared to WT *Arabidopsis thaliana* Col-0 plants, and potentially also increase the growth of WT plants in their vicinity due to their production of the acetoin volatile.

An additional aim of the study was to generate a transformed *Escherichia coli* strain that can produce the volatile acetoin and assess this strain's ability to enhance plant growth. Acetoin-producing bacterial strains, such as *Bacillus*, will produce a selection of volatile compounds, not only acetoin, which could possibly contribute to enhanced plant growth. The newly developed *E. coli* strain should produce only acetoin, which creates an opportunity to study the effects of this single compound on plants. Additionally, the availability of such a strain will allow plant growth experiments involving potential continuous exposure to

acetoin to be performed, which is difficult to achieve using synthetic acetoin. This part of the study had the following objectives, firstly, a recombinant pRSETA vector was constructed containing the α -acetolactate decarboxylase gene, which was then transformed into the *E. coli* BL21-CodonPlus(DE3)-RIPL strain. Secondly, the transcription and translation of the gene to protein was analysed, thereafter the bacteria were used in plant growth trials to investigate the growth enhancement abilities of the produced acetoin. It was hypothesized that exposure to the transgenic bacteria would enhance the growth and increase salinity tolerance of WT *Arabidopsis thaliana* Col-0 plants compared to untreated plants due to the acetoin continuously being produced by the bacteria.

Chapter 2

Trials with synthetic volatile compounds

2.1 Introduction

2.1.1 Dose-dependent curve

Different studies have shown that lipophilic, low molecular weight volatile compounds emitted by certain rhizobacteria (particularly *Bacillus* spp.) can act as signal molecules over various distances, promote plant growth, and enhance tolerance to biotic and abiotic stresses (Ryu *et al.*, 2003; Ryu *et al.*, 2004; Zhang *et al.*, 2007; Kwon *et al.*, 2010; Forni *et al.*, 2017; Numan *et al.*, 2018; Cappellari and Banchio, 2020). These rhizobacteria produce highly complex blends of volatiles and although the volatile(s) in the highest abundance are considered the most likely triggers for effects on growth, a specific blend of volatiles may also be a factor to consider (Bailly and Weisskopf, 2012). The utilization of pure (synthetic) compounds to supplement experimentation with volatile-producing bacteria provides an opportunity to characterize the effects of specific volatiles. Thus, several studies investigated the plant response when exposed to a specific synthetic volatile compound to establish a dose-dependent reaction to confirm the efficacy and importance of an individual volatile compound (Ryu *et al.*, 2003; Sharifi and Ryu, 2018). These dose-response curves entail the exposure of plants to a range of volatile concentrations to establish dose-dependent effects on growth and/or stress responses. Better understanding of individual volatile compounds might allow scientists to mimic the effects of these compounds, either through bio-manufactured bacterial products or by engineering plant genomes (Rosier *et al.*, 2018).

2.1.2 Circadian clock and photoperiod

In addition to the dose-response curve, it is of importance to consider adaptations in plants due to changes in the photoperiod, as this could also influence the effects that volatile compounds, such as acetoin and 2,3-butanediol, have on plant growth and/or stress responses. Dempers (2015) found, for example, that synthetic acetoin had no significant effect on plant growth under a short day (10 h:14 h day:night) photoperiod and conversely, that acetoin treatments resulted in significantly higher plant growth than control treatments under a long day photoperiod (16 h:8 h day:night; Dempers, 2015). Other studies on the effects of synthetic PGPVs on *Arabidopsis* all conducted these trials under different length photoperiods including 12 h:12 h day:night, 16 h:8 h day:night and 10 h:14 h day:night (Ryu *et al.*, 2003; Dempers, 2015; Sharifi *et al.*, 2020).

Due to the circadian clock system, plants can adapt to changes in photoperiod by adjusting growth and flowering to the energy available in the form of starch, oxidized compounds (CO₂) or sugars (Imaizumi *et*

al., 2010). *Arabidopsis thaliana* is classified as a long-day-length plant and normally reaches the flowering stage earlier in late spring to early summer and later in winter (Cookson *et al.*, 2007; Giakountis *et al.*, 2010). This correlates to photoperiods of 14 h of light or longer for earlier flowering and photoperiods of 10h or shorter for delayed flowering (Giakountis *et al.*, 2010). *Arabidopsis* ecotype Columbia 0 plants tend to flower synchronously at photoperiods of 14 h to 16 h light (Giakountis *et al.*, 2010). A long-day-length has been found to increase dry mass, leaf expansion, photosynthetic area, and leaf size, which are associated with increased cell number and size (Adams *et al.*, 2005). Furthermore, other plant processes that can change dependent on the photoperiod include RNA processing, light signalling, hormone signalling and expression of certain transcripts specific to long-day-length (flavonoid metabolism and biotic stress) and short-day-length (sugar transport and photosynthesis; Baerenfaller *et al.*, 2015). The availability of CO₂ is also affected by the photoperiod and is essential as the substrate for carbon assimilation, which is key in developmental processes (Queval *et al.*, 2012). Thus, the level of CO₂ due to the photoperiod can affect the synthesis of carbohydrates and amino acids in plant metabolism. Furthermore, CO₂ availability also affects the intracellular energy metabolism, redox state (in, for example, chloroplasts) and rate of photorespiration (Queval *et al.*, 2012).

An analysis of growth development in *Arabidopsis* under long and short photoperiods approximately 13 d after sowing (leaf 6 initiation) showed the effect of the photoperiod on the development of plants (Baerenfaller *et al.*, 2015). Initially long-day-length plants grew faster for around 20 d, where after rosette leaf area and leaf expansion ceased to allow for the transition to the flowering stage. The measurement of diurnal turnover of carbon reserves at the end of the light period showed that the amount of starch accumulated did not vary over the 30 d analysis period and larger amounts of starch were still available at the end of the dark period (Baerenfaller *et al.*, 2015). On the other hand, short-day-length plants showed a decrease in starch availability at the end of the light period and most of the accumulated starch was consumed during the dark period (Baerenfaller *et al.*, 2015). The short-day-length plants accumulated starch more rapidly and had to degrade it more slowly during the dark period to ensure that there were sufficient resources to fuel metabolic processes (Sulpice *et al.*, 2014). It is clear that several plant growth-related processes are influenced by the photoperiod and therefore this should be considered when investigating the effects of volatile compounds such as acetoin and 2,3-butanediol on plant growth, as different mechanisms could be at play or prioritized under different photoperiods.

2.1.3 Aim of chapter

The main aim of this study was to determine the effects of the *in planta* production of acetoin in *Arabidopsis thaliana* plants. To achieve this, it was important to first determine the effects of the pure volatile on *Arabidopsis* to establish a baseline for the effects of the volatile on growth and salinity tolerance of *Arabidopsis* to support and provide a comparison for results obtained from trials with transgenic bacteria and transgenic plants in subsequent chapters. In this chapter, different concentrations of the synthetic volatiles were applied to study their effects on growth and determine the optimal photoperiod and volatile concentration to conduct future trials. The optimal concentrations and photoperiod for each individual volatile was then used to study the effect of the respective volatiles on plants experiencing salinity stress.

2.2 Materials and methods

2.2.1 Plant material

Wild-type *Arabidopsis thaliana* Col-0 seeds were surface-sterilized via gas-phase decontamination using hydrochloric acid (HCl) and bleach and then stratified at 4°C for 2 d (Lindsey *et al.*, 2017). Seeds were sown on half-strength Murashige and Skoog (½ MS; Murashige and Skoog, 1962) basal medium (Sigma-Aldrich) with 9 g/L Phyto-agar (Duchefa Biochemie) as the solidifying agent at pH 5.7 in deep tissue culture plates (Falcon 353003). Plants were maintained at 22 ± 2°C in a 14 h:10 h day:night photoperiod (50 µmol photons/m²/s¹) under cool white, fluorescent tubes (Osram L 36W/640) or cool white LED tubes (Philips TL-D 13W/33-640). Identically-sized 13 d old seedlings were used for all experiments. All trials in this study were conducted at same temperature and photoperiod described, unless stated otherwise.

2.2.2 Growth trials with synthetic volatiles exposure

Different amounts (200 ng, 2 µg and 20 µg) of synthetic acetoin (92%, Sigma-Aldrich) and synthetic 2,3-butanediol (99%, Fluka) were dissolved in sterilized milliQ-grade water. Untreated seedlings were utilised as controls in the trials. Trials were set-up in three 500 mL containers (F.RL500, VaalPac) with 50 mL of medium and containing 8 seedlings (generated as described in Section 2.2.1) each per treatment. The volatile-water mixture was pipetted into a smaller petri dish (REF 353001, FALCON) that was placed into the centre of the culture container, with seedlings spaced evenly on the surrounding medium (Figure 2.1). Seedlings were exposed to the volatile compounds for a period of 14 d under short-day-length (10 h:14 h day:night) or long-day-length (14 h:10 h day:night) photoperiods as per average summer and winter day lengths in South Africa (<https://www.timeanddate.com/sun/@8335359>). At the conclusion of each trial, fresh and dry mass of each plant were measured.

2.2.3 Salinity trials with synthetic volatiles exposure

The 200 ng optimal concentration for acetoin and 2,3-butanediol identified during growth trials was applied for salinity trials. Salinity trials were set-up similarly to growth trials, with the exception that 50 mM and 100 mM NaCl (Sigma-Aldrich) were added to the ½ MS medium used in these experiments and 6 replicate containers were set-up per treatment. Seedlings were exposed to the volatiles for a period of 14 d under a long-day-length (14 h:10 h day:night) photoperiod. Untreated seedlings, on media with and without added NaCl, served as controls for the trial. At the conclusion of the trial, rosette diameter, fresh mass, and dry mass of each plant were measured. The trial was repeated twice and measurements from the two repeats were pooled together for statistical analysis.

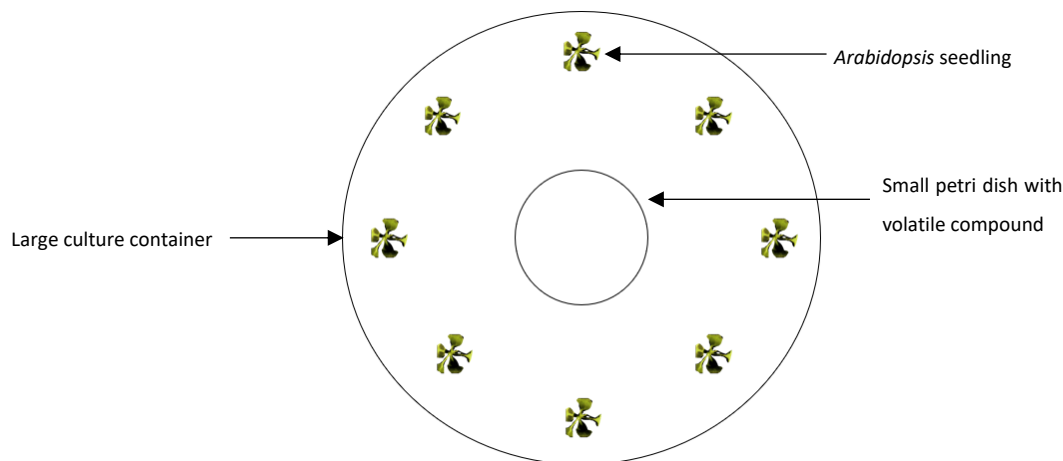


Figure 2.1: Setup of cultures for *in vitro* trial to expose plants to synthetic volatiles. A small petri dish was placed onto the medium surrounded by 8 plants, containing a specific concentration of synthetic volatiles diluted in sterile water.

2.2.4 Statistical analysis

The following assumptions of the ANOVA model were satisfied to allow interpretation of data: treatment levels in the experiment have approximately equal variances, residuals are normally distributed, and observations are independent. A one-way ANOVA and appropriate *post hoc* test for significant difference ($p \leq 0.05$) from the untreated or other treatments were applied for statistical analysis. All trials were independently repeated, and data was pooled together for statistical analysis, unless stated otherwise. For accurate dry mass measurement, three plants were pooled and measured together, unless stated otherwise. Tukey's multiple comparisons test was applied to compare treatments to two different untreated controls or to all other treatments. If data failed the Shapiro-Wilk normality test, the Kruskal-Wallis nonparametric test and Dunn's *post hoc* test were applied instead of one-way ANOVA.

2.3 Results

2.3.1 Growth trials with synthetic volatiles exposure

Growth trials were conducted with a range of concentrations (200 ng, 2 µg, 20 µg) for each of the synthetic volatiles, acetoin and 2,3-butanediol. Identically-sized 13 d old seedlings were used to set up trials and after two weeks of exposure to the synthetic volatiles, respectively, plants were measured and photographed (Figure 2.2). Under the short-day-length photoperiod (10 h:14 h day:night photoperiod), both independent trials generated highly similar results and all data were pooled to enhance the statistical analysis. All plants treated with either the synthetic acetoin or 2,3-butanediol had significantly smaller fresh and dry mass compared to the untreated control, except the treatment with 2 µg 2,3-butanediol (Figure 2.3).

All three independent repeats for the long-day-length trials generated different results. When comparing the fresh mass and dry mass of the untreated plants from each individual repeat, it was clear that there was a significant size difference between these untreated plants, even though they were grown under identical conditions (14 h:10 h day:night photoperiod; $22 \pm 2^\circ\text{C}$) and allowed the same germination time (13 d after 2 d stratification). Since all three independent trials gave different results, each was individually analysed to show different outcomes (Figure 2.4 and 2.5). For the three repeats there were an inexplicable but consistent trend in reduction in growth between repeats, including the untreated plants. Plants treated with 200 ng and 2 µg acetoin had significantly higher fresh mass than untreated plants in one of the three repetitions of the experiment. The dry mass data showed no significant differences, except in treatment of 20 µg acetoin, and 200 ng and 2 µg 2,3-butanediol for one of the repeats, in comparison to control plants. Considering the overall trend of the presented data, regardless of significance, the 200 ng acetoin treatments were the best performing out of the three volatile concentrations tested in terms of their enhancement of plant fresh and dry mass.

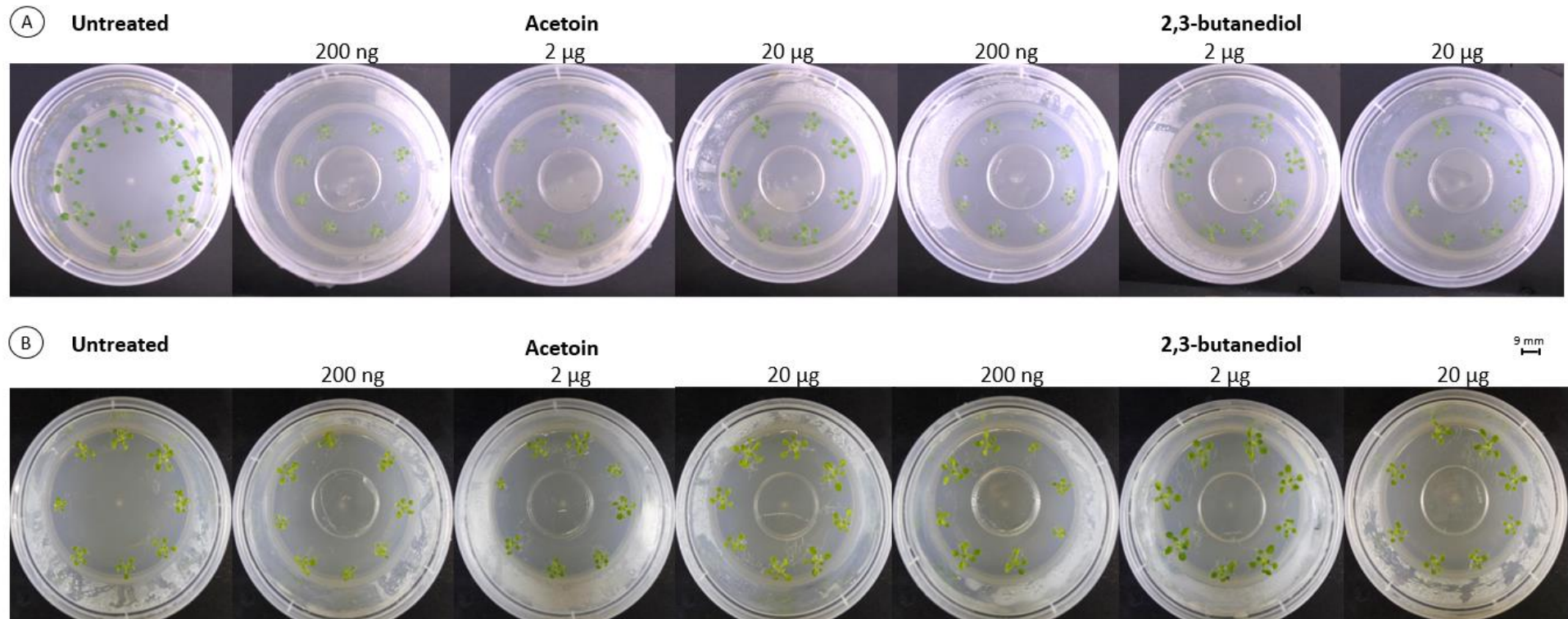


Figure 2.2: Growth trials to determine the effect of synthetic acetoin and 2,3-butanediol exposure on seedling growth. Identically-sized 13 d old seedlings were used to set up the experiment. After two weeks of exposure to the respective volatiles, the plates were photographed, and fresh and dry mass of plants were measured. Growth trials were conducted under both **A)** short-day-length (10 h:14 h photoperiod) and **B)** long-day-length (14 h:10 h photoperiod) conditions. Indicated are the different concentrations used for each respective synthetic volatile compound to which plants were exposed.

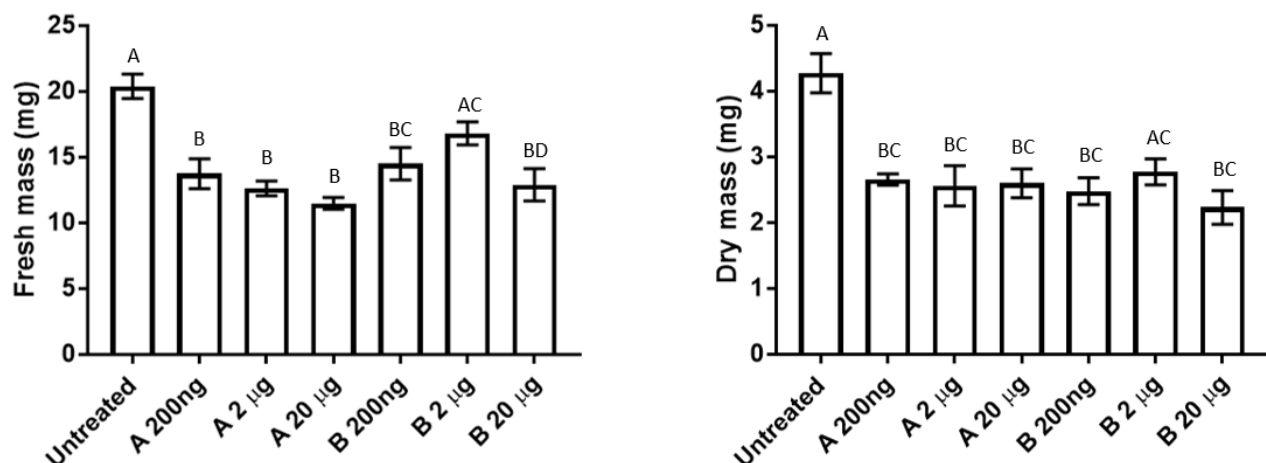


Figure 2.3: Analysis of effect of synthetic acetoin and 2,3-butanediol exposure on seedling growth at short-day-length photoperiod. Fresh mass (mg) and dry mass (mg) of 13 d old *Arabidopsis thaliana* Col-0 seedlings exposed for 14 d to synthetic acetoin (indicated by A before concentration tested) or 2,3-butanediol (indicated by B before concentration tested) grown under a 10 h:14 h light:dark photoperiod *in vitro*. Values represent the mean \pm SE (n = 48). Different letters indicate significantly different values ($p \leq 0.05$) as determined by Kruskal-Wallis and Dunn's multiple comparisons test.

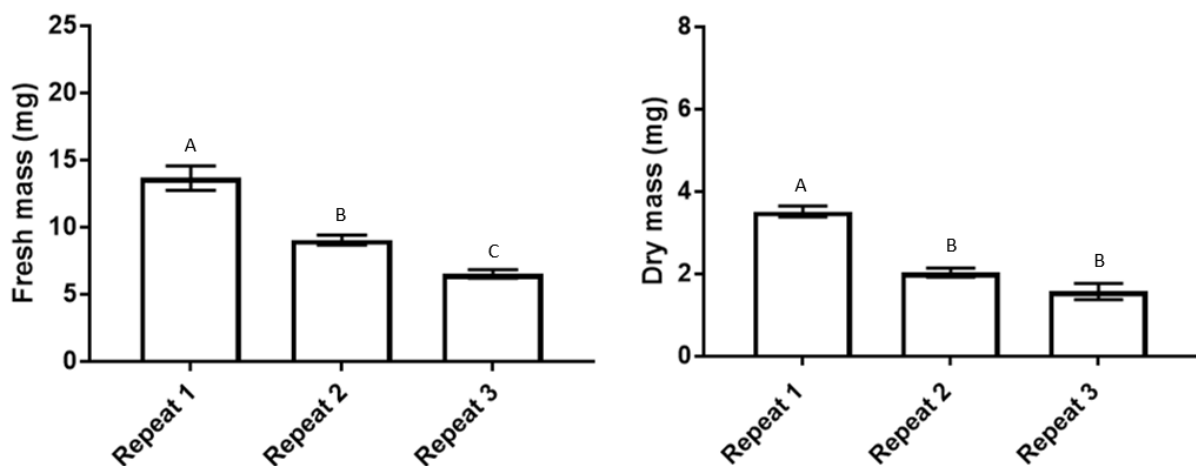


Figure 2.4: Analysis of untreated plants of each individual repeat for long-day-length synthetic volatile growth trials. Fresh mass (mg) and dry mass (mg) of 13 d old *Arabidopsis thaliana* Col-0 seedlings grown for 14 d grown under a 14 h:10 h light:dark photoperiod *in vitro*. Values represent the mean \pm SE (n = 24). Different letters indicate significantly different values ($p \leq 0.05$) as determined by one-way ANOVA and Tukey's multiple comparisons test.

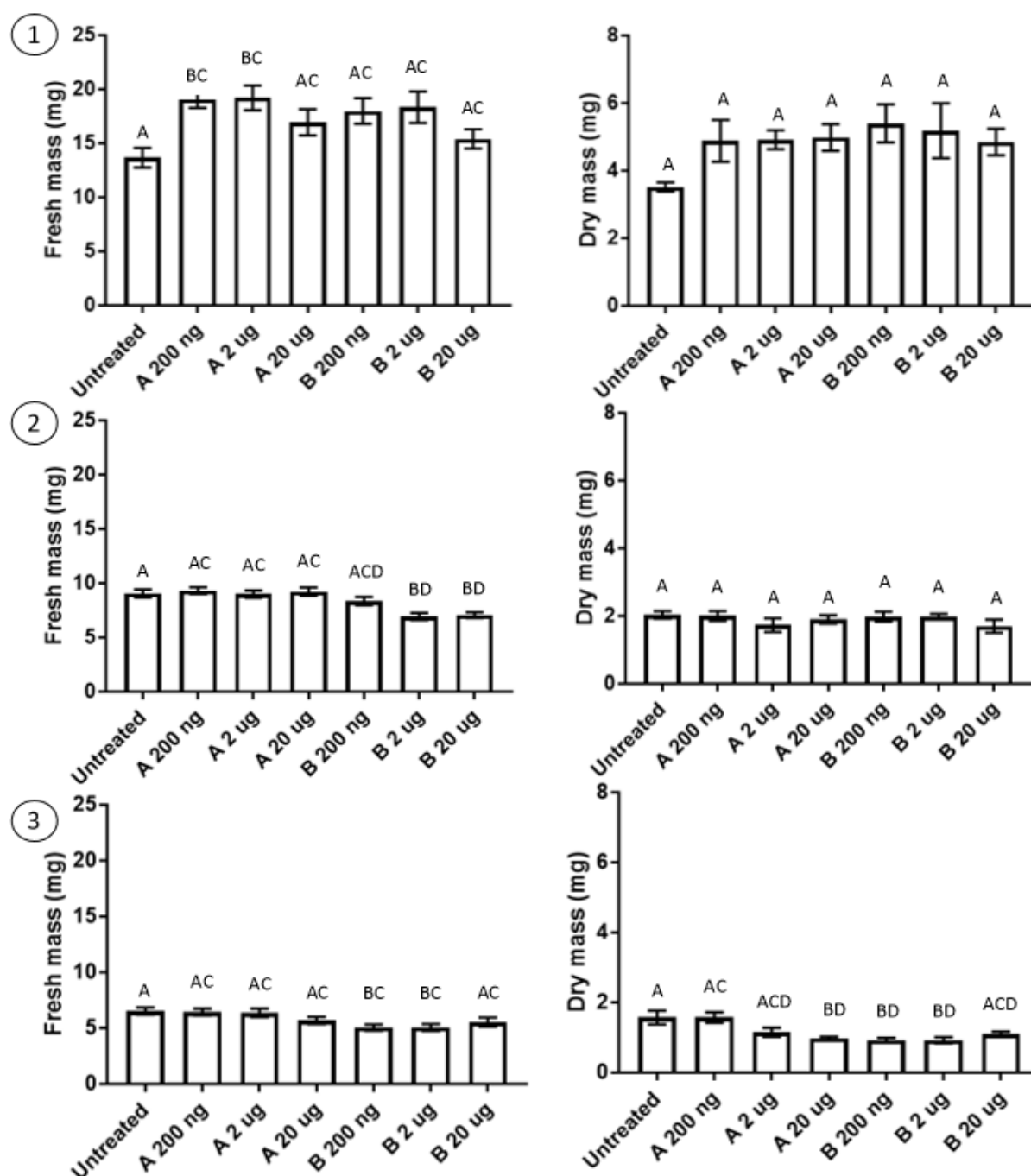


Figure 2.5: Analysis of effect of synthetic acetoin and 2,3-butanediol exposure on seedling growth during long-day-length photoperiods. Experimental repeats are indicated by numbers 1 to 3 to show the different outcomes under the same treatment conditions. Fresh mass (mg) and dry mass (mg) of 13 d old *in vitro* *Arabidopsis thaliana* Col-0 seedlings exposed for 14 d to synthetic acetoin (indicated by A before concentration tested) or 2,3-butanediol (indicated by B before concentration tested) grown under a 14 h:10 h light:dark photoperiod *in vitro*. Values represent the mean \pm SE ($n = 24$). Different letters indicate significantly different values ($p \leq 0.05$) as determined by one-way ANOVA and Tukey's multiple comparisons test.

2.3.2 Salinity trials with synthetic volatiles exposure

Based on results from the growth trials described above, the salinity trials were conducted with 200 ng concentration of each of the two volatiles at a photoperiod of 14 h:10 h day:night (long-day-length). After two weeks of exposure to the respective volatiles and salt concentration, the plates were photographed, and, across all treatments, there was a visibly higher survival rate of between 70-75% on the 50 mM NaCl treatments compared to the 100 mM NaCl treatments, which had a survival rate of between 20 and 30% (Figure 2.6). Growth parameters including rosette diameter, fresh mass, and dry mass were measured from plants that survived the 100 mM NaCl conditions (Figure 2.7). Untreated plants on medium without added NaCl (hereafter referred to as untreated control) were added to the experiment as an additional control. However, a significant difference in growth parameters between salinity-stressed untreated plants (hereafter referred to as salt control) and salinity-stressed plants exposed to 200 ng of acetoin or 2,3-butanediol were considered the true representation of the effects of volatiles on salinity tolerance in plants.

There was only a significant difference in rosette diameter between the salt control and the acetoin-treated plants on 100 mM salt plates, while rosette diameter of all three treatments with salt stress was significantly smaller than in the untreated controls. The fresh mass for the volatile-treated plants were significantly higher than the salt control, while the volatile treatments did not significantly differ from each other. The overall size of plants made it difficult to obtain an accurate dry mass measurement in this trial and all plants per treatment for each of the repeats were pooled for measurement, thus only two values were obtained for dry mass when combining the two independent repeats' results. Although statistical analysis was performed on the data set, the statistical reliability was comprised by this reduction in the number of samples due to pooling. The growth parameters measured showed a similar trend relating to which treatment was best performing for rosette diameter and fresh mass. Although 200 ng acetoin and 200 ng 2,3-butanediol treatments did not significantly differ from each other for fresh mass and rosette diameter, the trend showed that plants exposed to acetoin performed slightly better under salinity stress. Furthermore, the acetoin treatment also resulted in the highest survival rate of 32% compared to untreated salt (30%) and the 2,3-butanediol treatment (28%).

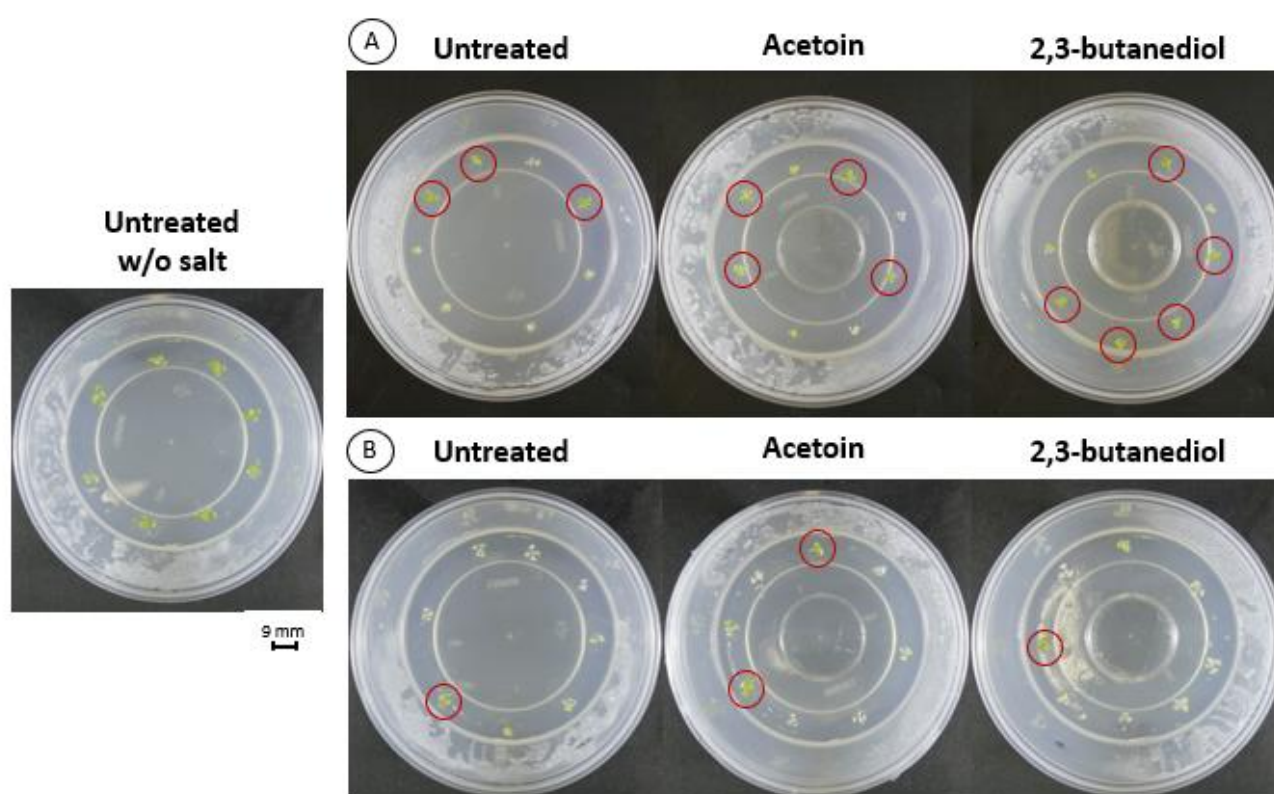


Figure 2.6: *in vitro* growth trials to determine the effect of salinity stress and exposure to synthetic volatiles on seedling growth and survival. Identically-sized 13 d old seedlings were used to set up the experiment. After two weeks of exposure to the respective volatiles (200 ng), the seedlings grown on medium with **A)** 50 mM NaCl or **B)** 100 mM NaCl were photographed, and fresh and dry mass of plants were measured of plants that survived. The 50 mM NaCl treatment had a visibly higher survival (indicated by red circle) rate for plants than the 100 mM NaCl treatment.

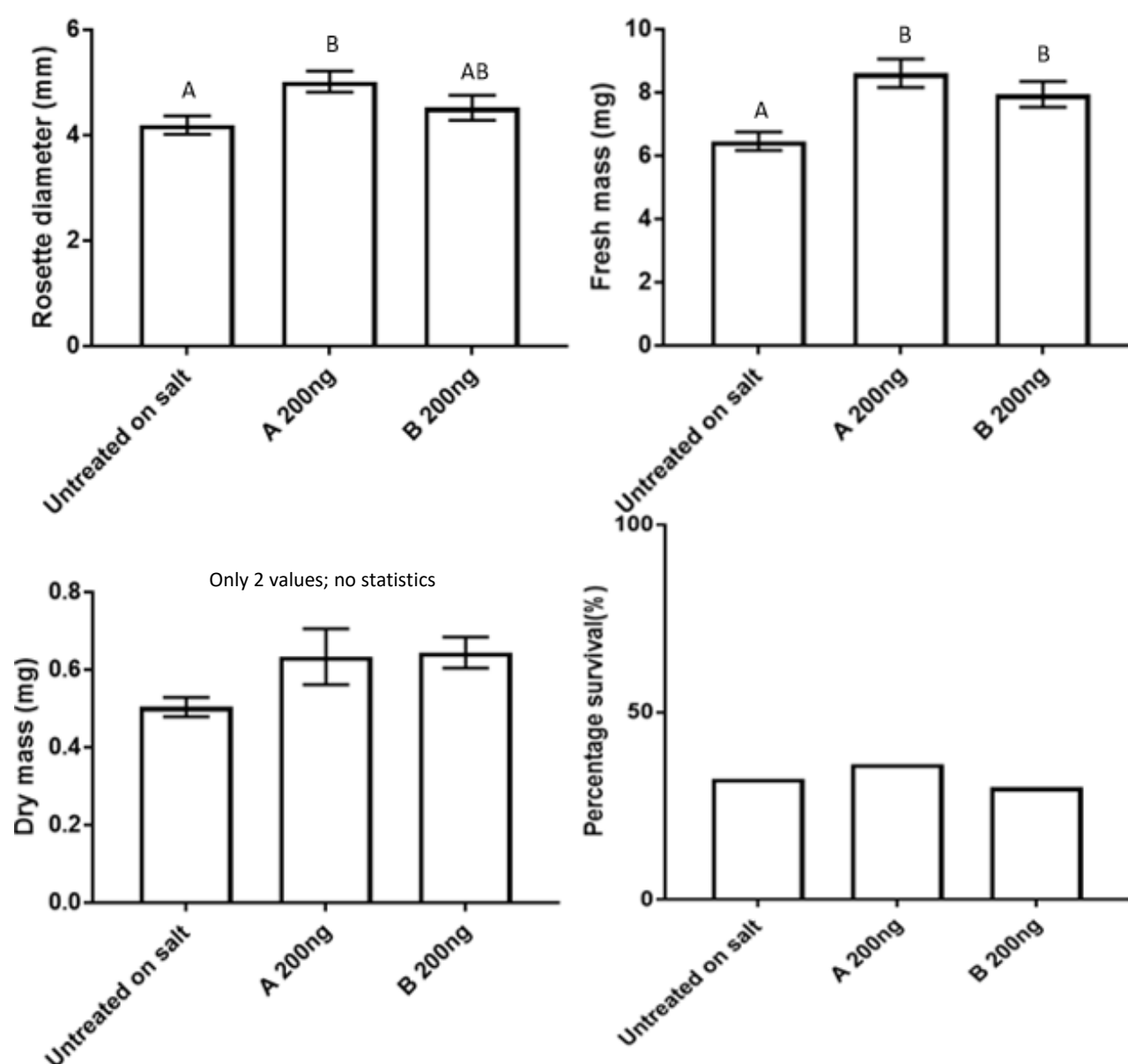


Figure 2.7: Analysis of volatile effects on seedling growth during salinity stress. The growth parameters of 13 d old *Arabidopsis thaliana* Col-0 seedlings exposed for 14 d to 100 mM NaCl and synthetic acetoin (indicated by A before concentration tested) or 2,3-butanediol (indicated by B before concentration tested) grown under a 14 h:10 h light:dark photoperiod *in vitro*, was measured. Values represent the mean \pm SE (n varied based on survival rate, n for untreated = 96). Different letters indicate significantly different values ($p \leq 0.05$) as determined by one-way ANOVA and Tukey's multiple comparisons test. All plants per treatment were combined to determine the average dry mass (mg) per plant for each repeat of experiment.

2.4 Discussion

2.4.1 Growth trials with exposure to synthetic volatiles

The growth trials suggested that the effects of acetoin on plant growth were more beneficial under long-day-length rather than short-day-length conditions, as fresh mass and dry mass were not significantly increased under a short photoperiod, but rather significantly decreased. In the short- and long-day-length trials conducted in this study, plants were used in the trials approximately 13 d after sowing (leaf 6 initiation) and the trials were concluded approximately around the time (20 d after germination) that rosette leaf area and leaf expansion is expected to cease in *Arabidopsis* plants under long-day-length conditions to allow for the transition to the flowering stage (Baerenfaller *et al.*, 2015). Thus, it can be reasoned that an initial faster growth in plants under a long-day-length photoperiod is responsible for the higher biomass, fresh and dry, observed for the 14 h:10 h day:night photoperiod compared to the 10 h:14 h day:night photoperiod (Baerenfaller *et al.*, 2015). Moreover, the observation that PGPV-treated plants had lower fresh and dry mass than untreated plants under the 10 h:14 h day:night photoperiod could be assumed to be attributed to the fact that these plants had to divert all resources into essential processes due to a decrease in starch availability at the end of the light period as most of the accumulated starch was consumed during the dark period, rather than pathways where PGPVs might exert their effects (Baerenfaller *et al.*, 2015). It is also possible that during different developmental stages of leaves, synthetic PGPVs could be interacting with different pathways such as hormone biosynthesis or hormone signalling pathways, resulting in diverse growth effects under different photoperiods (Dempers, 2015).

All three independent long-day-length repeat experiments (Figure 2.4) generated different fresh- and dry mass measurements for the untreated plants, even though they were grown under identical conditions (14 h:10 h day:night photoperiod; $22 \pm 2^\circ\text{C}$) and allowed the same germination time (13 d after 2 d stratification). The most plausible explanation for this observation is that seeds did not have the same germination rate and the seeds from the first repeat may have germinated earlier in the 13 d compared to the other two repeats, considering that the fresh and dry mass were significantly higher. This could consequently mean that plants were at different developmental stages during the exposure to the volatiles. Dry mass for repeats 2 and 3 did not significantly differ, however, a significantly smaller average fresh mass was recorded for plants in repeat 3 than in repeat 2. These differences could possibly be attributed to circadian rhythms, seed batch age, and slight differences in media composition, particularly the amount and age of the gelling agent used, all of which could have affected the time taken for the seed batches to germinate.

Previous studies on the effect of synthetic PGPVs on *Arabidopsis* all conducted their growth trials under different photoperiods (12 h:12 h day:night, 16 h:8 h day:night, 10 h:14 h day:night), duration periods (14 d, 10 d) and utilized seedlings of different ages (2 d or 14 d old; Table 2.1). Other studies

investigated the effects of PGPVs by dissolving 2,3-butanediol in dichloromethane or lanolin wax (Ryu *et al.*, 2003; Dempers, 2015). This study observed that at an equal 12 h:12 h day:night photoperiod, different concentrations of 2,3-butanediol (2 ng and 20 µg) treatments resulted in significantly larger leaf surface areas compared to the solvent and water controls after 14 d (Ryu *et al.*, 2003). A recent study by Sharifi *et al.* (2020) repeated the work of Ryu and his colleagues with acetoin instead of 2,3-butanediol. In that study, a significantly higher fresh mass was observed for the plants when exposed to different concentrations of acetoin, between 0.2 µg and 200 µg, compared to the untreated control plants, with the best performing treatment being 20 µg (Sharifi *et al.*, 2020). A similar study using older *Arabidopsis* seedlings (14 d) conducted 10 d trials at long (16 h:8 h day:night) and short photoperiods (10 h:14 h day:night) with both acetoin and 2,3-butanediol (Dempers, 2015). The synthetic acetoin had no significant effect at the short photoperiod, whereas the 2,3-butanediol treatments resulted in significantly lower biomass than the controls. Conversely, 2,3-butanediol treatments had no effect at the long photoperiod and the seedlings exposed to the 20 µg, 200 ng and 2 ng acetoin treatments were significantly larger than the control seedlings (Dempers, 2015).

In the current study, which had a similar design to that of Dempers (2015), both short-day-length (10 h:14 h day:night photoperiod) and long-day-length (14 h:10 h day:night photoperiod) trials were conducted to test the effects of the synthetic volatiles, acetoin and 2,3-butanediol (Figure 2.5). Regardless of the treatment, under a short-day-length photoperiod plant growth was not enhanced since the fresh mass, dry mass and leaf surface area of the plants did not increase significantly. In fact, several parameters were significantly decreased by some of the treatments. The comparison of the observed effect of volatiles and long-day-length on *Arabidopsis* for the four studies is nearly impossible since different variables (seedling age, photoperiods, volatile concentrations, and exposure time) were used. Future studies should investigate a larger range of concentrations (0.02 µg to 20 µg) and measure all growth traits (fresh mass, dry mass, rosette size and leaf surface area) at long-day-length. However, the results do suggest that acetoin is more effective at enhancing plant growth over a wider range of concentrations than 2,3-butanediol.

2.4.2 Salinity trials with exposure to synthetic volatiles

In the past, a number of studies have investigated the effect of salinity stress on plant growth and development. The vegetative rosette of *Arabidopsis* seedlings, experiencing salinity stress since germination, has been shown to be affected 21 d after sowing (Carrasco *et al.*, 2007). Furthermore, the dry mass of these plants was only slightly reduced compared to control plants, suggesting structural modifications including an increase in protein, chlorophyll content and leaf thickness as causes (Carrasco *et al.*, 2007). In peppermint plants experiencing salinity stress, root dry mass was up to 60% higher for salinity-stressed plants compared to control plants not exposed to salt, whereas

the fresh mass of the plants was lower under salinity stress conditions as fresh mass is mostly a reflection of water content (Cappellari and Banchio, 2020). The 13 d old *Arabidopsis* plants exposed to salinity stress for 14 d in this study, exhibited similar behaviour (Figure 2.6, Figure 2.7). Seven days from the onset of salinity exposure, the *Arabidopsis* plants in this study were approximately at the same growth stage as seeds exposed to salinity for 21 d by Carrasco (2007) and vegetative rosette diameter was significantly affected as leaves folded inwards. During the 14 d exposure, no significant difference was seen between the fresh mass of untreated controls with and without salt (data not shown). Although fresh mass was indistinguishable, untreated control plants on salt had a 25% higher dry mass than untreated plants without salt. This observation was unexpected, since stress is considered to reduce the growth rate. However, as seen in other species and *Arabidopsis* seedlings experiencing salinity stress, the time scale can have an influence on differences observed. Furthermore, the higher dry mass could be due to a similar increase in root mass seen for peppermint plants, since whole *Arabidopsis* plants were measured. Alternatively, the higher dry mass seen in untreated plants exposed to salt could be the result of structural modifications within the salinity-stressed *Arabidopsis* plants.

Exposure to acetoin and 2,3-butanediol resulted in higher fresh mass for *Arabidopsis* plants experiencing salinity stress compared to the salt control. In other research, the enhanced fresh mass was contributed to structural modification, stress response, and hormone regulation that are triggered by the volatile compounds (Cho *et al.*, 2008; Cappellari and Banchio, 2020). The cell wall of peppermint plants was loosened when exposed to salinity stress and acetoin, suggesting that plants had an improved ability to take up water and nutrients, consequently increasing dry mass to potentially make plants less susceptible to oxidative stress (Cappellari and Banchio, 2020). Similarly, a significant change in relative water content was only observed in *Arabidopsis* plants after 13 d of exposure to salinity stress and *Arabidopsis* plants exposed to acetoin and salinity had a lower reduction in relative water content after the same period of time (Cho *et al.*, 2008). These observations could suggest that similar structural modifications as seen for the peppermint plants could be responsible for the increased fresh mass seen for volatile treatments.

Although there were insufficient measurements for statistical analysis of the dry mass data, the average dry mass of the volatile-treated plants was much larger than the average dry mass measured for untreated plants. Thus, it is possible to speculate that the significant increase seen in fresh mass might also be true for dry mass. The increase in fresh mass is an indication of overall enhancement of water uptake and probably biomass accumulation as a result of the treatment with volatile compounds.

Table 2.1: Effect of synthetic volatiles at different photoperiods on growth traits of *Arabidopsis thaliana*.

Seedling age	Daylengths	Duration periods	Volatile	Amount of volatile	Significant effect on growth trait		Reference
2d old	12h:12h day:night	14	2,3-butanediol	20 µg, 0.2 µg (200 ng), 2 ng, 20 pg, 0.2 pg	Leaf surface area	↑ 2 ng, 20 pg	Ryu et al., 2003
2d old	12h:12h day:night	14	Acetoin	2 ng, 200 pg, 20 pg, 2 pg, 0.2 pg, 0.02 pg	Fresh mass	↑ 200 pg, 20 pg, 2 pg, 0.2 pg	Sharifi et al., 2020
14d old	16h:8h day:night	10	2,3-butanediol	20 µg, 200 ng, 2 ng, 20 pg	Leaf surface area	None significant	Dempers, 2015
			Acetoin			↑ 20 µg, 200 ng, 2 ng	
14d old	10h:14h day:night	10	2,3-butanediol	20 µg, 200 ng, 2 ng, 20 pg	Leaf surface area	↓ 20 µg, 20 pg	Dempers, 2015
			Acetoin			None significant	
12d old	14h:10h day:night	14	2,3-butanediol Acetoin	200 ng, 2 µg, 20 µg	Dry mass Fresh mass	See results as data for each repeat varies	This study
12d old	10h:14h day:night	14	2,3-butanediol	200 ng, 2 µg, 20 µg	Dry mass Fresh mass	↓ 200 ng, 2 µg, 20 µg ↓ 200 ng, 20 µg	This study
			Acetoin		Dry mass Fresh mass	↓ 200 ng, 2 µg, 20 µg ↓ 200 ng, 2 µg, 20 µg	

2.5 Conclusion

The growth trials suggested that the effects of acetoin on plant growth were more beneficial under long-day-length rather than short-day-length conditions, as fresh mass, dry mass, and leaf surface area were not significantly increased under a short photoperiod, but rather significantly decreased. However, it proved difficult to obtain consistent results for the effect of volatiles on plant growth under a long photoperiod. Acetoin either enhanced growth or resulted in similar growth to the untreated plants, while 2,3-butanediol treatment varied between improved and decreased growth in comparison to the untreated control plants. Despite the difficulties with different repeats of the experiment yielding different results, the overall trend was that the presence of acetoin was more beneficial than 2,3-butanediol. Furthermore, acetoin was effective at a wider range of concentrations compared to 2,3-butanediol. Similarly, in the salinity trials, the presence of acetoin appeared to induce salinity tolerance and treated plants showed higher measurements of rosette diameter and fresh mass compared to the salt control plants. It is suggested that the synthetic acetoin could promote plant growth and salinity tolerance *in vitro* and future studies should investigate this further. Future studies should include a wider range of acetoin concentration (0.02 µg – 20 µg) and broader photoperiod comparison (10 h:14 h day:night, 12 h:12 h day:night, 14 h:10 h day:night, 16 h:8 h day:night) in order to better understand the link between the photoperiod and the effect it could have on the ability of a volatile compound to enhance plant growth and IST. Additionally, future trials should use DAG (days after germination) rather than DAS (days after sowing) employed in this study and most studies in literature. Conducting trials with plants at the same DAG should generate more consistent results and exclude the issue of seeds germinating at different stages, possibly skewing results.

Chapter 3

Acetoin-production in *Escherichia coli*

3.1 Introduction

3.1.1 Volatile production by PGPR

Members of the *Bacillus* and *Pseudomonas* spp. are the predominant PGPR in the rhizosphere and possess plant growth promoting abilities. In some instances, these plant-growth-promoting abilities may be attributed to the production of volatile compounds that communicate with the plant in order to regulate biosynthesis of plant hormones (Beneduzi *et al.*, 2012; Shafi *et al.*, 2017; Fincheira and Quiroz, 2018). These volatile compounds also play a role in priming plants for biotic and abiotic stresses via cross-protection by taking advantage of natural cross-talk between stress-response pathways (Shafi *et al.*, 2017; Rosier *et al.*, 2018). Acetoin and 2,3-butanediol, emitted by *Bacillus amyloliquefaciens* GB03 and *Bacillus amyloliquefaciens* IN937a, can induce or suppress gene expression related to the biosynthesis or signalling responses of phytohormones to promote plant growth or elicit ISR (Table 1.2). In acetoin-producing bacteria, pyruvate is converted to α -acetolactate by acetolactate synthase and further converted to acetoin by means of α -acetolactate decarboxylase (ALDC; EC 4.1.1.5) via the catabolic pathway. Alternatively, α -acetolactate can be converted to leucine and valine via the anabolic pathway (Figure 1.5; Xu *et al.*, 2011). Acetoin is further converted to 2,3-butanediol by acetoin reductase/2,3-butanediol dehydrogenase (BDH1; EC 1.1.1.4; Xu *et al.*, 2011).

3.1.2 Deficiencies in bacterial and synthetic volatile studies

All past research studying the effect of volatiles, including 2,3-butanediol and acetoin, on plant growth has either utilised the pure compound or a bacterial strain releasing a complex blend of volatile compounds (Bailly and Weisskopf, 2012). The importance of continual or constant exposure to volatile emissions, whether from bacteria or synthetic sources, was highlighted by the observation that during exposure to the volatiles, photosynthetic capabilities and iron levels of plants were elevated, but after withdrawal of the volatiles these returned to levels equal to those of WT plants (Xie *et al.*, 2009). Similarly, effects on differential transcriptional expression of genes relating to iron regulation and cell wall functions were only observed during exposure to these PGPRs (Xie *et al.*, 2009). Exposure to the synthetic volatile compounds is not continuous, but rather takes the form of a fixed amount of volatile that spikes at the start of a trial, gradually decreases over time and which is available at low concentrations, if at all, by the end of the trial, which could influence the plant's overall growth and stress response.

Studying the effect of a single, purified volatile will enable an accurate assessment of the growth promotion ability of that specific volatile, rather than a blend of several different compounds potentially affecting the phenotype. In this study, an *Escherichia coli* bacterial strain was engineered, known to not promote plant growth, to produce the PGPV acetoin, which could allow us to study the effect of a single volatile that is continuously produced by the transgenic bacteria on plant growth.

3.1.3 *Escherichia coli* BL21

In previous research studying the effect of volatiles, *Bacillus* strains were investigated which produced other volatile compounds in addition to acetoin that could possibly contribute to the enhanced plant growth observed. In these studies, *Arabidopsis* plants were exposed to *Escherichia coli* strains as control cultures as *E. coli* are considered not to produce plant growth promoting volatiles, and plants treated with these *E. coli* strains were indistinguishable from untreated plants in terms of their growth in these experiments (Ryu *et al.* 2003; Ryu *et al.*, 2004; Farag *et al.*, 2013; Chung *et al.*, 2016; Tahir *et al.*, 2017a; Tahir *et al.*, 2017b). In addition to not promoting plant growth, *E. coli*, in particular *E. coli* BL21 derivatives with IPTG-inducible T7 polymerase, is a well-established heterologous system for the production of recombinant proteins (Joseph *et al.*, 2015). The T7 RNA polymerase allows high-level expression from the T7 bacteriophage promotor once induced with IPTG and is less likely to terminate transcription prematurely in comparison with other polymerases (Joseph *et al.*, 2015). *Escherichia coli* BL21 strains also lack the Lon and OmpT proteases that are responsible for the degradation of foreign proteins, thus allowing for increased stability of the heterologous protein (Joseph *et al.*, 2015). The *E. coli* BL21-CodonPlus(DE3)-RIPL strain is engineered to contain extra copies of genes responsible for encoding tRNAs that frequently limit the translation of heterologous proteins, especially from eukaryotic sources (Joseph *et al.*, 2015). The tRNAs include argU, ileY, leuW, and proL, recognizing arginine (AGA, AGG), isoleucine (AUA), leucine (CUA), and proline (CCC) codons, respectively (Joseph *et al.*, 2015). Furthermore, this strain can rescue heterologous protein expression from either AT- or CG-rich genomes (Joseph *et al.*, 2015).

3.1.4 Aim of chapter

This chapter was focussed on the generation of a transformed *E. coli* BL21-CodonPlus(DE3)-RIPL strain that produces acetoin, in order to study the effects of continuous exposure of acetoin on *Arabidopsis thaliana*. This was achieved by generating a recombinant pRSETA vector containing the α -acetolactate decarboxylase gene from *Aspergillus niger*, which was then transformed into the *E. coli* BL21-CodonPlus(DE3)-RIPL strain. It was hypothesized that WT *Arabidopsis thaliana* Col-0 plants exposed to the transformed bacteria would exhibit growth enhancement and increased salinity tolerance compared to untreated plants due to the acetoin continuously being produced by the bacteria.

3.2 Materials and methods

3.2.1 DNA and RNA isolations

The Wizard Plus SV Minipreps DNA Purification System (Promega) was utilized to isolate plasmid DNA from liquid cultures grown from bacteria colonies. The Wizard SV Gel and PCR Clean-up System (Promega) was employed to purify DNA fragments, including linearized plasmids, digested fragments, and amplified DNA. All kits were used according to the manufacturers' instructions. RNA was extracted from bacterial samples using the Maxwell 16 LEV Plant RNA Kit (Promega) according to the manufacturer's protocol, starting from step 4 ("Adding homogenizing solution"), utilising the Maxwell 16 RNA robot (Promega). All DNA and RNA concentrations and purity were assessed using a Nanodrop Lite spectrophotometer (Thermo Fisher 439262) and the integrity was further analysed on a 1% (m/v) TBE agarose gel with added ethidium bromide (0.05 µl/mL) to allow visualization under UV light. The fragments were separated at 120 V.

3.2.2 Polymerase chain reaction (PCR)

Unless otherwise specified, the polymerase chain reaction (PCR) was conducted with GoTaq DNA Polymerase (Promega) using the conditions shown in Table 3.1. The extension time was adjusted depending on amplicon size, and annealing temperatures were modified depending on the T_m of the primer pairs applied in the specific reaction.

Table 3.1: Standard PCR cycling protocol for GoTaq DNA Polymerase

PCR cycle	Cycling conditions		No. of cycles
	Temperature	Time (min)	
Initial denature	95°C	02:00	1
Denature	95°C	00:30	25
Annealing (T_m)	58 – 60°C	00:30	
Extension	72°C	1 kb/min	
Final Elongation	72°C	05:00	1
Hold	12°C	-	

All primers used in this study were designed by using SnapGene Viewer software (GSL Biotech LLC) and synthesised by Inqaba Biotechnical Industries (Pty) Ltd (Table 3.2). The following primers in the table below were designed by Rosmarin (2020) for different sized amplicons within the *ALDC* and *BDH1* genes: AF2, AR1, BF1 and BR1.

Table 3.2: Primer pairs and sequences used in this study

Primer name	Sequence (5'-3')	Product size	T _m	Purpose
F_BamHI	<u>GGATCC</u> ATGACCACCGCT	1167 bp	58°C	Amplify <i>ALDC</i> for Gateway Cloning
A_BamHI	<u>GGATCCT</u> TAGTGAGAAGTGGGG A			
AF2	GTCGAAGACGCGGATATAATT	275 bp	58°C	Confirming <i>ALDC</i> insert
AR1	AGCGTGCCCTGTATATGTCT			
AF3	CAGTGTGGTACCTAAAAAGCC	607 bp	60°C	Expression levels of <i>ALDC</i> gene (RT-sqPCR)
AR1	CA AGCGTGCCCTGTATATGTCT			
AF3	CAGTGTGGTACCTAAAAAGCC	120 bp	58°C	Expression levels of <i>ALDC</i> gene (RT-PCR)
AR3	CA CGGAGGCGGTGAATTGAGG			
BF1	GAATGTATCTGCAACTGGGAA	1036 bp	58°C	Confirming <i>BDH1</i> insert
BR1	GTCTTCGACAACATAGCCGA			
EF-1α F	GTCAAGCAGATGATCTGCTGTT	607 bp	58°C	Plant reference gene
EF-1α R	G GGGCGTAACCGTTACCAATCTG			
U968	ACGCGAAGAACCTTAC	450 bp	60°C	Bacterial reference gene (16S rDNA)
L1401	GCGTGTGTACAAGACCC			
pRSET_ALDC F	<u>GGGATCC</u> ATGGAGACATGGG (<i>Bam</i> HI) <u>CGAATTCT</u> TAGTGAGAAGTGGG	974 bp	60°C	Amplification of <i>ALDC</i> with restriction sites for pRSETA
pRSET_ALDC R	GAC (<i>Eco</i> RI)			

3.2.3 Restriction enzymes

All enzymes and buffers utilized for digestion of plasmids or amplified DNA were obtained from New England Biolabs (NEB). The digestions were carried out according to protocols for specific enzymes obtained from NEB website (<https://nebcloner.neb.com/#!/redigest>). Unless otherwise specified, all digestions were performed using the CutSmart buffer and incubating at 37°C for 1 h.

3.2.4 Competent cells of *Escherichia coli*

All *Escherichia coli* (*E. coli*) strains were made competent and transformed according to a protocol by Chang *et al.* (2017). The calcium chloride (CaCl₂) solutions were applied to render the cells chemically competent. The CaCl₂ buffers included a 0.1 M CaCl₂ solution, filter sterilized and a

solution of 0.1 M CaCl_2 with 15% sterile glycerol added. Buffers were prepared the day before and kept at 4°C until use.

3.2.5 Bacterial growth

Liquid and solid lysogeny broth (LB) medium was used to culture the different bacteria utilised in this study. Liquid LB medium consisted of 10 g/L tryptone, 5 g/L yeast extract and 10 g/L sodium chloride (NaCl), with the addition of 15 g/L bacterial agar for semi-solid media, added before autoclaving (121°C, 1.2 kPa, 20 min). If required for specific strain or selection of cells, antibiotics were added when the autoclaved medium had cooled to around 60°C. All bacterial cultures in this chapter were grown at 37°C, except for transgene inductions (Section 3.2.8).

3.2.6 Construction of a protein expression vector

The *ALDC* gene (EC 4.1.1.5), originally isolated from *Aspergillus niger*, was amplified from the already available pUBI510::ALDC vector (Rosmarin, 2020) template using primers pRSET_ALDC F and pRSET_ALDC R (Figure 3.2) at a PCR annealing temperature of 60°C and extension time of 1 min. The PCR product was purified, and both the purified *ALDC* fragment and pRSETA vector were digested with *Bam*HI-HF and *Eco*RI-HF to allow for directional cloning. The *ALDC* gene was then ligated into the pRSETA vector using T4 DNA Ligase (New England Biolabs) and transformed into *E. coli* Top10 competent cells using a standard heat shock protocol (Chang *et al.*, 2017). The transformed cells were grown overnight on LB medium with ampicillin (100 µg/mL) and positive colonies were identified through colony PCR (Table 3.1) using the AF2/AR1 primer pair (Table 3.2). Liquid cultures with ampicillin (100 µg/mL) were grown overnight from transformed colonies and plasmid DNA was isolated. The integrity of the transgene was confirmed with PCR analysis using a combination of vector and transgene specific primers. Additionally, the plasmid DNA was sent to the Central Analytical Facilities (CAF), Stellenbosch University for DNA sequencing. After confirmation that the *ALDC* gene was in frame with the six histidine α -amino acids that form part of the Xpress™ tag in the pRSETA vector, plasmid DNA was transformed into *E. coli* BL21-CodonPlus(DE3)-RIPL competent cells. The same transformation was performed with the empty pRSETA vector to serve as a control for the protein induction.

3.2.7 Semi-quantitative analysis of *ALDC* expression in transformed bacteria

The *E. coli* BL21-CodonPlus(DE3)-RIPL bacteria, with or without the pRSETA::ALDC recombinant vector or the empty pRSETA vector, were cultured overnight at 37°C. Starter cultures were prepared and allowed to grow until an OD_{600} of 0.8 was reached. Thereafter, 5 mL of culture was centrifuged (6 000 $\times g$) for 2 min at 4°C. The pellet was resuspended in 400 µL TE (Tris-EDTA, pH 8) buffer and 400 µg of lysozyme, and samples were incubated on a shaker at 4°C for 15 min. RNA was extracted from samples using the Maxwell 16 LEV Plant RNA Kit (Promega) according to the manufacturer's

protocol, starting from step 4 (“Adding homogenizing solution”), using the Maxwell 16 RNA robot (Promega). Thereafter, cDNA was synthesized via the RevertAid H Minus First Strand cDNA Synthesis Kit (Thermo Scientific) using the random primer from the kit, according to the manufacturer’s instructions. Transcription of the gene was confirmed via Reverse Transcriptase semi-quantitative PCR (RT-sqPCR, Table 3.3). The U968/L1401 primer set was used to amplify a section of the bacterial 16S rDNA reference gene, and the AF3/AR1 primer set to test the expression of the *ALDC* transgene (Table 3.2).

Table 3.3: RT-sqPCR conditions

PCR cycle	Cycling conditions		No. of cycles
	Temperature	Time (min)	
Initial denature	95°C	03:00	1
Denature	95°C	00:30	26
Annealing (T_m)	60°C	00:30	
Extension	72°C	00:30	
Final Elongation	72°C	02:00	1
Hold	12°C	-	

3.2.8 Analysis of *ALDC* protein expression

A colony of *E. coli* BL21-CodonPlus(DE3)-RIPL transformed with the pRSETA::*ALDC* vector was grown overnight in 2 mL liquid LB medium with ampicillin (100 µg/mL) and chloramphenicol (25 µg/mL). The following day, 50 mL of liquid LB with ampicillin and chloramphenicol was inoculated with the overnight culture and grown at 37°C to reach an OD₆₀₀ of 0.5, where after 50 mL was divided into two 25 mL cultures. Isopropyl-β-D-thiogalactoside (IPTG, 0.5 mM) was added to one of the 25 mL cultures, whilst the other culture served as a non-induced control. The above-mentioned procedure was repeated for different induction conditions, including duration (4 h, 8 h and overnight) and temperature (room temperature, 28°C and 37°C). The same process was repeated for the empty pRSETA vector. Finally, 2 mL of each culture was centrifuged (15 900 xg) for 5 min and the supernatant removed. The pellets were resuspended in 2X SDS-PAGE sample buffer (0.5 M Tris [pH6.8]; 2% [m/v] SDS; 25% [v/v] glycerol; 5% [v/v] β-mercaptoethanol; 0.01% [v/v] bromophenol blue) and boiled for 5 min at 95°C.

A Bradford protein assay was conducted to determine the concentration of protein present in samples (Bradford, 1976). A linear range from 0.0625 – 1 mg/mL for bovine serum albumin (BSA)

was set up in 1 mL cuvettes and the absorbance measured at 595 nm. The standard curve was then utilized to determine protein concentrations (See Addendum 2 Figure 5.4).

Sodium dodecyl sulfate-polyacrylamide gel electrophoresis (SDS-PAGE) was conducted using a Bio-Rad gel apparatus (Mini-PROTEAN® Tetra Vertical Electrophoresis Cell for Mini Precast Gels, 4-gel #1658004), according to the Bio-Rad Guide to Polyacrylamide Gel Electrophoresis and Detection manual (http://www.bio-rad.com/webroot/web/pdf/lisr/literature/Bulletin_6040.pdf). The 12% (m/v) SDS-PAGE polyacrylamide resolving gel (5 mL H₂O, 6 mL 30% [v/v] acrylamide/*bis*-acrylamide, 3.8 mL 1.5 M Tris [pH 8.8], 150 µL 20% [m/v] SDS, 150 µL 10% [m/v] ammonium persulfate, 6 µL TEMED) was prepared according to the protocol in the manual. Once the gel had polymerized, the 5% stacking gel (2.1 mL H₂O, 0.5 mL 30% [v/v] acrylamide/*bis*-acrylamide, 0.38 mL 1 M Tris [pH 6.8], 30 µL 20% [m/v] SDS, 30 µL 10% [m/v] ammonium persulfate, 3 µL TEMED) was added. After setting up the apparatus, samples were boiled in sample buffer for 5 min at 95°C, equal amounts of protein (20 µg) loaded in each lane and the gel was allowed to run for approximately 1 h at 140 V until the marker dye front had reached the end of resolving gel. The gel was removed from apparatus and stained under gentle agitation with the staining solution (2.5 g Coomassie Brilliant Blue R-250, 45% [v/v] methanol, 10% [v/v] acetic acid, 40% [v/v] ddH₂O). Subsequently the gels were de-stained in a de-staining solution (45% [v/v] methanol, 10% [v/v] acetic acid, 40% [v/v] ddH₂O). De-staining was allowed until individual bands were clearly visible, whereafter the gel was rinsed in ddH₂O water.

3.2.9 Protein immunoblots

For immunoblotting, an SDS-PAGE gel was run as described in Section 3.2.8. Filter paper and a nitrocellulose blotting membrane (PVDF, 0.45 µm, GE Healthcare) were cut to the size of the gel. The filter paper was immersed in blotting buffer (13.1 g/L Tris, 94 g/L glycine, 50 mL ddH₂O water) with 20% (v/v) methanol and the membrane in 100% methanol. Proteins were transferred from the gel to the membrane using the Bio-Rad Trans-Blot SD Semi-Dry Electrophoretic Transfer Cell apparatus at 30 V for 1 h, where after the membrane was blocked overnight at 4°C in 2% (m/v) BSA. The membrane was washed once for 5 min in PBS (8 g/L NaCl, 0.2 g/L KCl, 1.44 g/L Na₂HPO₄, 0.24 g/L KH₂PO₄) and 0.1% Tween20. A 6x-His Tag monoclonal antibody (HIS.H8, DyLight 550, mouse/IgG2b host, Invitrogen) diluted in PBS (1:1 000) was added to the membrane and incubated for 2 h, where after excess antibody was removed by three washes in the PBS solution. A secondary anti-mouse antibody (1:7 500) was added to the membrane and allowed to incubate for 2 h, followed by washing the membrane three times. Finally, a substrate tablet (BCIP®/NBT Alkaline Phosphatase Substrate, B5655, Sigma-Aldrich) to detect alkaline phosphatase was dissolved in 10 mL of water and added to the membrane until bands appeared, whereafter the membrane was allowed to dry.

3.2.10 Detection of acetoin production

The Voges-Proskauer test was employed to detect acetoin produced by *E. coli* BL21-CodonPlus(DE3)-RIPL bacteria transformed with the pRSETA::ALDC vector based on colour changes (Barry and Feeney, 1967). Prior to use, 5 mL of MR-VP broth (3.5 g/L casein, 3.5 g/L soy peptone, 5 g/L D-(+)-glucose, 5 g/L KH₂PO₄, pH 6.9) was aliquoted into test tubes (12 mL, Z666114, Greiner) or 200 µL of broth into microfuge tubes (1.5 mL, Cat.-No.:616201, Greiner Bio-one). The different tubes were used to account for the possible effect of different amounts of oxygen exposure in the different size tubes that could influence the results. Each tube was inoculated with a colony of the appropriate overnight culture and incubated at 37°C for either 4 h or overnight. As a positive control for acetoin presence, 200 µL of undiluted acetoin (92%, Aldrich) was used instead of culture. Thereafter, 600 µL of 5% (m/v) α-naphthol reagent (Sigma-Aldrich) and 200 µL of 40% (m/v) potassium hydroxide (Merck) was added to each tube and the tube contents gently mixed after each addition. The tubes were incubated at room temperature for 15 min before the colour change was interpreted. A pink or red colour at the surface was indicative of acetoin presence, whereas a yellow or copper surface colour indicated the absence of acetoin.

3.2.11 Growth trials with bacterial exposure

A growth trial was set-up as described in Section 2.2.2, except that the synthetic volatiles compounds in the small petri dish (10 mm, REF 353001, FALCON) were replaced by different *E. coli* strains, including *E. coli* DH5α, *E. coli* BL21-CodonPlus(DE3)-RIPL, *E. coli* BL21-CodonPlus(DE3)-RIPL with the empty pRSETA vector, and transformed *E. coli* BL21-CodonPlus(DE3)-RIPL expressing the ALDC gene from the pRSETA::ALDC vector (Figure 3.1). For this, a small petri dish containing LB media was inoculated with 25 µL of bacterial culture and allowed to grow overnight, as per Section 3.2.5. The following day, eight seedlings were evenly spaced in a tissue culture container containing ½ MS medium (as described in Section 2.2.1) around the small bacterial culture plate. Each treatment was replicated 3 times within same trial repeat, with 8 seedlings in each replicate. The trial was conducted for a period of 14 d under long-day-length (14 h:10 h day:night) conditions as per Section 2.2.1. At the conclusion of the trial, fresh mass, dry mass, and rosette diameter of each plant were measured. The trial was repeated, whereafter measurements from the two repeats were pooled together for statistical analysis.

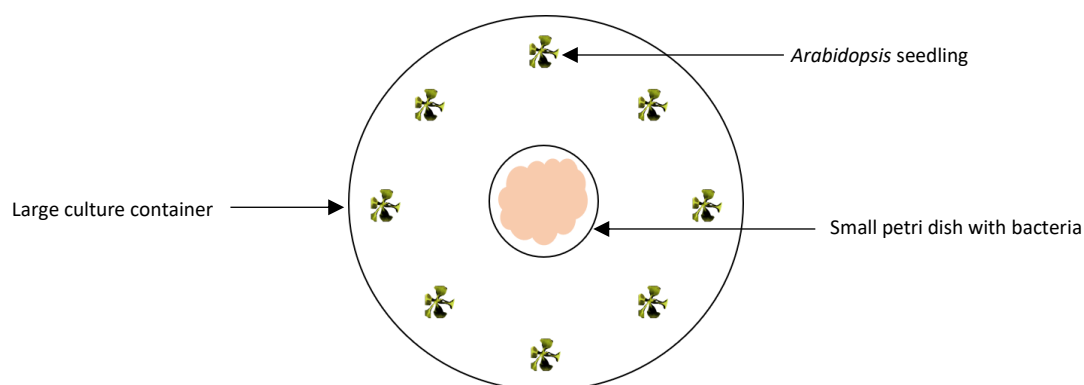


Figure 3.1: Setup of cultures for *in vitro* trial to expose plants to transgenic bacteria. A small petri dish containing bacteria was placed in the middle of a large culture container containing $\frac{1}{2}$ MS media onto which 8 *Arabidopsis* plants were evenly spaced. The small petri dish contains semi-solid LB-media with overnight culture of *E. coli* BL21-CodonPlus(DE3)-RIPL bacteria with pRSETA vector (with and without *ALDC* gene). The untreated plates lacked the small petri dish in the centre.

3.2.12 Salinity trials with bacterial exposure

The salinity trials were set-up similarly to growth trials, with the exception that 100 mM sodium chloride (NaCl, 99.5%, Sigma-Aldrich) was added to the $\frac{1}{2}$ MS medium and phyto-agar in the larger tissue culture container. At the conclusion of the trial, rosette diameter, fresh mass, and dry mass of each plant were measured. The trial was repeated, whereafter measurements for each treatment from the two repeats were pooled together for statistical analysis.

3.2.13 GC-MS analysis of acetoin production in transgenic bacteria

Escherichia coli BL21-CodonPlus(DE3)-RIPL strains were cultured in solid phase micro-extraction (SPME) headspace vials (SU86009, 20 mL, Merck) containing 2 mL LB medium at 37°C overnight, whereafter they were kept at 22°C for 5 d before gas chromatography-mass spectrometry (GC-MS) analysis. Head-space solid phase micro-extraction (HS-SPME) analysis was executed by the Central Analytic Facilities (Mass spectrometry unit, CAF).

Volatile compounds were trapped and extracted from the headspace vials using the HS-SPME method. An SPME vial was equilibrated for 10 min at 50°C in the Triplus RSH auto-sampler incubator (SPME, Thermo Fisher Scientific) agitated at 250 rpm. Subsequently, the polyethylene glycerol (PEG, 60 μ m, metal alloy, purple, Supelco) coated fibre was exposed to the sample headspace for 20 min at 50°C. After extraction, desorption of the volatile compounds from the fibre coating was carried out in the injection port of the GC–MS for 2 min.

Separation and quantification of the acetoin was performed on a Thermo Scientific TRACE™ 1310 gas chromatograph coupled with a TSQ 8000 mass spectrometer detector (Thermo Fisher

Scientific). The GC–MS system was equipped with a polar ZB-wax column (Model number: 7GH-G007-11, Supelco) capillary column with nominal length of 30 m; 250 µm internal diameter; and 0.25 µm film thickness. Analyses were carried out using helium as carrier gas at a flow of 1 mL/min. The injector temperature was maintained at 220°C. The oven program was as follows: 35°C held for 8 min; and then ramped to up to 240° at 10°C min⁻¹ and held for 3 min. The MSD was operated in full scan mode and the ion source and quadrupole temperatures were maintained at 230°C and 150°C respectively. The transfer line temperature was maintained at 250°C. Compounds were tentatively identified by comparison of retention times (T_R) and, by comparison with the NIST11 mass spectral library (Addendum 2 Figure 5.5; <https://www.nist.gov/system/files/documents/srd/NIST1a11Ver2-0Man.pdf>).

3.2.14 Statistical analysis

The following assumptions of the ANOVA model were satisfied to allow interpretation of data: treatment levels in the experiment have approximately equal variances, residuals are normally distributed, and observations are independent. A one-way ANOVA and appropriate *post hoc* test for significant difference ($p \leq 0.05$) from the untreated or other treatments were applied for statistical analysis. All trials were independently repeated, and data was pooled together for statistical analysis, unless stated otherwise. For accurate dry mass measurement, three plants were measured together, unless stated otherwise. Tukey's multiple comparisons test was applied to compare treatments to all other treatments.

3.3 Results

3.3.1 Construction of a protein expression vector

The *ALDC* gene was successfully cloned into the pRSETA vector shown by the 974 bp and 275 bp products, respectively (Figure 3.2). Sequencing confirmed the in-frame cloning of the gene with the six histidine codons that form part of Xpress™ tag to allow for purification of the expressed protein. The nucleotide sequence and alignment of the transgene with the tag and vector construct are shown in Addendum 1 (Figure 5.1; Figure 5.2). The pRSETA::ALDC vector was then transformed into *E. coli* BL21-CodonPlus (DE3)-RIPL bacteria as the expression host and successful transformation was shown by PCR product of 275 bp (Figure 3.3). RNA was successfully extracted from bacteria and converted to cDNA for RT-sqPCR analysis. The 16S rDNA gene was employed as a reference for expression and was expressed at a consistent level in the wild-type (WT) and the transformed *E. coli* BL21 strains. The transgene was only expressed in the *E. coli* BL21 strain transformed with the transgene (hereafter referred to as AA) but no expression was detected in the WT or the *E. coli* BL21 strain transformed with the empty vector (EV; Figure 3.4). A product of 450 bp was expected for the reference gene and 605 bp product for the transgene specific primer set.

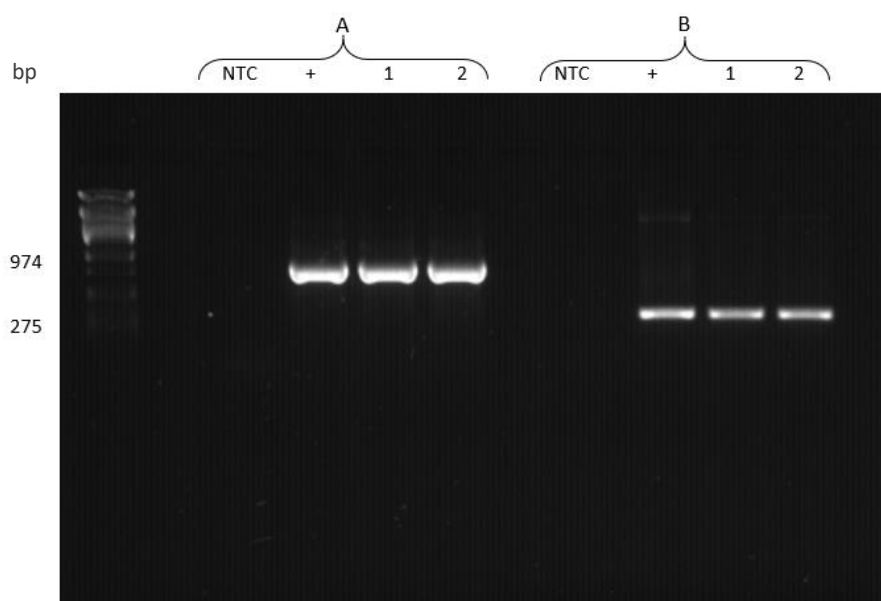


Figure 3.2: PCR analysis confirming the cloning of the *ALDC* gene into the pRSETA vector using gene-specific primers.

The recombinant vector was additionally sequenced and the integrity of the transgene in relation to the 6xHis-tag confirmed. The following primer sets were used **A)** pRSET_ALDC F/pRSET_ALDC R and **B)** AF2 /AR1. Indicated are base pairs (bp); the pUbi510:ALDC plasmid as positive control (+); and a negative non-template control (NTC); and lanes 1 and 2 individual clones.

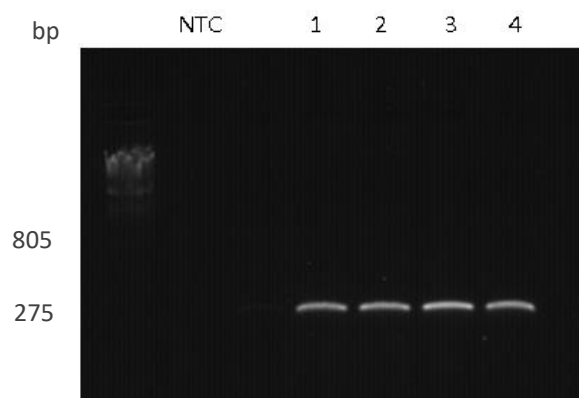


Figure 3.3: Colony PCR to confirm transformation of the recombinant pRSETA:ALDC vector into *E. coli* BL21-CodonPlus (DE3)-RIPL using gene-specific primer set. Four of the colonies obtained were confirmed for incorporation of the transgene by colony PCR using transgene specific primers (AF2/AR1). All the colonies yielded positive results for the transformation. Indicated are base pairs (bp); a negative non-template control (NTC); and lane 1, 2, 3, and 4 individual colonies.



Figure 3.4: Semi quantitative PCR analysis confirming the expression of ALDC in *E. coli* BL21-CodonPlus(DE3)-RIPL. PCR analysis was performed with the primer pairs specific for the **A**) 16S rDNA reference gene (U968/L1401) and **B**) a transgene specific (AF2/AR1). Indicated are base pairs (bp); the non-template control (NTC); wild-type strain without modifications (WT); bacteria transformed with empty pRSETA vector (EV) and bacteria transformed with pRSETA::ALDC vector (AA).

3.3.2 Analysis of ALDC protein expression

Transformed *E. coli* BL21 carrying the pRSETA:ALDC vector was analysed with SDS-PAGE after induction with IPTG. Gel electrophoresis revealed no evident recombinant protein at the expected protein size of 39 kDa. Different induction conditions including a temperature range from between RT (room temperature) to 37°C, and induction times of 4 h, 8 h or 16 h (not all data shown) were used, but no differential protein band could be detected for any of the conditions (Figure 3.5). In a further attempt to identify the ALDC protein, protein expression was analysed through immunoblotting using a 6x-His Tag monoclonal antibody which should target the His-tag coupled with the ALDC protein. However, no discernible band was visible at 39 kDa for any of the protein samples on the immunoblots (Figure 3.6).

The presence of acetoin was detected using the Voges-Proskauer test (Figure 3.7). A pinkish colour, indicating the presence of acetoin, was detected in the pRSETA:ALDC transformed bacteria, while the positive control developed a strong red colour. The negative empty vector control remained yellow, indicating the absence of acetoin.

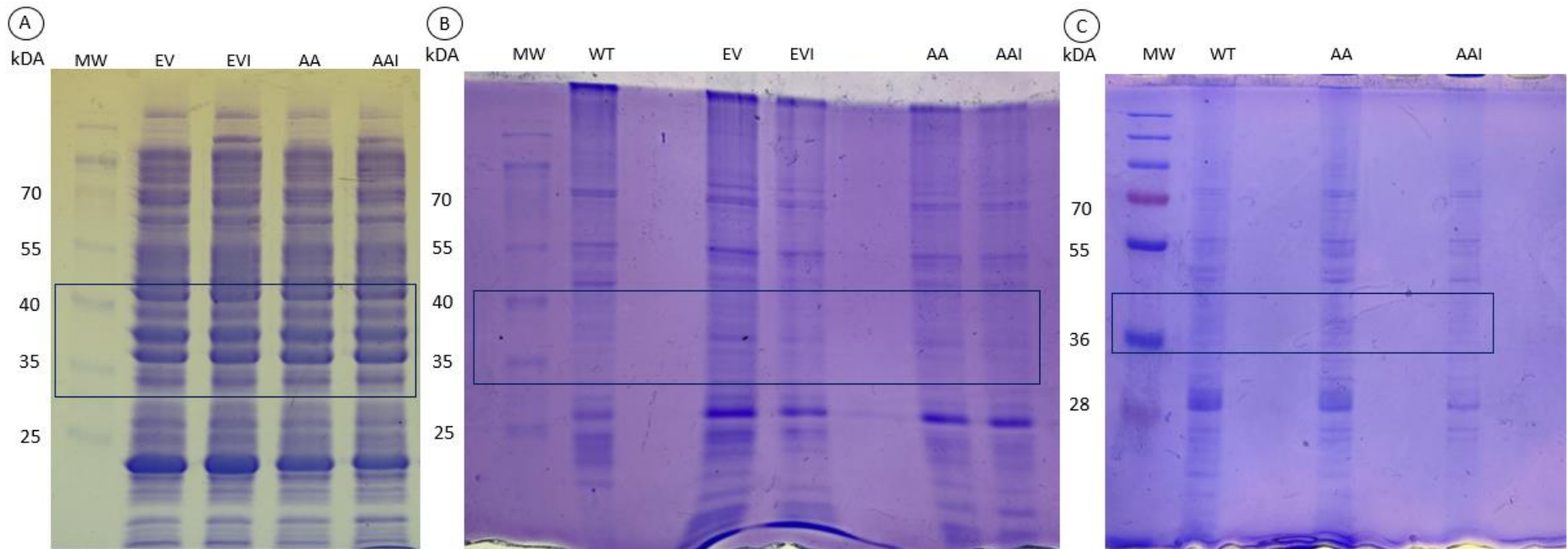


Figure 3.5: SDS-PAGE gel analysis of induction ALDC-encoded protein (39 kDa) expressed by transgenic *E. coli* BL21-CodonPlus(DE3)-RIPL. Different conditions were tested for protein expression namely, **A)** induction at 37°C; or **B)** at 20°C; or **C)** at 20°C with 5% sugar added to growth medium. Boxes represent the area in which protein would be expected. Also indicated are the molecular weight marker (MW); the wild-type BL21 bacteria (WT); empty pRSETA vector (EV); empty pRSETA vector induced (EVI); pRSETA::ALDC (AA); and pRSETA::ALDC vector induced (AAI).

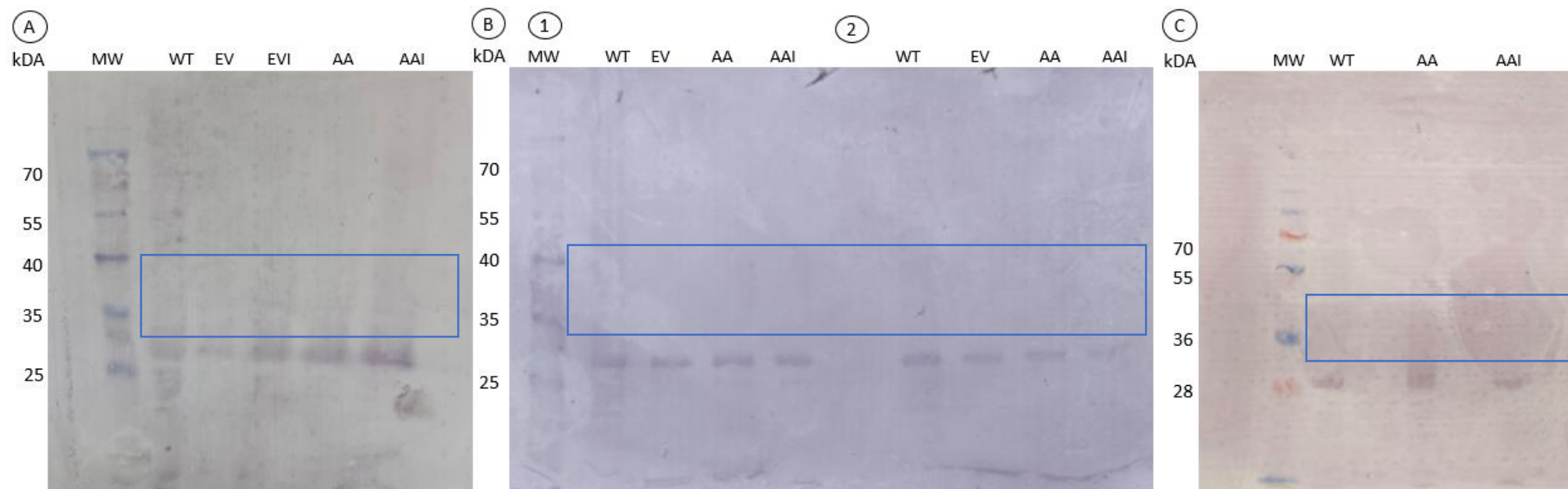


Figure 3.6: Western blot to analyse ALDC protein expression in transgenic *E. coli* BL21-CodonPlus(DE3)-RIPL using a His-tag antibody. Western blot was performed on *E. coli* BL21-CodonPlus(DE3)-RIPL pRSETA::ALDC induced with IPTG to identify the ALDC-encoded protein (39 kDa) linked to a His-tag. 6x-His tag monoclonal (HIS.H8), DyLight 550 Mouse/IgG2b host was used with anti-mouse as secondary antibody. Different conditions were tested: **A)** Induction at 37°C, **B1)** Induction at 20°C, **B2)** Induction of different strain at 20°C (Rosette Origami (DE3) 2), **C)** Induction at 20°C with 5% sugar added to medium. Boxes represent area where protein would be expected. Also indicated are the molecular weight marker (MW); the wild-type BL21 bacteria (WT); empty pRSETA vector (EV); empty pRSETA vector induced (EVI); pRSETA::ALDC (AA); and pRSETA::ALDC vector induced (AAI).

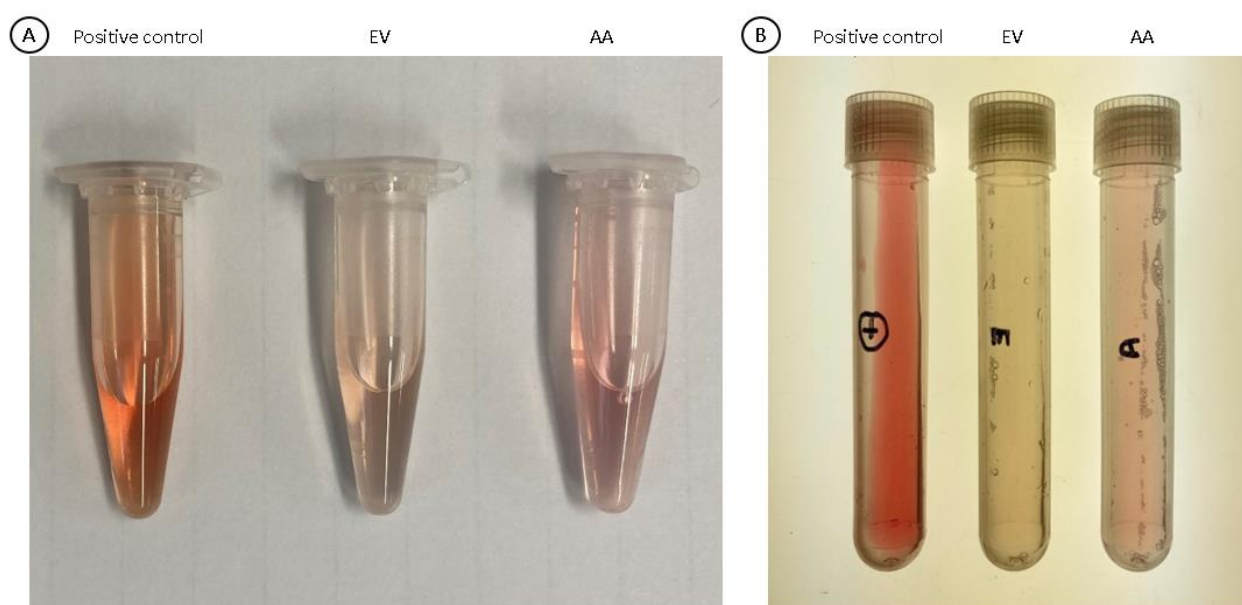


Figure 3.7: Voges-Proskauer test to detect acetoin in transgenic *E. coli* BL21-CodonPlus(DE3)-RIPL transformed with the pRSETA:ALDC recombinant vector. The Voges-Proskauer test was performed on cultures grown for **A)** 4 h or **B)** overnight in MR-VP media. Synthetic pure acetoin was used as a positive control and developed a red-pinkish colour. As a negative control the BL21-CodonPlus(DE3)-RIPL transformed with an empty pRSETA vector (EV) appear yellowish. The *E. coli* BL21 strain transformed with the transgene exhibited a pale pink colour (AA) indicating low levels of acetoin.

3.3.3 GC-MS analysis of acetoin production in transgenic bacteria

Both AA and EV strains underwent GC-MS headspace analysis with SPME after 6 d of allowing bacteria to grow and produce volatiles in the SPME headspace vials. Acetoin was detected at between 14,50 and 14,85 min retention time within the used system. Compounds were tentatively identified by comparison of retention times (T_R) and, by comparison with NIST11 mass spectral library. The y-axis in the chromatogram represents the relative abundance or intensity based on the number of counts for analyte taken at a certain time point by the MS detector. Acetoin was detected in the AA sample at 14.66 min with 50% relative abundance, while no acetoin was detected in EV (Figure 3.8).

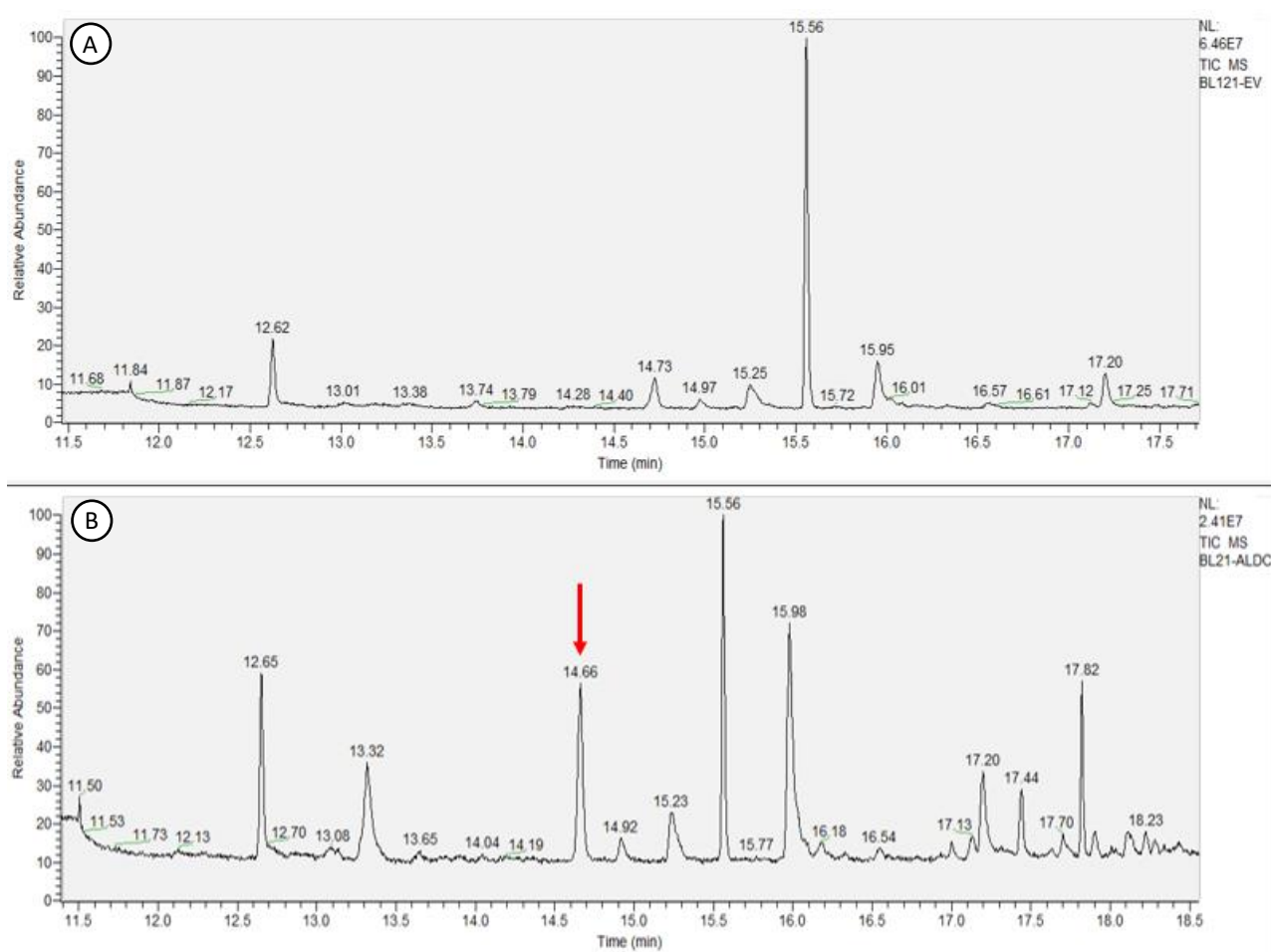


Figure 3.8: Gas chromatography-mass spectrometric analysis of transgenic bacteria to detect the presence of acetoin. *E. coli* BL21-CodonPlus(DE3)-RIPL was grown in SPME headspace vials containing 2 mL LB medium for 6 d. **A)** EV detected no acetoin and **B)** AA detected acetoin at 14,66 min indicated by red arrow.

3.3.4 *Arabidopsis* growth trials with transgenic *E. coli* exposure

Plant growth trials were conducted by exposing *Arabidopsis* to *E. coli* strains including BL21-CodonPlus(DE3)-RIPL wild-type (WT), and BL21 transformed with an empty pRSETA vector (EV) and pRSETA::ALDC (AA), respectively. Different controls were utilised to account for possible variations in the plant growth responses. These included untreated *Arabidopsis* plants without exposure to bacteria (absence of the small petri dish in the experimental setup), and various non-acetoin producing *E. coli* BL21-CodonPlus(DE3)-RIPL strains were added as treatments to confirm whether or not the presence of the *ALDC* transgene was solely responsible for a possible increase in growth.

Identically-sized 13 d old seedlings were used to set up growth trials and after two weeks of exposure to bacterial strains, plants were measured in terms of rosette diameter, fresh mass, and dry mass, and photographed. Two independent trials were conducted under a long-day-length (14 h:10 h day:night) photoperiod. Both independent trials generated highly similar results and all data was pooled to enhance statistical analysis. Bacterial treatments on visual inspection seemed to exhibit similar effects on plant growth (Figure 3.9). Plants exposed to bacteria appeared to have larger and more roots compared to untreated plants, however, this was not quantified and requires further investigation in future studies (See Addendum 2 Figure 5.6 for preliminary representation). Furthermore, plants exposed to AA had longer stems when compared to plants exposed to EV.

The analysis of fresh mass and rosette diameter showed significant differences between plants in the WT and AA treatments, although there was no significant difference between plants in the EV treatment and either of the other two treatments (Figure 3.10). The p value for comparison of fresh mass as a result of AA and EV treatments, was 0.09 and just short of significance set at 0.05. The plants treated with AA had the highest average measured fresh mass (35.3 mg), compared to the non-acetoin producing strain treatments with average fresh mass ranging from 26.4 mg to 30.2 mg. The AA treatments resulted in an average dry mass of 8 mg, while the WT and EV treated plants had dry mass of approximately 6 mg. However, the dry mass of plants from all of the different bacterial treatments did not significantly differ from each other.

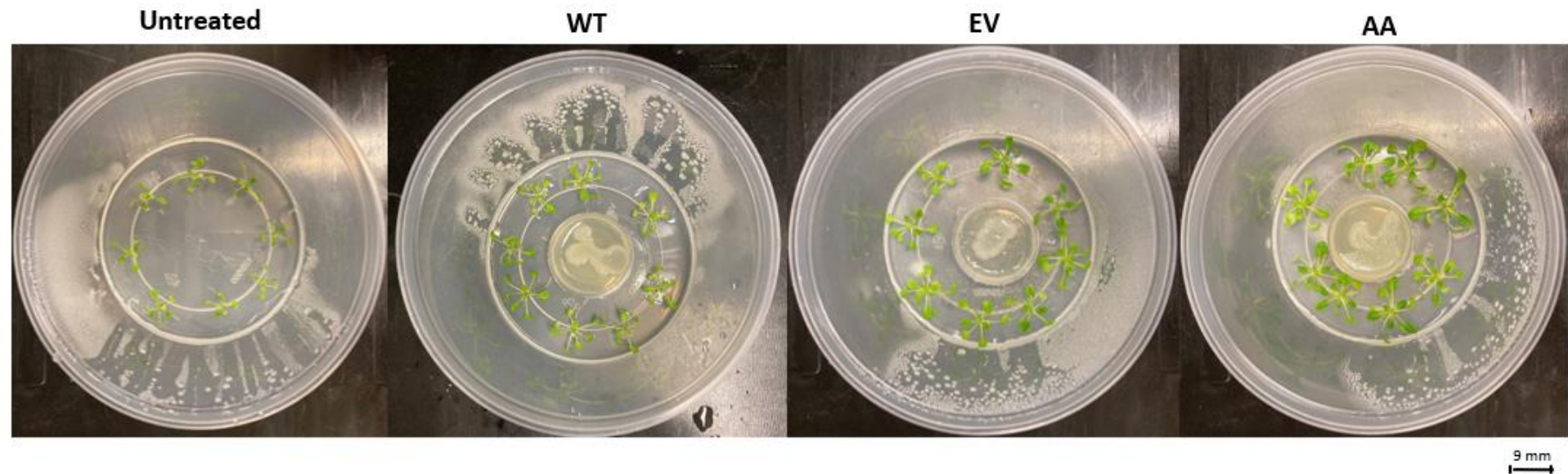


Figure 3.9: Growth performance of *Arabidopsis* seedlings exposure to the transgenic *E. coli* expressing the *ALDC* gene. Identically-sized 13 d old seedlings were used to set up the experiment. After two weeks of exposure to the respective *E. coli* BL21-CodonPlus (DE3)-RIPL strains, the plates were photographed, and fresh and dry mass of plants were measured. Growth trial was conducted *in vitro* at long-day-length (14 h:10 h photoperiod) conditions. Indicated are the wild-type *E. coli* BL21-CodonPlus (DE3)-RIPL (WT); empty pRSETA vector (EV); and pRSETA::ALDC (AA) to which plants were exposed.

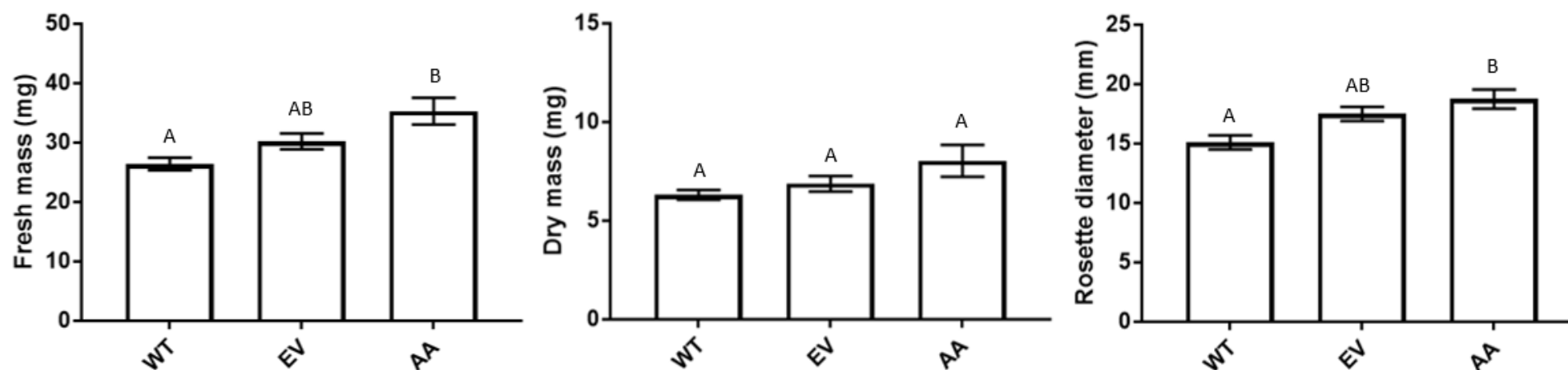


Figure 3.10: Analysis of plant growth in response to exposure to transgenic *E. coli* expressing the *ALDC* gene. Fresh mass (mg), dry mass (mg), and rosette diameter (mm) of 13 d old *Arabidopsis thaliana* Col-0 seedlings, grown under a 14 h:10 h light:dark photoperiod *in vitro*, exposed for 14 d to *E. coli* BL21 bacteria with and without *ALDC* gene. Values represent the mean \pm SE ($n = 48$). For the dry mass, three plants were measured together for greater accuracy of measurement. Each different letter indicates a value that was determined to be significantly different ($p \leq 0.05$) by one-way ANOVA and Tukey's multiple comparisons test. Indicated are the wild-type *E. coli* BL21-CodonPlus (DE3)-RIPL (WT); empty pRSETA vector (EV); and pRSETA::*ALDC* (AA) to which plants were exposed.

3.3.5 *Arabidopsis* salinity trials with transgenic *E. coli* exposure

The salinity trials were conducted on plants grown on a medium containing 100 mM NaCl. After two weeks of exposure to the respective bacterial strains, plates were photographed, and plants exposed to bacteria had a visibly higher survival rate compared to the untreated control, where none of plants survived (Figure 3.11). Bacterial treatments on visual inspection seemed to exhibit similar effects on growth to each other under saline conditions. Plants exposed to bacteria had seemingly similar roots as determined by visual inspection (See Addendum 2 Figure 5.7). Plants exposed to the WT treatment retained a green colour while showing early signs of necrosis and leaf folding under saline conditions. Furthermore, plants exposed to EV and AA treatments had shorter stems with visibly thicker leaves compared to other bacterial control treatments, with some leaves folded inwards towards the stem. The AA-treated plants had a slightly darker green colour compared to the EV-treated plants, some of which were a paler green colour with early signs of necrosis and retarded growth.

Growth parameters including rosette diameter, fresh mass, and dry mass were measured for plants that survived the salt culture conditions (Figure 3.12). For both fresh mass and rosette diameter, plants treated with EV and AA were significantly larger compared to WT treated plants. It is noteworthy that the p value for a significant difference between the EV and AA treated plant fresh mass was 0.062, only short of significance (≤ 0.05) by a narrow margin. The analysis of the dry mass of plants exposed to bacteria showed no significant differences between treatments. However, the p value (0.065) was again only marginally outside of the 0.05 cut-off for significance.

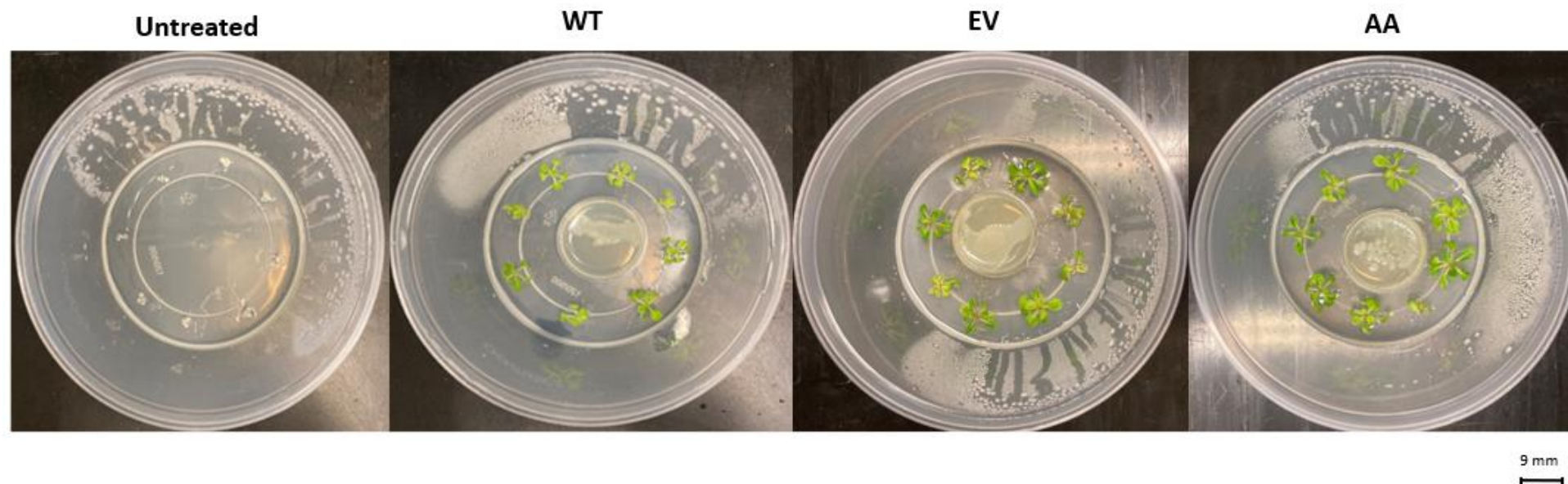


Figure 3.11: Salinity stress tolerance of *Arabidopsis* seedlings exposure to the transgenic *E. coli* expressing the *ALDC* gene. Identically-sized 13 d old seedlings were used to set up the experiment. After two weeks of exposure to the respective *E. coli* BL21-CodonPlus (DE3)-RIPL strains, the plates were photographed, and fresh and dry mass of plants were measured. Salinity stress tolerance trial was conducted *in vitro* at long-day-length (14 h:10 h photoperiod) conditions. Indicated are the wild-type *E. coli* BL21-CodonPlus (DE3)-RIPL (WT); empty pRSETA vector (EV); and pRSETA::ALDC (AA) to which plants were exposed.

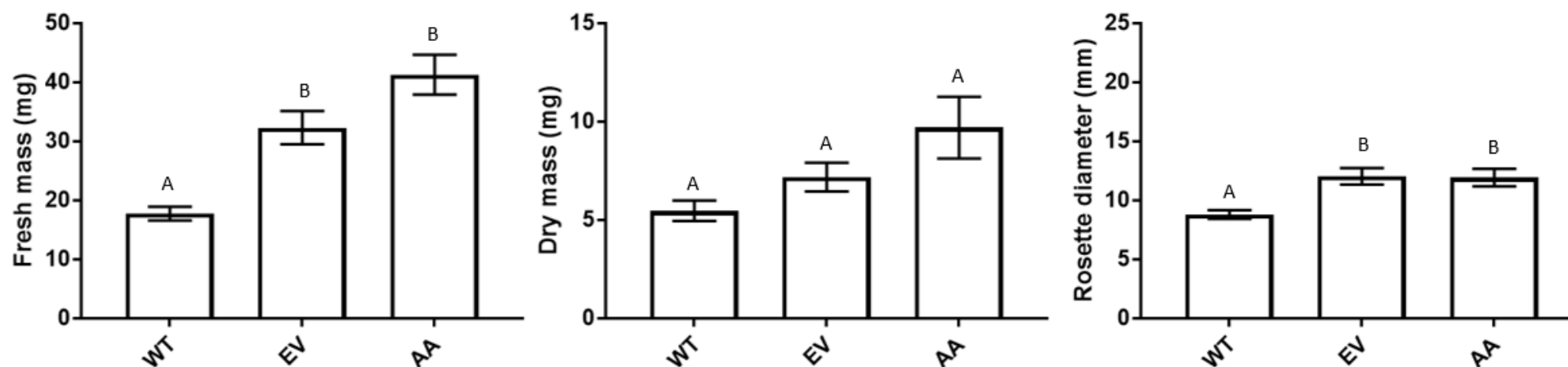


Figure 3.12: Analysis of plant growth under saline conditions (100 mM NaCl) in response to exposure to transgenic *E. coli* expressing *ALDC*. Fresh mass (mg), dry mass (mg), and rosette diameter (mm) of 13 d old *Arabidopsis thaliana* Col-0 seedlings, grown under a 14 h:10 h light:dark photoperiod *in vitro* on medium containing 100 mM NaCl, exposed for 14 d to *E. coli* BL21 bacteria with and without *ALDC* gene. Values represent the mean \pm SE ($n = 48$). For the dry mass, three plants were measured together for greater accuracy of measurement. Each different letter indicates a value that was determined to be significantly different ($p \leq 0.05$) by one-way ANOVA and Tukey's multiple comparisons test. Indicated are the wild-type *E. coli* BL21-CodonPlus (DE3)-RIPL (WT); empty pRSETA vector (EV); and pRSETA::ALDC (AA) to which plants were exposed.

3.4 Discussion

3.4.1 Protein expression and detection

Although the *ALDC* transgene was clearly transcribed to mRNA in the transformed bacteria, the protein was not detected by SDS-PAGE or immunoblotting at any of the induction conditions (Figure 3.4; Figure 3.5; Figure 3.6). Missing bands on an SDS-PAGE gel is commonly due to low protein concentrations or insensitivity of the detection method. Coomassie blue stain is suitable for protein concentrations between 0.3 – 1 µg, which might not be sensitive enough for ALDC in this instance. Furthermore, the protein may not be produced during the specific time point in the culture growth phase that was analysed in this study. Low expression levels of proteins can further be due to insolubility of protein or inability to interact with cellular machinery due to mRNA secondary structure and posttranslational modifications (Goelling *et al.*, 1988; Joseph *et al.*, 2015). The possibility of posttranslational modifications, including possible phosphorylation of the target protein, could not be confirmed in this study as specific antibodies were not available to test against phosphorylated residues (Ghosh *et al.*, 2014). As the immunoblot also lacked a positive control for the ALDC protein, it could not be concluded whether the basic protocol was ineffective, if the primary antibody could not detect protein in the denatured state or if the detection signal decayed too quickly (Ghosh *et al.*, 2014). No purification using immobilized metal ions or other methods was attempted with the His-tag due to time constraints, although purification would likely have addressed the issue of possible low levels of the protein being present. However, considering that HS-SPME analysis did detect acetoin being produced by the bacteria transformed with the *ALDC* gene (AA), it can be assumed that the protein was indeed produced by the transgenic bacteria (Figure 3.8).

The pale pink colour seen for the AA sample after the Voges-Proskauer test further suggests that low levels of acetoin were present in the AA samples (Figure 3.7). This could suggest low expression levels of the protein, correlating to the absence of a visible band for protein on the SDS-PAGE gels and immunoblots. Several studies attempting to engineer *E. coli* to produce either acetoin or 2,3-butanediol at high levels during fermentation introduced α -acetolactate synthase (ALS, EC. 4.1.3.18), responsible for the production of α -acetolactate, alongside α -acetolactate decarboxylase (Nielsen *et al.*, 2010; Xu *et al.*, 2015; Zhang *et al.*, 2015). The genes were obtained from original strains previously used in successful recombinant acetoin-producing *E. coli* such as *Staphylococcus aureus*, *Serratia marcescens* and *Enterobacter cloacae* (Xu *et al.*, 2014; Xu *et al.*, 2015; Zhang *et al.*, 2015). A comparison between the employment of overexpressed native *E. coli* ALS and *B. subtilis* ALS in introducing the 2,3-butanediol pathway into *E. coli* BL21 (DE3) strains revealed that the conversion of glucose to 2,3-butanediol by the strain with the native ALS was very slow and ended rapidly after approximately 3 h (Kay and Jewett, 2015). This could indicate that *E. coli* cannot produce acetolactate fast enough to sustain high levels of acetoin/2,3-butanediol production. In

addition to decreased enzyme activity, the pH of the culture also decreased during fermentation, meaning acetoin production could not neutralise acidification induced during anaerobic fermentation (Kay and Jewett, 2015). Although *E. coli* has a native version of ALS producing α -acetolactate, is the activity of this native enzyme is insufficient to support the high-level production of acetoin if ALDC is introduced into *E. coli* genome alone for fermentation purposes (Nielsen *et al.*, 2010). Furthermore, depending on the bacterial origin of the *ALS* and *ALDC* transgenes, the proteins could have different physical and chemical properties and might be insufficient to compete with native endogenous pathways utilizing pyruvate (Nielsen *et al.*, 2010; Zhang *et al.*, 2015). In such cases, it is necessary to block pathways converting pyruvate to acetate and acetyl-CoA to ensure sufficient quantities of pyruvate is available (Nielsen *et al.*, 2010). The fact that the *E. coli* BL21-CodonPlus(DE3)-RIPL bacterial strain in this study only possessed the native ALS, that all other pathways were active, and that fermentation conditions were not utilised as discussed above, should be considered as factors in the levels of acetoin produced. Previous research has shown that extremely low levels of acetoin (2 ng) are capable of enhancing plant growth, and a transgenic *E. coli* might produce enough to be effective (Ryu *et al.*, 2003). The native ALS was sufficient to allow for production of some acetoin, which were nowhere near the high quantities usually associated with fermentation, however, the levels of acetoin is potentially sufficient for plant growth promoting activity.

3.4.2 *Arabidopsis* growth trials with transgenic *E. coli* exposure

Treatment with the transgenic bacterial strain possessing the *ALDC* gene (AA) showed a significantly higher fresh mass and rosette diameter for plants than WT treated plants (Figure 3.10). WT and EV treatments should theoretically be identical and as expected they did not differ significantly; however, natural variations lead to AA-treated plants significantly differing from WT-treated plants but not the EV treatment. The effect of natural variation could be overcome by increasing the replicates utilized as the plants were very small and data points were over a narrow range. These results suggest that the presence of the transgene enhances the growth effect of fresh mass and rosette diameter as seen by increase in fresh mass, but only by a narrow margin. This may be due to increased water uptake, as dry mass for plants exposed to bacterial treatments did not differ. Furthermore, plants exposed to AA had longer stems when compared to plants exposed to EV. Auxin is known for a role in stem elongation in addition to root development (Hwang *et al.*, 2012). As seen in previous studies, the presence of the volatile acetoin is suggested to regulate, but is not limited to, the biosynthesis of auxin by upregulating several genes, such as *Expansins*, involved in cell division (Table 1.1; Zhang *et al.*, 2007; Bailly and Weisskopf, 2012; Sharifi and Ryu, 2018). *Expansins* drive turgor pressure to allow cell enlargement in which the protoplast pressures the cell wall to yield and enabling water uptake to counteract reduced pressure within the cell due to cell wall expansion (Cosgrove, 1987). It is thus theorised that the acetoin produced by the AA bacterial strain may have influenced auxin and/or other phytohormones to promote stem elongation and root development. However, a

transcriptomic analysis of phytohormone gene expression would be required to determine whether acetoin does indeed interact with any phytohormones to elicit plant growth promotion. A transcriptome analysis would identify differentially expressed genes that could be further investigated. Due to time-constraints, the investigation into the particular genes involved will be left to future studies.

Considering that the presence of the transgene enhances fresh mass and rosette diameter in plants exposed to the AA strain only in comparison with WT treated plants and that all bacterial treatments resulted in significantly larger plants than the untreated control, it is possible that *E. coli* BL21-CodonPlus(DE3)-RIPL strains might release unidentified compounds that could enhance plant growth in some way. A headspace GC-MS analysis of *E. coli* identified the most abundant volatile released from the bacteria as indole, a volatile produced by many Gram-positive and Gram-negative bacteria (Addendum 2 Figure 5.8; Chung *et al.*, 2016; Devaraj *et al.*, 2018). Indole has been shown to promote *Arabidopsis* growth by acting as messenger for plant growth and development regulations via auxin-signalling systems (Chung *et al.*, 2016). Furthermore, indole can also act as bioprotectant by priming defence responses through jasmonic acid signalling (Chung *et al.*, 2016). Interestingly, most studies investigating PGPV released from bacteria employed *E. coli* DH5 α as the control bacterium, as it did not elicit significant plant growth promoting or defence response priming compared to untreated plants (Ryu *et al.* 2003; Ryu *et al.*, 2004; Farag *et al.*, 2013; Chung *et al.*, 2016; Tahir *et al.*, 2017a; Tahir *et al.*, 2017b). However, in this study *E. coli* DH5 α , like *E. coli* BL21-CodonPlus(DE3)-RIPL, significantly enhanced growth parameters compared to the untreated control (data not shown). This suggests that the increase seen for bacterial treatments may be due to the presence of indole or that untreated control plants simply, for some reason, did not grow as well. Future investigations would be required to determine the true effect of indole in the bacterial strains used in this study.

3.4.3 *Arabidopsis* salinity trials with transgenic *E. coli* exposure

As described in Chapter 1, salinity can exhibit different effects depending on developmental stage of plant or exposure period to stress conditions (Table 1.1). Signs of necrosis, retarded growth and leaves folded inwards towards the stem observed for untreated plants are generally expected for plants experiencing salinity stress for periods of days to weeks (Munns, 2002b). After days of exposure, the root to shoot ratio usually increases, and cell dimensions change, resulting in smaller, thicker leaves with a higher chloroplast density (Munns and Tester, 2008). The EV and AA treatment resulted in plants that had shorter stems with visibly thicker leaves, with some folded inwards towards the stem as seen in plants experiencing salinity stress for a period of days (Figure 3.11). The AA-treated plants had a slightly darker green colour, possibly indicating healthier plants compared to the EV-treated plants, of which some were a lighter green colour with early signs of necrosis and

retarded growth. Salinity stress can damage the chloroplasts of plants and decrease chlorophyll content (Acosta-Motos *et al.*, 2017). The exposure to acetoin has been shown to increase chlorophyll content in salinity-stressed white clover through hormone regulation, in particular auxin (IAA; Niu *et al.*, 2016; Sharifi and Ryu, 2018). It is suggested that the presence of acetoin resulted in darker plants compared to EV-treated plants due to higher chlorophyll content.

Plants treated with AA had a significantly higher fresh mass and rosette diameter compared to WT treated plants, however, they again did not significantly differ for the specific growth parameters from EV-treated plants (Figure 3.12). Based on the p value, the difference between EV and AA treated plant fresh mass were only slightly short of significance by 0.012 (p value = 0.062). The EV-treated plants had a significantly higher fresh mass and rosette diameter compared to WT, which is unexpected as they are essential similar with the exception of the addition of the empty pRSETA vector in EV. Most likely the lack of significant difference between AA and EV is due to an insufficient number of replicates and a high range of natural variation influenced the statistical power.

The increase in growth parameters seen for bacterial treatments in compared with the untreated control plants could be attributed to structural modifications, stress responses, and hormone regulation that are triggered by volatile compounds, including both acetoin and indole (Cho *et al.*, 2008; Cappellari and Banchio, 2020). The non-significant difference seen between bacterial EV treatments and AA might be explained by the suggestion that indole requires jasmonic acid signalling and acetoin decreases jasmonic acid levels (Chung *et al.*, 2016; Cappellari and Banchio, 2020).

3.5 Conclusion

The presence of acetoin produced by the AA-strain of bacteria in growth and salinity stress tolerance trials resulted in significantly increased fresh mass and rosette diameters compared with the WT treated plants. There was no significant difference for individual treatment dry mass measurements in either the growth or the salinity trials, suggesting that plant growth promotion and salinity stress tolerance observed between untreated plants and treated-plants may be related to the fresh mass rather than the dry mass. Recombinant *E. coli* BL21-CodonPlus(DE3)-RIPL containing the pRSETA::ALDC vector did produce acetoin to elicit some level of growth promotion and salinity tolerance, although only low levels of acetoin were produced, probably due to a lack of sufficient α -acetolactate (precursor to acetoin) being produced by the endogenous *E. coli* ALS. However, the AA treated plant did not differ from plants treated with EV, which was unexpected and could indicate that the acetoin production might not be optimal at this stage or an insufficient number of replicates were used. In the future, *E. coli* could be transformed with both *ALS* and *ALDC*, instead of just *ALDC*, as overexpression of *ALS* will result in more α -acetolactate available for acetoin production, possibly having a greater effect on plant growth and resistance. Further investigation on bacterial-treated plants at transcriptomic level is also recommended and future growth trials should include the analysis of root development.

Chapter 4

Acetoin-production in *Arabidopsis thaliana*

4.1 Introduction

Plant transformation is a useful research tool for gene discovery and new insights into gene function, which allows investigation of genetically controlled characteristics (Narusaka *et al.*, 2010). Moreover, it enabled the introduction of useful genes and the generation of genetically modified organisms in a relative short period of time (Narusaka *et al.*, 2010).

4.1.1 *Agrobacterium* transformation method

There are two major strategies to generate transgenic plants, namely *Agrobacterium*-based transformations, and direct DNA transfer methods such as particle bombardment (Gase *et al.*, 2011). Mostly, *in planta* transformations required tissue culture and *in vitro* plant regeneration systems, but Clough and Bent (1998) developed the efficient *Agrobacterium*-mediated floral dipping method to transform *Arabidopsis thaliana*, which involved flower buds being dipped into an *Agrobacterium* cell suspension. This method was later simplified and improved by Narusaka and colleagues (2010) to the inoculation of individual *Arabidopsis* flowers with small amounts of *Agrobacterium* inoculum, resulting in many independent transformation events (Narusaka *et al.*, 2010). *Agrobacterium*-mediated transformation involves the utilization of virulence genes present on a tumour-inducing (Ti) plasmid, host intracellular transport and DNA repair machinery to transfer the T-DNA molecule into the host cell for integration into the host genome (Gase *et al.*, 2011).

4.1.2 Vector construct

A vector system is employed as vehicle to transport a transgene into plant cells for replication and expression (Low *et al.*, 2018). *Agrobacterium*-based plant transformation generally uses a Ti plasmid, which contains three regions, the transfer DNA (T-DNA), virulence, and opine catabolism regions. The T-DNA region is flanked by a left and right border; the region between these two borders is transferred into the plant genome (Gase *et al.*, 2011). The virulence region functions as an aid for the transfer of the T-DNA by encoding *vir* genes that translate to proteins responsible for excision, processing, coating, and protection of the T-DNA (Low *et al.*, 2018). The transgene and selectable marker gene with its respective promoter and terminator regions, responsible for the transcriptional regulation in the host cells, is cloned into the T-DNA region of the Ti-plasmid system (Low *et al.*, 2018). The selectable marker gene, often an antibiotic resistance gene, functions to eliminate non-transformants during transformant selection.

After transformation of the plant, the resulting transformants need to meet strict criteria, such as retaining the same ploidy level as the wild-type (WT) plant, lacking any deletions or rearrangement in the T-DNA region inserted into the plant genome, and ideally only a single transgenic locus with one T-DNA copy should exist (Gase *et al.*, 2011). Furthermore, the insertion of the transgene should not disrupt any other functional genes in the transgenic plant genome (Gase *et al.*, 2011). Mutations in this instance are linked, but not limited, to insertional inactivation of endogenous genes or alterations in the expression of these genes due to the disruption of expression-control regions (e.g. promotor, activator and repressor regions).

4.1.3 Transgenic plants

Once a transgene has been inserted into the plant genome, it is usually inherited as a dominant trait by the next generation according to the Mendelian laws of inheritance (Low *et al.*, 2018). Plants transformed via the *Agrobacterium*-mediated method are considered the T₀ generation after the genetic transformation process and are heterozygous for the transgene, meaning only one allele of the gene is present at a gene locus (Passricha *et al.*, 2016). The seed from T₀ plants will be considered the T₁ generation and grow into T₁ plants of which the genotypic representation will be 25% homozygous for the transgene, 50% heterozygous, and a further 25% will be homozygous with no insertion of the transgene (wild-type). Phenotypically, the heterozygous and homozygous transgenic plants will look similar due to presence of the transgene, consequently the antibiotic selection marker will be of value to determine which plants are homozygous (Passricha *et al.*, 2016). Seeds from a homozygous plant will be able to germinate at 90-95% on the appropriate antibiotic selection, while only around 75% of heterozygous seed will germinate. Ideally, studies aim to make use of homozygous lines as they maintain a higher degree of consistency for traits linked to the transgene in subsequent generations and all future progeny/generations will be homozygous (Passricha *et al.*, 2016). Furthermore, it would render the need for selection agents to ensure presence of the transgene obsolete, which could interfere with experiments such as growth comparisons between transgenic and wild-type plants.

4.1.4 Chloroplast transit peptides

Chloroplasts are able to perform other specialized functions in addition to photosynthesis, including, but not limited to, synthesis of amino acids, fatty acids, and carotenoids, making them the ideal location to enhance plant abilities through biotechnological methods (Shen *et al.*, 2017). Thus, biotechnological metabolic engineering can aim to achieve improved photosynthesis, stress resistance, grain quality, and yield to name a few, by efficiently targeting novel or altered proteins into the chloroplast. Chloroplast transit peptides are one of the main methods used to guide foreign proteins to the chloroplast (Shen *et al.*, 2017). Chloroplast transit peptides are high in hydroxylated serine, threonine, and proline amino acid residues, while lacking acidic aspartate and glutamate amino acid residues. Furthermore, they tend to form α -helical structures in hydrophobic

environments (Shen *et al.*, 2017). As 95% of chloroplastic proteins are encoded in the nuclear genome, chloroplast transit peptides function as a guide to ensure transport of the protein to the chloroplast. These chloroplastic proteins are translated as precursors in the cytoplasm, whereafter they are imported into the chloroplast by the chloroplast transit peptide, which forms part of the precursor sequence. Once entry into the chloroplast is achieved, the chloroplast transit peptide is removed from the protein (Shen *et al.*, 2017).

Various nuclear-encoded chloroplast proteins have been identified to have chloroplast transit peptides, one of which is Ferredoxin-NADP⁺ reductase (Mulo, 2010). Ferredoxin-NADP⁺ reductase (FNR, EC 1.18.1.2) is a ubiquitous and hydrophilic enzyme found in mitochondria and plastids of higher plants. Furthermore, FNR is found in three distinct chloroplast compartments, namely the chloroplast inner envelope, soluble stroma, and thylakoid membranes (Mulo, 2010). The protein acts as the catalyst in the final step of the linear photosynthetic electron transfer chain by mediating transfer of electrons between reduced ferredoxin and NADP⁺ (Mulo, 2010). *Arabidopsis thaliana* has two isoforms of FNR (FNR1 and FNR2), both of which are predominantly expressed in rosette leaves, with minor amounts in flowers, siliques, and stems (Mulo, 2010). Ferredoxin-NADP⁺ reductase is synthesized on cytosolic polysomes as precursor containing an amino-terminal transit peptide which is responsible for targeting proteins to the chloroplast. The amino-terminal extension of FNR that function as transit peptide is approximately 5 kDa (29 aa) in size and allows the translocation across the plastid envelope (Arakaki *et al.*, 1997). Furthermore, the addition of the peptide to a protein increases stability and solubility (Arakaki *et al.*, 1997).

4.1.5 Aim of chapter

The main aim of this study was to enhance *Arabidopsis thaliana* growth by overexpressing the *ALDC* gene, isolated from fungi responsible for the production of acetoin, *in planta* and determining the functionality of the protein. The objectives of this chapter include the cloning of a recombinant vector construct containing the *ALDC* gene linked to the FNR chloroplastic transit peptide sequence to allow its targeting to chloroplast as α -acetolactate (precursor for acetoin) is only produced in the chloroplast in plants (Mifflin, 1974). The recombinant vector was then employed in the generation of transgenic *Arabidopsis thaliana* plants expressing the transgene, via the *Agrobacterium*-mediated floral inoculation method described by Narusaka and colleagues (2010). It was hypothesized that *Arabidopsis thaliana* plants with the ability to produce acetoin would display increased growth and salinity stress tolerance compared to WT *Arabidopsis thaliana* Col-0 plants, and potentially also increase the growth of WT plants in their vicinity due to their production of the acetoin volatile.

4.2 Materials and methods

4.2.1 Cloning of recombinant vector

The α -acetolactate decarboxylase (*ALDC*, EC 4.1.1.5) and acetoin reductase/2,3-butanediol dehydrogenase (*BDH1*, EC 1.1.1.4) genes were isolated from *Aspergillus niger* ATCC 10864 and *Saccharomyces cerevisiae* W3030, respectively, and individually cloned into the pUBI510 vector (Dempers, 2015; Van der Merwe, 2016; Rosmarin, 2020). Both genes were flanked by a ferredoxin-NADP⁺ reductase (FNR) chloroplastic transit peptide sequence (EC 1.18.1.2, from *Spinacia oleracea*) and octopine synthase (*ocs*, V00088.1) terminator.

The *ALDC* gene, together with the FNR transit peptide and terminator, was amplified from the pUBI510::FNR:ALDC vector template using the primers F_BamHI and A_BamHI (Table 3.2) designed for this purpose via PCR with Q5® High-Fidelity DNA Polymerase (New England Biolabs). The conditions of the PCR are shown in Table 4.1. The PCR product was purified according to Wizard SV Gel and PCR Clean-up System (Promega) manual (Section 3.2.1) and then A-tailed (Table 4.2) for cloning. The fragment was then cloned into the pCR8::GW::TOPO entry vector for Gateway Cloning according to the pCR™8/GW/TOPO® TA Cloning® Kit manual (Invitrogen), and transformed into *E. coli* Top10 competent cells. The putative transformed cells were grown overnight on LB medium containing 100 µg/mL spectinomycin. A verification PCR (Table 3.1) with an extension time of 30 s was executed on colonies obtained using the AF2/AR1 primer pair (Table 3.2). Liquid cultures with spectinomycin were grown overnight from colonies that were positive for the transgene and these were used for plasmid isolation. Plasmid DNA was obtained using the Wizard Plus SV Minipreps DNA Purification System (Promega).

The *ALDC* gene was then cloned into the pMDC32 destination vector using the pCR™8/GW/TOPO® TA Cloning® Kit (Invitrogen) following the manufacturer's instructions for LR Clonase reactions. The reactions were transformed into *E. coli* Top10 competent cells and selected overnight on LB medium containing 50 µg/mL kanamycin. Plasmid DNA was obtained from transformed colonies and PCR analysis (Table 3.1) confirmed the presence of the transgene using primers AF2 and AR1 (Table 3.2).

Additionally, the *BDH1* gene was cloned into the pCAMBIA2300 binary vector. For this, both the vector and *BDH1* gene linked with the FNR transit peptide and *ocs* terminator (from a pUBI510::BDH1 template) was digested with *Eco*RI-HF and *Hind*III-HF for directional cloning, whereafter the DNA was purified (Section 3.2.1). Ligation was performed using the ligation protocol for T4 DNA Ligase (New England Biolabs) and the plasmid transformed into *E. coli* Top10 competent cells. The cells were grown overnight on LB medium with kanamycin (50 µg/mL). A verification PCR (Table 3.1) was executed on colonies obtained using the BF1/BR1 primer pair (Table 3.2). Plasmid

DNA was extracted from transformed colonies using the Wizard Plus SV Minipreps DNA Purification System (Promega) kit (Section 3.2.1).

Table 4.1: PCR cycling protocol for Q5® High-Fidelity DNA Polymerase

PCR cycle	Cycling conditions		No. of cycles
	Temperature	Time (min)	
Initial denature	98°C	00:30	1
Denature	98°C	00:10	30
Annealing (T _m)	68°C	00:30	
Extension	72°C	01:00	
Final Elongation	72°C	02:00	1
Hold	12°C	-	

Table 4.2: A-tailing protocol for blunt PCR fragments

Blunt PCR fragment	1 µg
dATP (10mM)	2 µL
GoTaq Enzyme	0.25 µL
5x GoTaq Buffer (clear)	10 µL
Water	Up to 50 µL
Incubate @ 72°C for 30 min	

4.2.2 Competent cells for *Agrobacterium*

For *Agrobacterium tumefaciens* competent cells, a 5 mL liquid culture with appropriate antibiotic was prepared and incubated at 28°C for 24 h. The culture was then utilized to inoculate 50 mL LB containing the appropriate antibiotic. The antibiotic required for the *A. tumefaciens* GV3101 strain was rifampicin (25 µg/mL). Cultures were incubated at 28°C until an OD600 of 0.8 was reached and then transferred to an ice-cold conical tube for centrifugation (1 500 xg) at 4°C for 10 min. The supernatant was discarded, and the pellet resuspended in 50 mL ice-cold water. The centrifugation and re-suspension steps were repeated twice. The cells were centrifuged again at 4°C for 15 min, the cell pellet was resuspended first in 20 mL of cold sterile 10% (v/v) glycerol and finally in 0.5 mL ice-cold sterile 20% (v/v) glycerol, where after 100 µL cell aliquots were stored at 80°C.

4.2.3 Transformation of plants

The pMDC32::FNR:ALDC and pCAMBIA2300::BDH1 vectors were transformed into *Agrobacterium tumefaciens* GV3101 by electroporation. The *Agrobacterium* competent cells (100 µL) were thawed

and added to an ice-cold 2 mm electroporation cuvette, together with either plasmid DNA of pMDC32::FNR:ALDC or pCAMBIA2300::BDH1 (100 – 200 ng). The cuvette was placed into the Gene Pulser Xcell Electroporation machine (BioRad) with the following settings: voltage 2400 V, capacitance 25 μ F, resistance 200 Ω , and cuvette 2 mm. After electroporation, 1 mL of liquid LB medium was added to the cuvette and transferred to a 10 mL test tube (R/B S/CAP ST PP 16X100MM, Lasec). The cells were incubated at 28°C for 2 h, whereafter they were transferred to a microfuge tube and centrifuged at 15 900 $\times g$ for 5 min. After centrifugation, 800 μ L of the supernatant was removed and the pellet re-suspended in the remaining 200 μ L supernatant. The cells were plated out onto LB-agar medium containing 50 μ g/mL kanamycin and 25 μ g/mL rifampicin and were incubated at 28°C for 2 d. Liquid cultures with the antibiotics were grown overnight at 28°C for plasmid isolation and PCR analysis (Table 3.1).

Agrobacterium tumefaciens liquid cultures for both *ALDC* and *BDH1* genes were cultured with appropriate antibiotics, whereafter plants were transformed with the *Agrobacterium* according to the protocol described by Narusaka *et al.* (2010). In order to establish putative transformed A lines, plants were inoculated with the *Agrobacterium* containing the pMDC32::ALDC vector. Putative transformed AB lines were established by mixing equal amounts of the liquid cultures from both *Agrobacterium* cultures (pMDC32::ALDC and pCAMBIA2300::BDH1) before centrifugation and resuspension in transformation buffer.

4.2.4 Establishing homozygous transgenic lines

After seeds were collected from putative A and AB transgenic siliques of *Agrobacterium*-infected plants, they were surface-sterilized as described previously (Section 2.2.1). The surface-sterilized seeds were then sown on 1/2 MS medium with phyto-agar and appropriate antibiotics. The seeds from plants inoculated with only the *Agrobacterium* containing the pMDC32::ALDC vector (A lines) were sown on medium with 15 μ g/mL hygromycin. The seeds from plants inoculated with a combination of *Agrobacterium* containing the pMDC32::ALDC vector and *Agrobacterium* containing pCAMBIA2300::BHD1 (AB lines) were sown on medium with both kanamycin (50 μ g/mL) and hygromycin (15 μ g/mL). Plants that survived longer than two weeks and produced roots growing into the medium were considered putative transgenic T₁ lines and were hardened off.

The putative A and AB T₁ lines were analysed first by confirming insertion of the transgene and second by testing the level of expression of the transgene. Genomic DNA (gDNA) was extracted from leaf material of putative T₁ plants for both A and AB lines using a method modified from Lu (2011). Leaf material was flash frozen in liquid nitrogen and ground to a fine powder, whereafter 400 μ L of Edwards extraction buffer (200 mM Tris-Cl pH 7.5, 250 mM NaCl, 25 mM EDTA, 0.5% [m/v] SDS) was added (Lu, 2011). After vigorous vortexing, samples were centrifuged (13 000 $\times g$) for 10 min at RT and 300 μ L of the supernatant was added to 300 μ L isopropanol. The samples were

incubated at -20°C for 1 h and centrifuged (13 000 xg) for 15 min at RT, whereafter the supernatant was discarded. After washing the pellet with 70% ethanol and allowing it to air-dry, the pellet was resuspended in 50 µL of nuclease-free water. After analysing the quantity and purity of the gDNA, 100 ng of DNA from each sample was used for PCR to test for the insertion of the transgenes into the plant genome. The PCR (Table 3.1) had an annealing temperature gradient of 58 to 60°C and an extension time of 40 s. The AF2/AR1 primer pair (Table 3.2) was employed for the A lines, whilst for the AB lines, the AF2/AR1 and BF1/BR1 primer sets were employed. The plants that tested positive for the transgene(s) were allowed to seed in order to collect T₂ seed, and the process outlined above was repeated to obtain T₃ seed.

The T₂ and T₃ plants that tested positive for the transgene were utilized to analyse the levels of transgene expression. RNA was extracted from the plant material (single leaf) via the Maxwell 16 LEV Plant RNA Kit (Promega), according to the manufacturer's protocol. Thereafter, complementary DNA (cDNA) was synthesized (170 ng RNA for T₂ plants; 1000 ng RNA for T₃ plants) via the RevertAid H Minus First Strand cDNA Synthesis Kit (Thermo Scientific) using the Oligo(dT)18 primer, according to the manufacturer's instructions. Relative levels of gene expression were analysed via Reverse Transcriptase semi-quantitative PCR (RT-sqPCR) using the *elongation factor-1 alpha* (*EF-1α*) gene as an internal reference and the AF3/AR1 primer sets for the *ALDC* gene (Table 3.2; Table 4.3)

Table 4.3: RT-sqPCR conditions

PCR cycle	Cycling conditions		No. of cycles
	Temperature	Time (min)	
Initial denature	95°C	03:00	1
Denature	95°C	00:30	26-32
Annealing (T _m)	58-60°C	00:30	
Extension	72°C	00:40	
Final Elongation	72°C	02:00	1
Hold	12°C	-	

The seeds were collected from the A line transgenic siliques of T₂ generation plants, and a small batch from each individual line was surface-sterilized as described previously (Section 2.2.1). The surface-sterilized seeds were then sown on ½ MS medium with phyto-agar and 15 µg/mL hygromycin. After 16 days, the number of seeds that germinated was quantified in order to determine whether the line was homozygous for the transgene. A germination rate of 90-95% was classified as homozygous, while germination rates around 75% were considered heterozygous. A similar batch of seed from each line was also sown on non-selective ½ MS medium to determine the overall

viability of the seeds collected. Only two successfully homozygous line for T₃ generation (A8.5 and A6.8) were identified at the time and investigated in subsequent trials.

4.2.5 Transgenic versus wild-type plant trials

Plant growth and salinity tolerance of homozygous T₃ plants were compared to WT *Arabidopsis thaliana* Col-0 plants. Seeds from two A-lines (A8.5 and A6.8) and WT *Arabidopsis thaliana* Col-0 were surface-sterilized and sown on non-selective medium, as described in Section 2.2.1.

Growth trials were set-up in three replicate 500 mL culture containers (F.RL500, vaalPAC), each containing eight 13 d old seedlings of either WT or one of the transgenic lines (Figure 4.1). The trial was repeated a second time. Seedlings were allowed to grow for a period of 14 d under a long day length (14 h:10 h day:night) photoperiod. At the conclusion of each trial, the rosette diameter, fresh mass, and dry mass for each plant were measured. Trials to test the salinity tolerance for transgenic plants versus WT plants were conducted similarly, with the exception that 100 mM NaCl was added to the ½ MS medium on which the plants were grown.

Additionally, 5 seeds from the two A-lines and WT *Arabidopsis*, respectively were sown in water-saturated Jiffy-7® bags (Jiffy Production Int.) containing compressed peat to compare growth. Seeds were allowed to germinate and grow for 30 d at 22 ± 2°C under a 10 h:14 h light:dark photoperiod with a light intensity of 50 µmol photons/m²/s¹. Plants were watered every four days and fertilized with Phostrogen (1.4 g/L) biweekly, starting one week after sowing. At the conclusion of the 30 days, the rosette diameter, fresh mass, and dry mass for each plant were measured.

4.2.6 Trials with transgenic plants as an acetoin source

After screening T₃ seed for homozygous lines, the 16 d old transgenic plants obtained from the A8.5 and A6.8 transgenic lines were utilized in a trial to determine whether transgenic plants could act as an acetoin source to enhance the growth of WT *Arabidopsis thaliana* Col-0 plants. Trials were set-up in three 500 mL culture containers (F.RL500, vaalPAC), each containing eight 9 d old WT seedlings (as described in Section 2.2.1) and one transgenic A8.5 or A6.8 plant in the centre (Figure 4.1). Three containers containing only 8 WT seedlings each, were considered as control. Seedlings were exposed to the transgenic plant for a period of 14 d under a long-day-length (14 h:10 h day:night) photoperiod. At the conclusion of each trial, the fresh mass, dry mass, and the rosette diameter for each plant were measured.

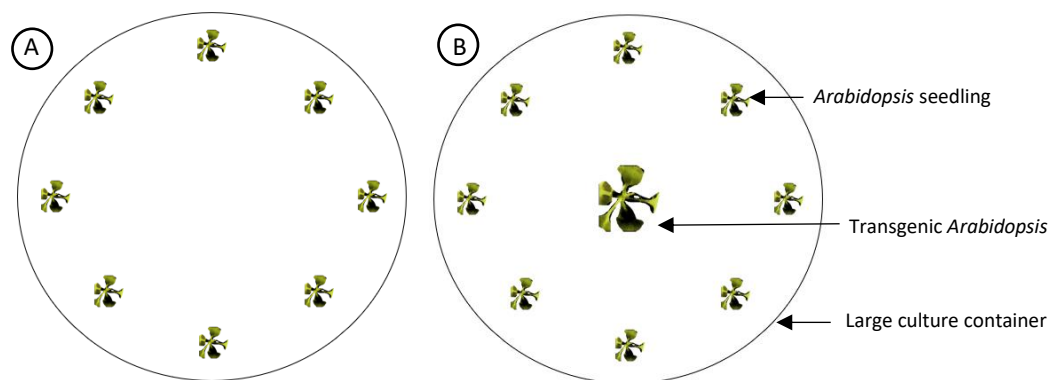


Figure 4.1: Layout for growth trials with transgenic plants. A) Control eight WT seedlings placed on $\frac{1}{2}$ MS media with or without 100 mM NaCl. **B)** Eight WT seedlings surrounding one transgenic plant in the centre of the container.

4.2.7 Gas chromatography-mass spectrometry analysis to detect acetoin

For GC-MS analysis of transgenic plants, A-line leaves or whole plants were placed in SPME headspace vials (SU86009, 20 mL, Merck) on 2 mL $\frac{1}{2}$ MS medium for 6 d or 11 d at 22°C. Wild-type *Arabidopsis* Col-0 leaves and WT leaves spiked with synthetic acetoin were considered as controls. Leaves were spiked by pipetting a 1 μ L droplet of pure acetoin onto a leaf. Head-space solid phase micro-extraction (HS-SPME) analysis was executed by the Central Analytic Facilities (Mass spectrometry unit, CAF) according to the method described in Section 3.2.13.

In the absence of an acetoin concentration curve, which was attempted but could not be standardised successfully, the chromatographic peak area was utilized to estimate the acetoin concentrations present in the samples. For this, a simple internal normalization procedure, as described by Guiochon and Guillemin, (1988) was utilized as a calculation method. Under the assumption that the detector is linear, the estimated concentration of acetoin was determined by calculating the fraction (%) of the peak area for acetoin to the total peak area of all compounds produced in the particular sample. The data was normalized by $A_j = \frac{P_j}{P_1 + P_2 + P_3} \times 100$ where P_j represents the peak area for acetoin and $P_1 + P_2 + P_3$ represents the area of the peaks for the other compounds in the sample (Guiochon and Guillemin, 1988; Brevard *et al.*, 2011). Thus, the ratio of acetoin present in each sample relative to total of all compounds detected, can be compared amongst different samples to estimate the increase, or decrease of acetoin. It should be noted that the fraction ratio calculated is differently from the relative abundance (or peak height; %) shown on the y-axis of the chromatogram, which represents the abundance of the particular peak to the most abundant peak (represented by 100%) in the particular volatile profile.

4.2.8 Statistical analysis

The following assumptions of the ANOVA model were satisfied to allow interpretation of data: treatment levels in the experiment have approximately equal variances, residuals are normally distributed, and observations are independent. A one-way ANOVA and appropriate *post hoc* test for significant difference ($p \leq 0.05$) from other treatments were applied for statistical analysis. All trials were independently repeated, and data was pooled together for statistical analysis. For accurate dry mass measurement, three plants were measured together, unless stated otherwise. The Fisher's LSD multiple comparisons test was applied to compare treatments.

4.3 Results

4.3.1 Establishing homozygous transgenic plants

The α -acetolactate decarboxylase (*ALDC*, EC4.1.1.5) and acetoin reductase/2,3-butanediol dehydrogenase (*BDH1*, EC1.1.1.4) genes that had previously been cloned into the pUBI510 vector (Dempers, 2016; Rosmarin, 2020), were successfully transformed into the pMDC32 and pCAMBIA2300 plant expression vectors, respectively (Figure 4.2). The final vector diagrams are shown in Addendum 1 (Figure 5.3). In order to transform plants with the two genes, singly or in combinations, both vectors were transformed into *Agrobacterium tumefaciens* GV3101.

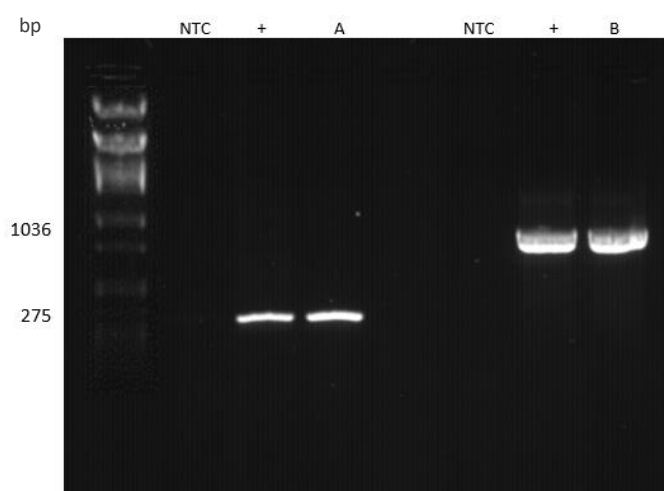


Figure 4.2: PCR confirmation of the transformation of the *ALDC* gene into the pMDC32 and the *BDH1* gene into the pCAMBIA2300 vector. The transformation of *ALDC* into pMDC32 vector was confirmed using the AF2/AR1 primer set, whereas BF1/BR1 primer set was used to confirm successful insertion of *BDH1* into pCAMBIA2300. Indicated are base pairs (bp); the non-template control (NTC); positive control pUBI510::*ALDC* (+); plasmid DNA of the pMDC32 vector containing *ALDC* (A); plasmid DNA of pCAMBIA2300 vector containing *BDH1* (B); and positive control pUBI510::*BDH1* (+).

After the *Arabidopsis* plants were transformed with the *ALDC* gene or a combination of the *ALDC* and *BDH1* genes, seeds were collected and screened using antibiotics (Figure 4.3). The 33 putative A-line plants and 2 putative AB-line plants obtained for the T_1 generation were allowed to grow and set seed. They were further screened by PCR analysis using extracted gDNA from each individual plant as template. A total of 24 putative A-line plants were shown to possess the transgene (Figure 4.4). Only one of the putative AB-line plants was found to possess both of the transgenes (data not shown) but did not survive to set seed, meaning that no AB lines were available for further experimentation.

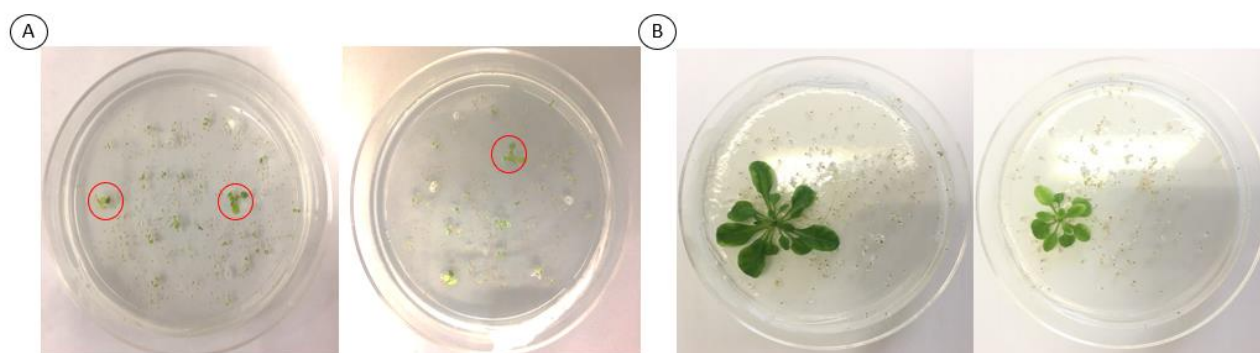


Figure 4.3: Screening T₁ putative transgenic *Arabidopsis* seedlings. Seeds obtained from plants inoculated with *Agrobacterium* to transform with **A)** *ALDC* only (A line) or **B)** a combination of *ALDC* and *BDH1* (AB line) were screened by making use of media containing the appropriate antibiotics, namely hygromycin for A-lines and hygromycin and kanamycin for the AB-lines. Germination and growth were allowed for 2-4 weeks depending on the growth rate and clear distinction between seedlings.

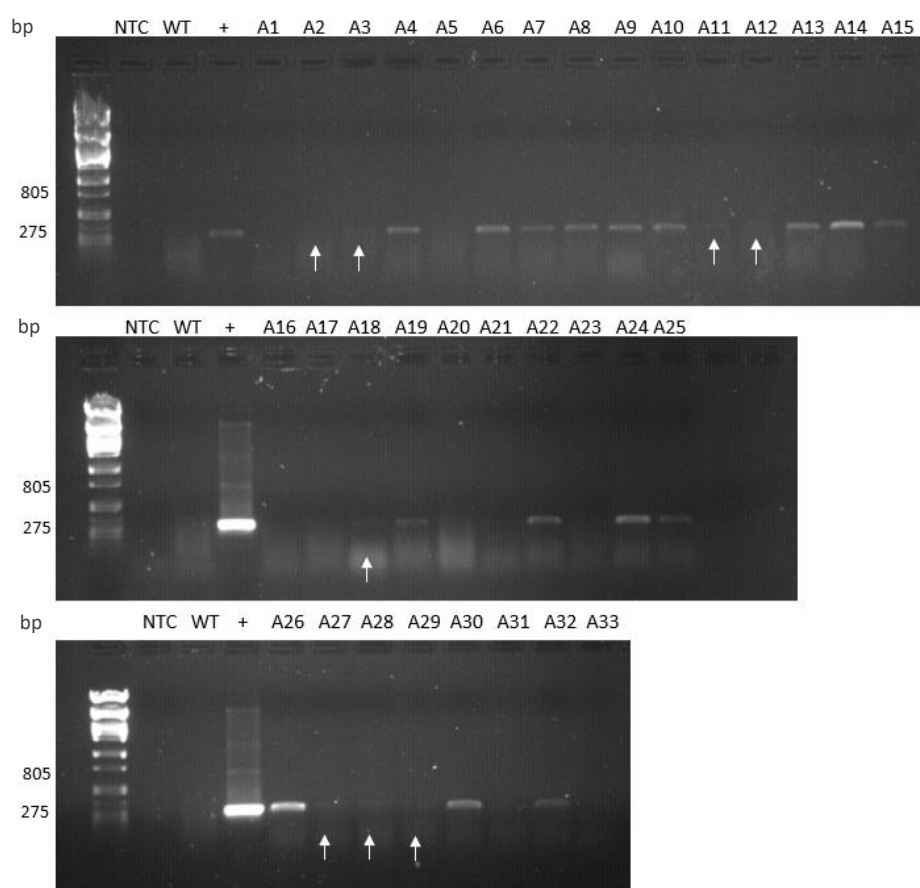


Figure 4.4: PCR analysis using genomic DNA extracted from putative T₁ plants as template to determine the insertion of the *ALDC* gene into the plant genome using gene-specific primers. Sixteen of the 33 putative A-line plants (A1 – A33) tested for the presence of the *ALDC* was positive for the transgene, while 8 of the plants yielded very faint bands. The plants showing clear bands for the transgene(s) were grown for T₂ seed collection. Indicated are base pairs (bp); *Arabidopsis thaliana* Col-0 (WT); positive control of pUBI50::*ALDC* plasmid DNA (+); single *ALDC* transformant (A); and arrows for faint bands.

The seed collected from the T₁ plants were screened and four T₂ generation lines (A6, A8, A10 and A14) were established. Two plants from each of the four lines were tested for the presence of the transgene and all plants were confirmed to contain the *ALDC* gene (Figure 4.5). The expression level of *ALDC* in the T₂ generation of A-line plants was analysed by RT-sqPCR using *EF-1α* as the reference gene (Figure 4.6). Based on the intensity of the bands, lines were classified as having low, medium, or relative high expression levels for the transgene. Lines A10.1 and A10.2 showed low levels of expression, while the A6, A8 and A14 lines were classified as having high levels of transgene expression. The independent plants within each of the four lines (A6, A8, A10 and A14) were allowed to set seed to establish the T₃ generation of plants.

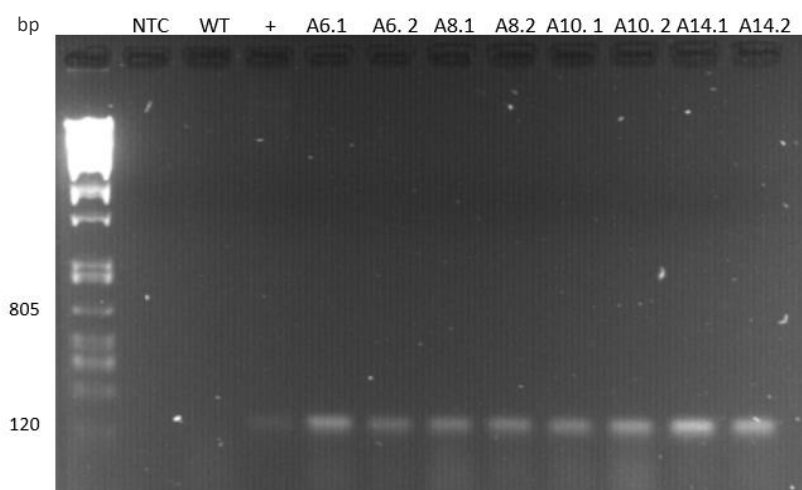


Figure 4.5: PCR analysis using genomic DNA extracted from putative transgenic T₂ plants as template to determine the insertion of the *ALDC* gene into the plant genome using gene-specific primers. All T₂ generation plants from each line that was tested yielded an amplicon corresponding to the transgene the AF3/AR3 primer set. Indicated are base pairs (bp); *Arabidopsis thaliana* Col-0 (WT); positive control of pUBI50 plasmid DNA (+); single *ALDC* transformant (A).

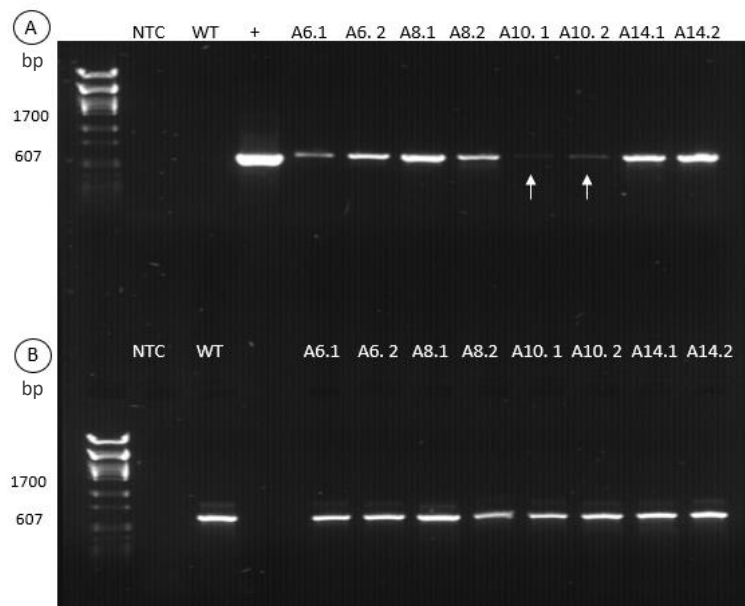


Figure 4.6: Semi-quantitative PCR analysis of the expression of *ALDC* in T_2 generation A-line transgenic plants. The expression levels of the *ALDC* gene were determined using a **A**) gene-specific primer set (AF3 /AR1) in comparison with the expression of the **B**) *EF-1 α* reference gene (*EF-1 α* F/ *EF-1 α* R). Indicated are base pairs (bp); *Arabidopsis thaliana* Col-0 (WT); positive control of pUBI50::*ALDC* plasmid DNA (+); single *ALDC* transformant (A); and arrows for faint bands.

The seeds for the T_3 generation were collected from plants of the four A-lines (A6, A8, A10 and A14) and a small batch of seed for each of the group's independent lines were sown on selective media to determine which of the T_3 A-lines were homozygous for the *ALDC* gene. Of all the lines tested, only A6.8 and A8.5 proved to be homozygous for the *ALDC* transgene (Figure 4.7). The expression of *ALDC* was assessed in two independent plants for each of the two homozygous T_3 generation A-line plants using *elongation factor 1-alpha* (*EF-1 α*) as the reference gene (Figure 4.8). All the plants for A6.8 and A8.5 showed equal expression of *ALDC*.

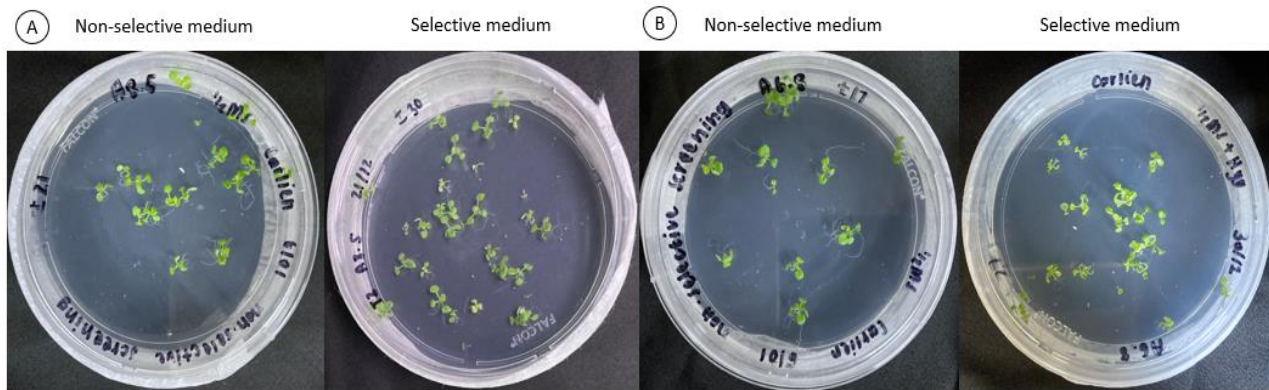


Figure 4.7: Screening T_3 putative seedlings for homozygous line. Seeds obtained from T_2 A-line plants were screened for homozygosity by sowing a small batch of seed on media containing 15 $\mu\text{g/mL}$ hygromycin. Germination and growth were allowed for 16 days, whereafter the germination percentage was determined, taking into consideration seed viability which was calculated by sowing seeds on non-selective plates. Lines showing 90-95% germination were considered homozygous and used in further experiments. Homozygous lines identified were **A)** A8.5 and **B)** A6.8 which are shown on non-selective and selective media.

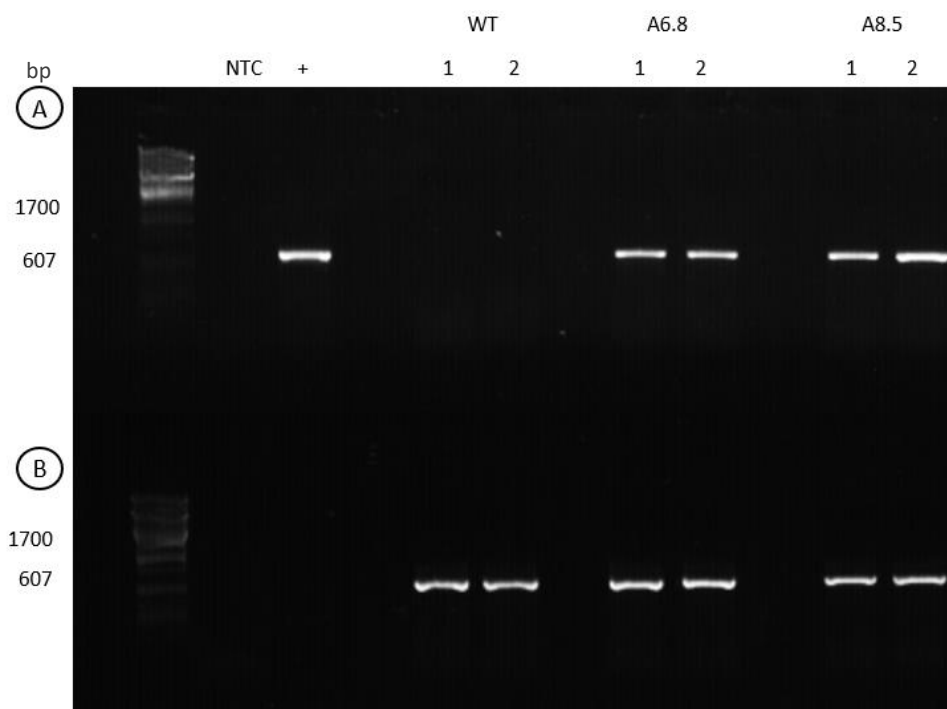


Figure 4.8: Expression level of *ALDC* in T_3 generation A-line plants.. The expression level of the *ALDC* gene was determined using **A)** gene-specific primer set (AF3/AR1) and **B)** *EF-1α* as reference gene (*EF-1α F*/*EF-1α R*). Indicated are base pairs (bp); non-template control (NTC); positive control of pUBI50::*ALDC* plasmid DNA (+); *Arabidopsis thaliana* Col-0 (WT); homozygous T_3 A-line 6.8 (A6.8); homozygous T_3 A-line 8.5 (A8.5); and 1 and 2 indicate individual plants.

4.3.2 Detection of acetoin production *in planta*

Two 30 d-old T₃ A-line transgenic plants (A8.7 and A10.6) were placed in SPME vials for 6 d to show successful production of acetoin due to the presence of the *ALDC* gene *in planta* (Figure 4.9). The negative control (WT *Arabidopsis* Col-0) showed no peak for acetoin at the expected retention time of between 14.50 and 14.85 min. The WT leaf spiked with pure synthetic acetoin showed a saturated peak for acetoin at a retention time of 14.83 min. Acetoin was detected at 14.57 and 14.59 min retention time for A8.7 and A10.6, respectively.

Furthermore, the acetoin production of the two identified homozygous lines (A6.8 and A8.5) for the T₃ A-line transgenic plants were analysed at different growth stages to determine the effects of plant developmental age on acetoin production (Table 4.4). Due to time constraints only the first two growth stages were analysed for A6.8. For the A6.8 plant at 13 d (four leaf stage), acetoin was detected at a retention time of 14.52 min with a relative abundance (peak height) of 12%, whereas acetoin detected at 14.57 min for the 21 d old A6.8 plant had a relative abundance of 14% (Figure 4.10). Analysing the peak area for acetoin through the simple internal normalization procedure in both A6.8 growth stages resulted in an estimate acetoin concentration value of 0.22% and 0.07%, respectively. Thus, the percentage of acetoin detected based on the peak area decreased from the 13 d old plant to the 21 d old plants.

Four different growth stages were analysed for A8.5 and the acetoin relative abundance increased from a minute amount at age 13 d (4 leaf stage) to 66% at 30 d (10 leaf stage) but decreased to 52% relative abundance at the age of 52 d (14 leaf stage; Figure 4.11). A similar trend to the relative abundance was seen for the calculated simple internal normalization value (Table 4.4). The different A8.5 growth stages produced an estimate acetoin concentration of 0.01%, 0.08%, 0.49% and 0.44% respectively. The percentage of acetoin peak area increased from the 13 d old plant to the 30 d old plants, whereafter it decreased to 0.44% for the 52 d old plant.

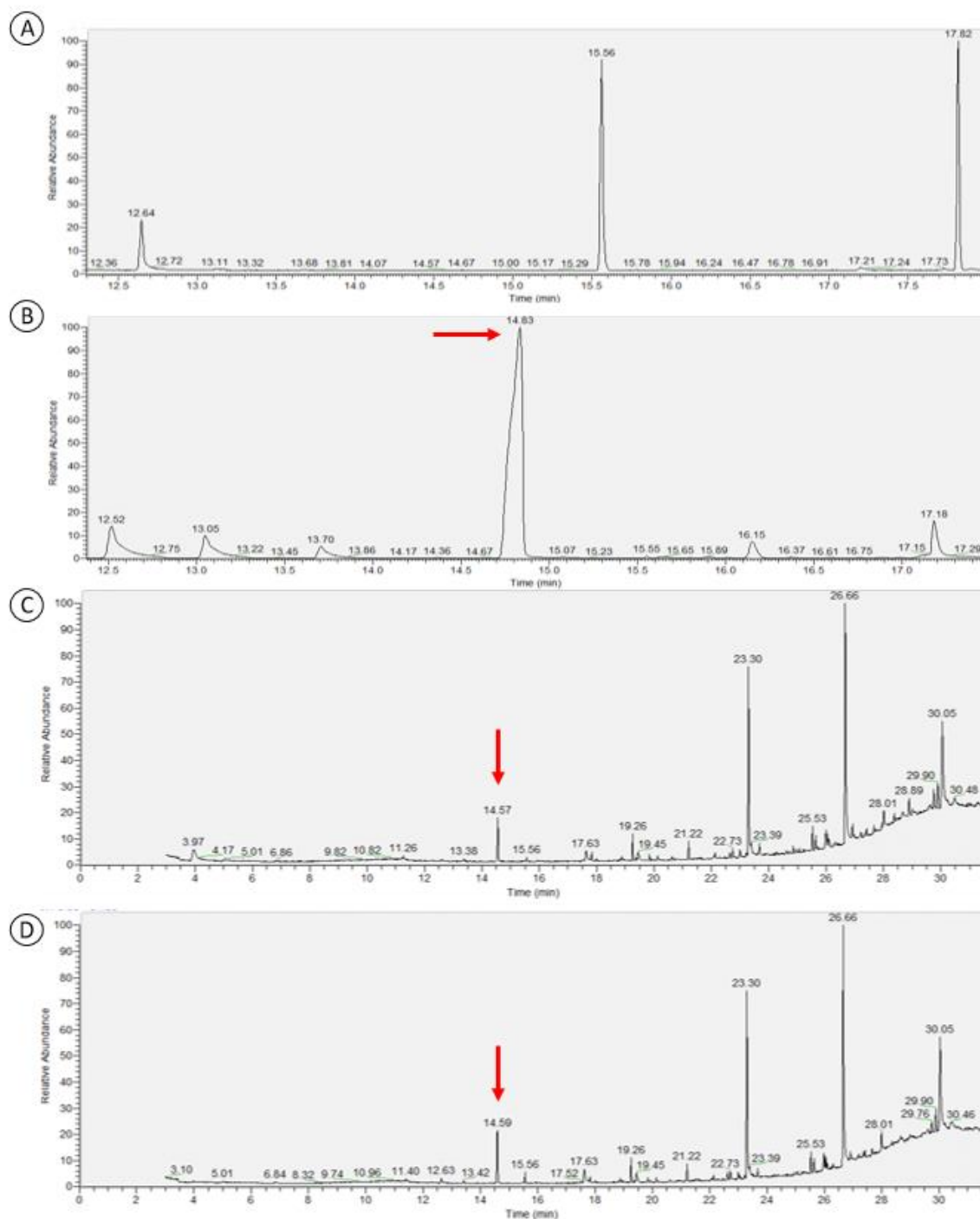


Figure 4.9: Gas chromatography-mass spectrometric analysis of transgenic T_3 plants. Whole 30 d old T_3 transgenic *Arabidopsis* plants were placed in a SPME headspace vials with 2 ml $\frac{1}{2}$ MS media for 6 days to determine if plants produced the volatile compound, acetoin. **A)** Wild-type *Arabidopsis* Col-0 leaf (WT) and **B)** WT leaf spiked with synthetic acetoin were used as controls. Acetoin was detected in the WT leaf spiked with acetoin at a retention time of 14.83 min. Acetoin was detected in the two transgenic A-line plants, **C)** A8.7 at 14.57 min and **D)** A10.6 at 14.59 min. (A8.7: T_3 A-line transgenic *Arabidopsis* plant; A10.6: T_3 A-line transgenic *Arabidopsis* plant; Red arrow: Indicates acetoin peak)

Table 4.4: Growth stages of two transgenic lines analysed by GC-MS to determine the effect of age on acetoin production

A-line	Age	# of leaves	Whole plant or only leaf	Vegetative or reproductive	Simple internal normalization value (%)
A6.8	13 d	4	Whole	Vegetative stage	0.22
	21 d	8	Whole	Vegetative stage	0.07
A8.5	13 d	4	Whole	Vegetative stage	0.01
	21 d	8	Whole	Vegetative stage	0.08
	30 d	10	Whole	Vegetative stage	0.49
	52 d	14	Leaf	Start of reproductive stage	0.44

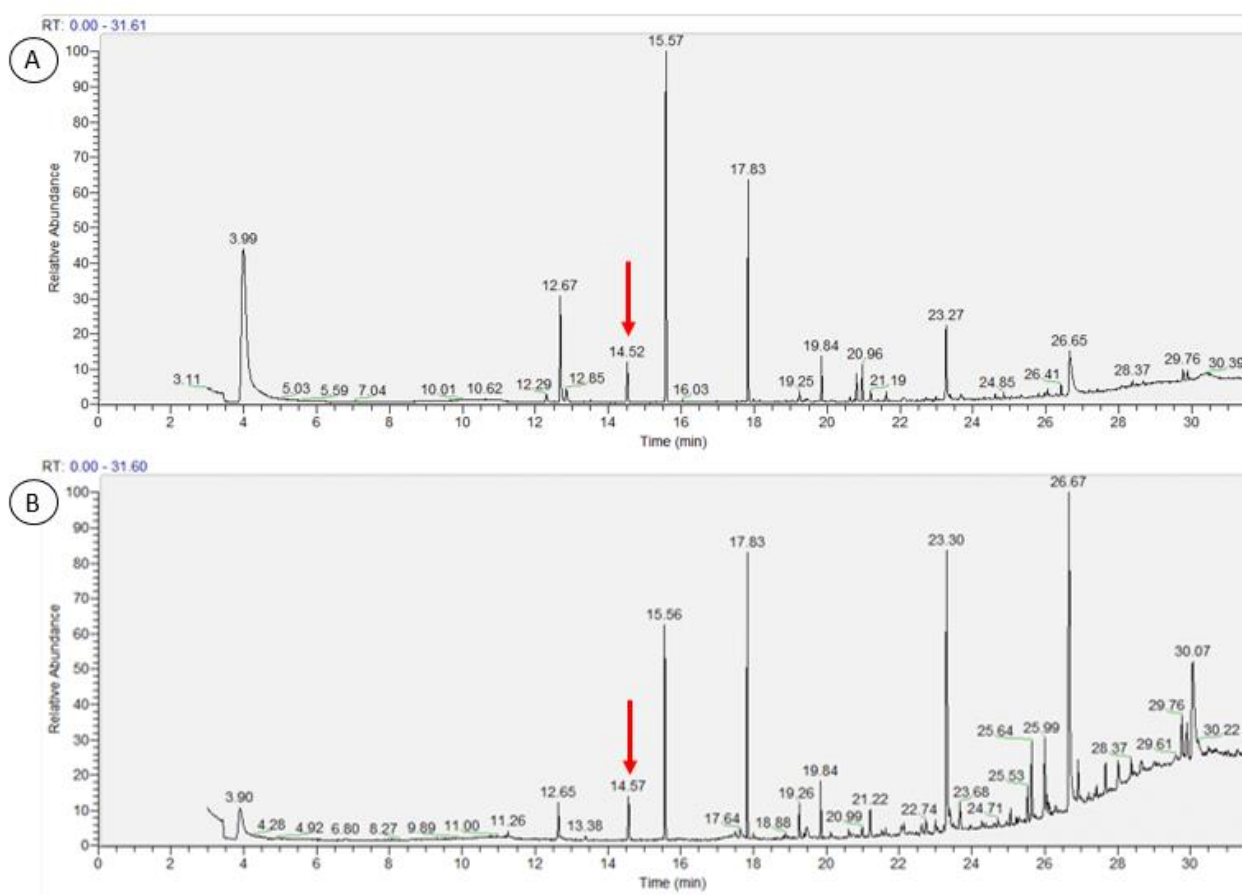


Figure 4.10: Gas chromatography-mass spectrometric analysis at different growth stage of transgenic T₃ A6.8 plants. Whole T₃ A6.8 *Arabidopsis* plants at different age and leaf stage were placed in a SPME headspace vials with 2 ml ½ MS media for 6 days to estimate the amount of acetoin produced. Acetoin was detected in the **A**) whole 13 d old plant (4 leaves) at 14.52 min and in the **B**) whole 21 d old plant (8 leaves) at retention time of 14.57 min. Acetoin peak is indicated by red arrow.

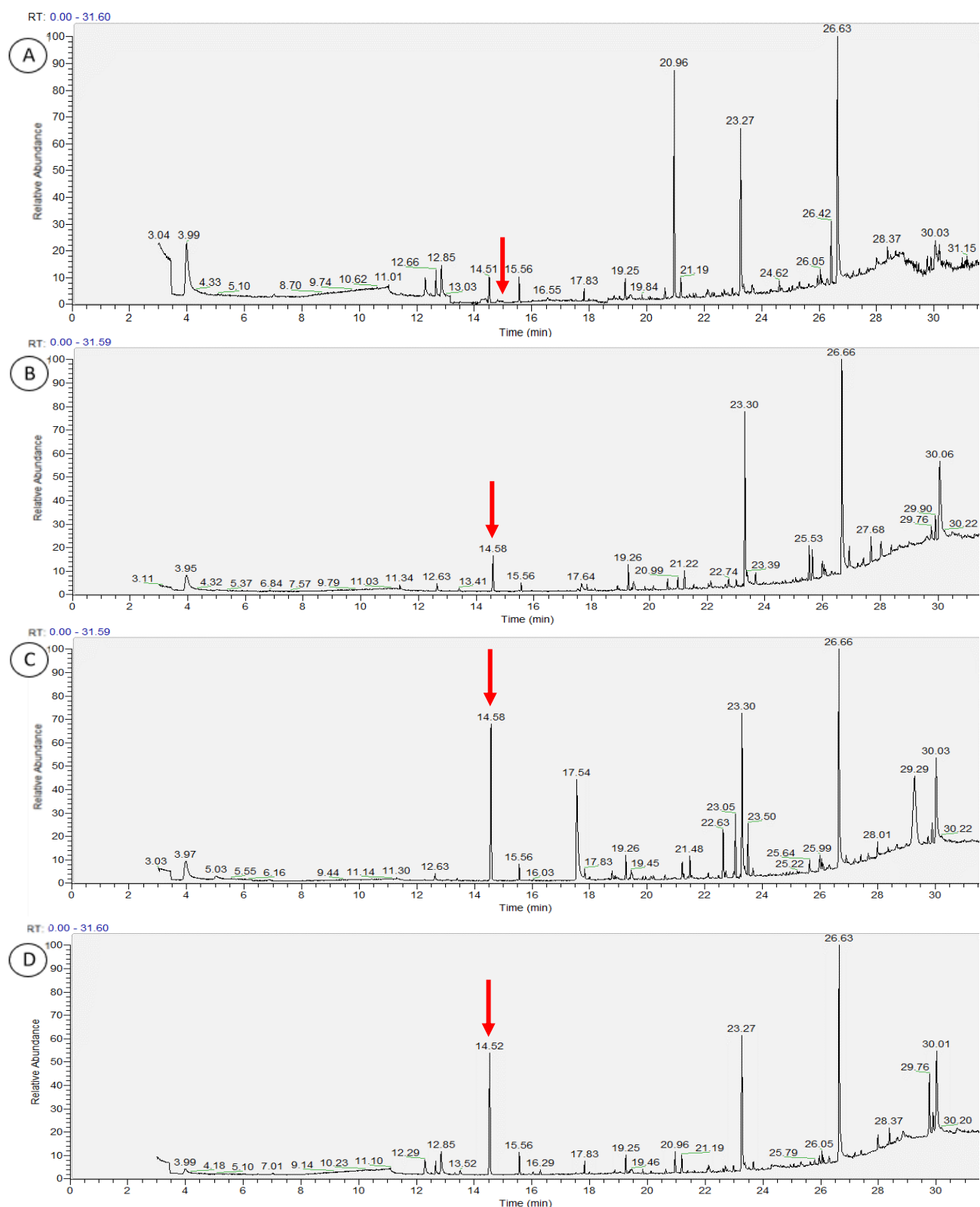


Figure 4.11: Gas chromatography-mass spectrometric analysis at different growth stage of transgenic T_3 A8.5 plants. The T_3 A8.5 *Arabidopsis* plants at different growth were placed in a SPME headspace vials for 6 days to estimate the amount of volatile compound, acetoin produced. Acetoin was detected in the **A)** whole 13 d old plant with 4 leaves at 14.86 min in trace amounts, **B)** whole 21 d old plant with 8 leaves at 14.58 min, **C)** whole 30 d old plant with 10 leaves at 14.58 min, and **D)** single leaf of 52 d old plant with 14 leaves at start of reproductive stage at retention time of 14.52 min. Acetoin peak is indicated by red arrow.

4.3.3 Transgenic plant growth versus wild-type plant growth

The growth and salinity stress tolerance of WT *Arabidopsis* was compared to the plants from two independent homozygous transgenic A-lines using identically-sized 13 d old seedlings to set up trials. After two weeks of growth, the plants were measured and photographed (Figure 4.12). Visual comparison of the plates did not show a distinct difference between plant lines, however A8.5 appeared slightly larger and more leaves were distinguishable compared to A6.8 and WT plants. Analysis of the plant growth data showed that the fresh mass measurement for A6.8 and A8.5 transgenic plants did not significantly differ from WT plants, while the dry mass of the A6.8 plants in comparison to A8.5 and WT was significantly decreased with a p value of 0.012 (Figure 4.13). The A8.5 plants had a similar rosette diameter to both WT and A6.8 plants, while the rosette diameter measurement for the A6.8 plants were significantly decreased compared to the WT with a p value of 0.002. There were no significant differences for growth parameters between WT and transgenic lines experiencing salinity stress (100 mM NaCl; Figure 4.14).

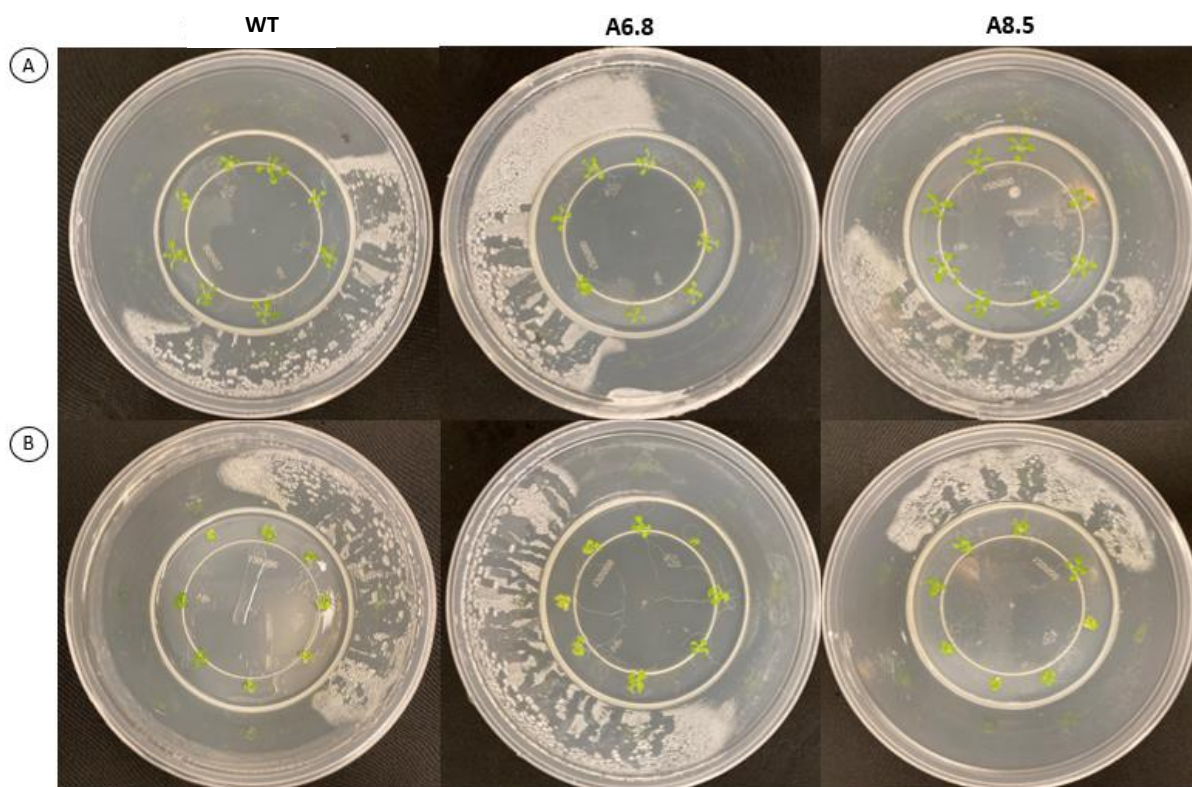


Figure 4.12: Growth and salinity stress trials to compare WT *Arabidopsis* to transgenic *Arabidopsis* plants. The growth parameters were compared between wild-type *Arabidopsis thaliana* Col-0 (WT) and T₃ homozygous A-lines (A6.8 and A8.5) through **A)** growth and **B)** salinity stress trials. After two weeks at long-day-length (14 h:10 h photoperiod) conditions, the plates were photographed, and fresh mass, rosette diameter, and dry mass of plants were measured.

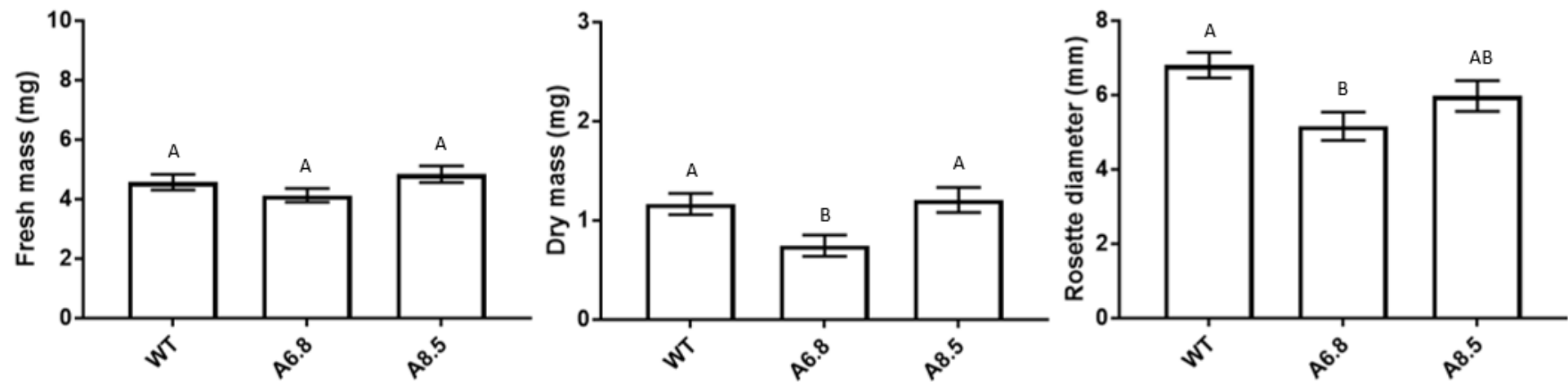


Figure 4.13: Analysis of *in vitro* plant growth of wild-type *Arabidopsis* compared to transgenic *Arabidopsis* possessing the *ALDC* gene. The fresh mass (mg), rosette diameter (mm) and dry mass (mg) of 13 d old wild-type *Arabidopsis thaliana* Col-0 (WT) and two T₃ homozygous transgenic *Arabidopsis thaliana* lines (A6.8 and A8.5), grown under a 14 h:10 h light:dark photoperiod *in vitro* for 14 d was compared. Values represent the mean \pm SE ($n = 48$). For the dry mass, three plants were measured together for greater accuracy of measurement. Different letters indicate a value that was determined to be significantly different ($p \leq 0.05$) by one-way ANOVA and Fisher's LSD multiple comparisons test.

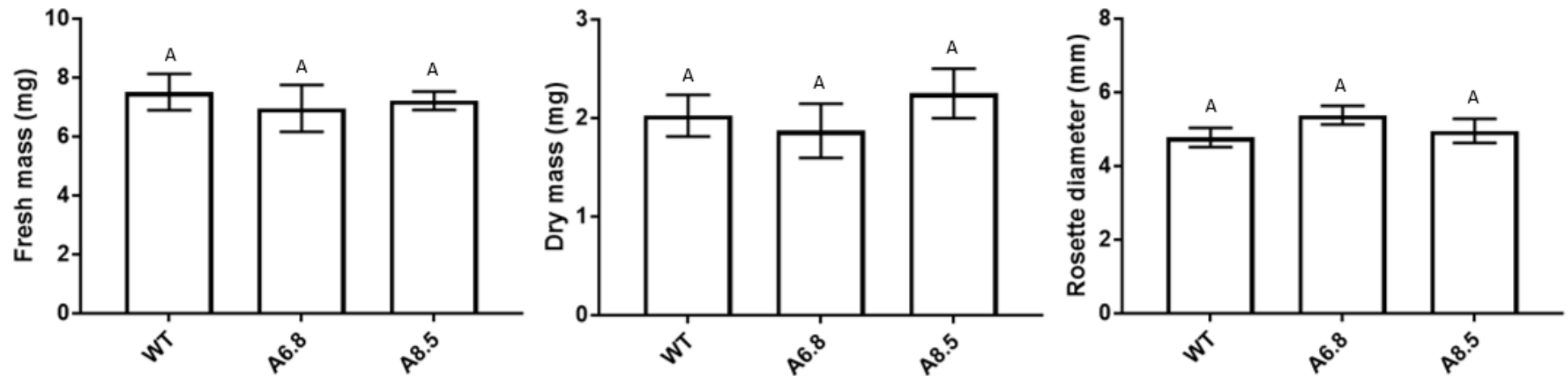


Figure 4.14: Analysis of *in vitro* salinity stress tolerance of wild-type *Arabidopsis* compared to transgenic *Arabidopsis* possessing *ALDC* gene. The fresh mass (mg), rosette diameter (mm) and dry mass (mg) of 13 d old wild-type *Arabidopsis thaliana* Col-0 (WT) and two transgenic *Arabidopsis thaliana* lines (A6.8 and A8.5), grown under a 14 h:10 h light:dark photoperiod *in vitro* for 14 d was compared. Values represent the mean \pm SE (n = 24). For the dry mass, three plants were measured together for greater accuracy of measurement. Different letters indicate a value that was determined to be significantly different ($p \leq 0.05$) by one-way ANOVA and Fisher's LSD multiple comparisons test.

Additionally to *in vitro* growth trials, the growth of WT *Arabidopsis* was compared to the two independent transgenic A-line plants (A6.8 and A8.5) grown *ex vitro* in peat from seeds for 30 d. Five plants for each genotype were photographed and measured for comparison of growth (Figure 14.16). Unlike the *in vitro* growth trial which showed no significant increase in fresh mass for the transgenic lines, A6.8 plants had a significantly higher fresh mass compared to WT and A8.5 plants *ex vitro* (Figure 14.17). Furthermore, the A6.8 plants also had a significantly higher dry mass than WT and A8.5 plants grown *ex vitro*, but A6.8 showed a significant decrease in dry mass when grown *in vitro*. The growth of the A8.5 plants, however, did not significantly differ from WT plants either *in vitro* or in the peat disks.



Figure 4.15: *Ex vitro* growth trials to compare wild-type *Arabidopsis* to transgenic *Arabidopsis* plants. Seeds of wild-type *Arabidopsis* (WT) and two transgenic *Arabidopsis thaliana* lines (A6.8 and A8.5), were sown in water saturated peat, respectively and allowed to germinate. After 30 days at long-day-length (14 h:10 h photoperiod) conditions, the plants were photographed, and fresh mass, rosette diameter, and dry mass of plants were measured.

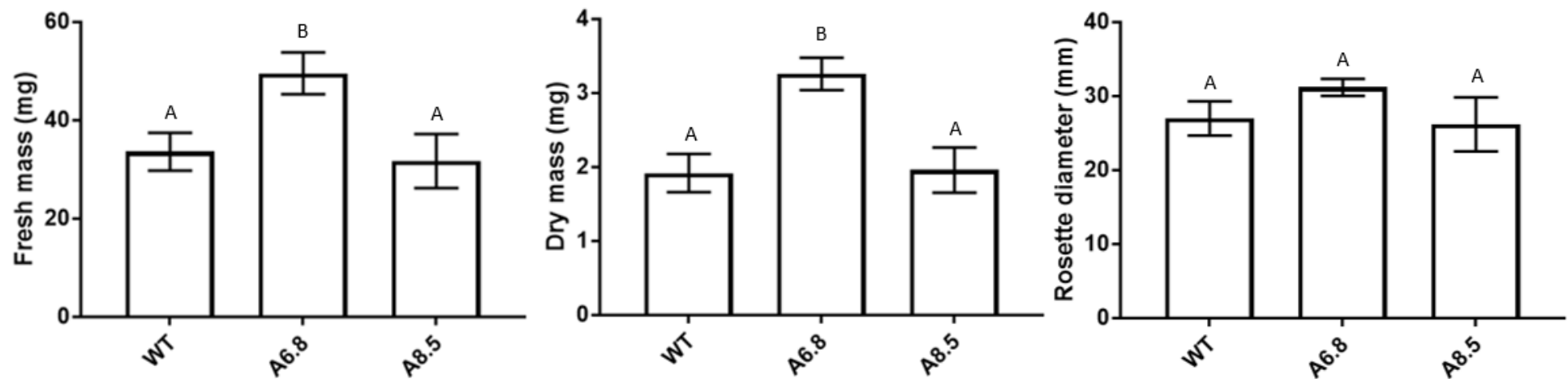


Figure 4.16: Analysis of *ex vitro* plant growth of wild-type *Arabidopsis* compared to transgenic *Arabidopsis* possessing *ALDC* gene. The fresh mass (mg), rosette diameter (mm) and dry mass (mg) of 30 d old wild-type *Arabidopsis thaliana* Col-0 (WT) and two transgenic *Arabidopsis thaliana* lines (A6.8 and A8.5), grown in peat under a 14 h:10 h light:dark photoperiod was compared. Values represent the mean \pm SE (n = 5). For the dry mass, each plant was measured separately. Different letters indicate a value that was determined to be significantly different ($p \leq 0.05$) by one-way ANOVA and Fisher's LSD multiple comparisons test.

4.3.4 Trials with transgenic plant as acetoin source

The growth trials were conducted by exposing WT *Arabidopsis* to plants from two independent homozygous transgenic T₃ A-lines (A6.8 and A8.5) as a potential acetoin source to enhance the growth of the WT plants. Identically-sized 9 d old WT seedlings were employed to set up trials and after two weeks of exposure to 16 d old A8.5 or A6.8 plants, WT plants were measured and photographed (Figure 4.17). Visual comparison of the plates showed a similar sized WT plant for the untreated and treatment with A8.5 plants, while the WT plants in the A6.8 treatment were clearly smaller, with fewer developed leaves. The transgenic plants utilized for A6.8 as acetoin source were also smaller than the transgenic plants used for A8.5. Analysis of the data pertaining to plant growth of WT *Arabidopsis* exposed to transgenic *Arabidopsis* as a potential acetoin source showed that all growth parameters measured were significantly decreased in WT plants exposed to A6.8 plants, in comparison with untreated WT plants (Figure 4.18). However, the exposure to A8.5 plants resulted in measured growth parameters that were similar to the untreated plants.

Additionally, an intact 16 d old plant from both the A8.5 and A6.8 lines were placed in SPME vials and sent for GC-MS analysis for an estimate of the acetoin production from these plants over the period of the conducted growth trial (Figure 4.19). Acetoin was detected for both the A6.8 and A8.5 plants, at retention times of 14.55 min (relative abundance of 28%) and 14.56 min (relative abundance of 36%), respectively. The estimated acetoin concentration values calculated by the simple internal normalization procedure was 0.17% for A6.8 and 0.24% for A8.5 respectively.

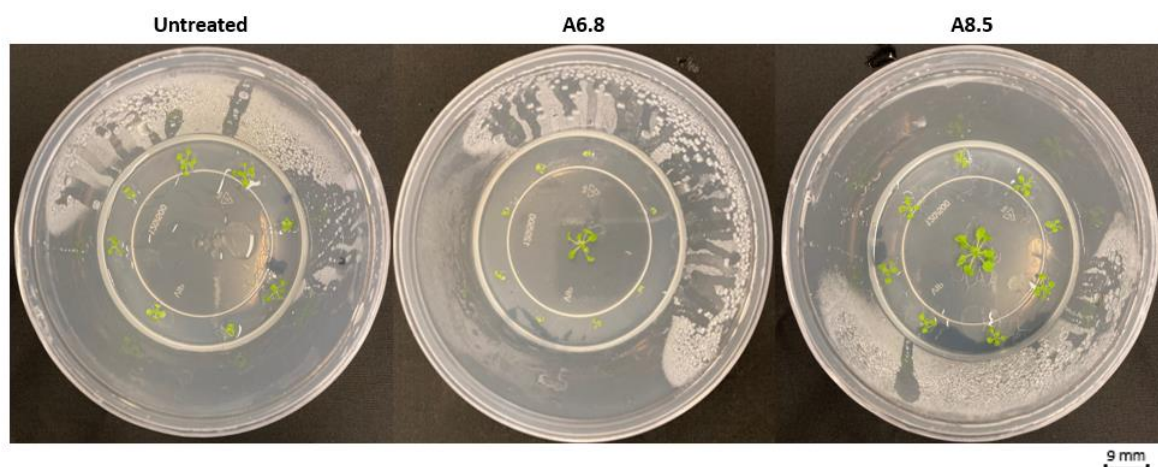


Figure 4.17: *In vitro* growth trials to study effect of transgenic *Arabidopsis* plants as acetoin source on neighbouring wild-type *Arabidopsis* plants. Identically-sized 13 d old WT seedlings surrounding a 16 d old transgenic plant (A6.8 and A8.5) were used to set up the experiment. After two weeks of exposure to the respective transgenic A-line plants, the plates were photographed, and fresh mass, rosette diameter, and dry mass of plants were measured. Growth trials were conducted at long-day-length (14 h:10 h photoperiod) conditions.

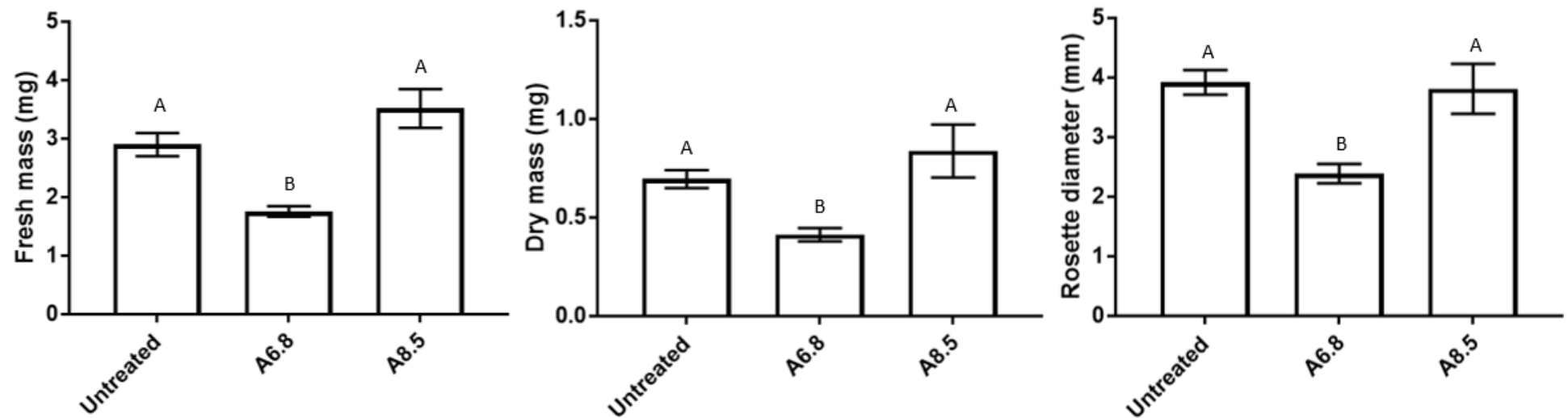


Figure 4.18: Analysis of *in vitro* plant growth of wild-type *Arabidopsis* exposed to transgenic *Arabidopsis* possessing *ALDC* gene. The fresh mass (mg), rosette diameter (mm) and dry mass (mg) of 13 d old *Arabidopsis thaliana* Col-0 exposed to 16 d old transgenic *Arabidopsis thaliana* plants (A6.8 and A8.5), grown under a 14 h:10 h light:dark photoperiod *in vitro* for 14 d was compared. Values represent the mean \pm SE (n = 48). For the dry mass, three plants were measured together for greater accuracy of measurement. Different letters indicate a value that was determined to be significantly different ($p \leq 0.05$) by one-way ANOVA and Fisher's LSD multiple comparisons test.

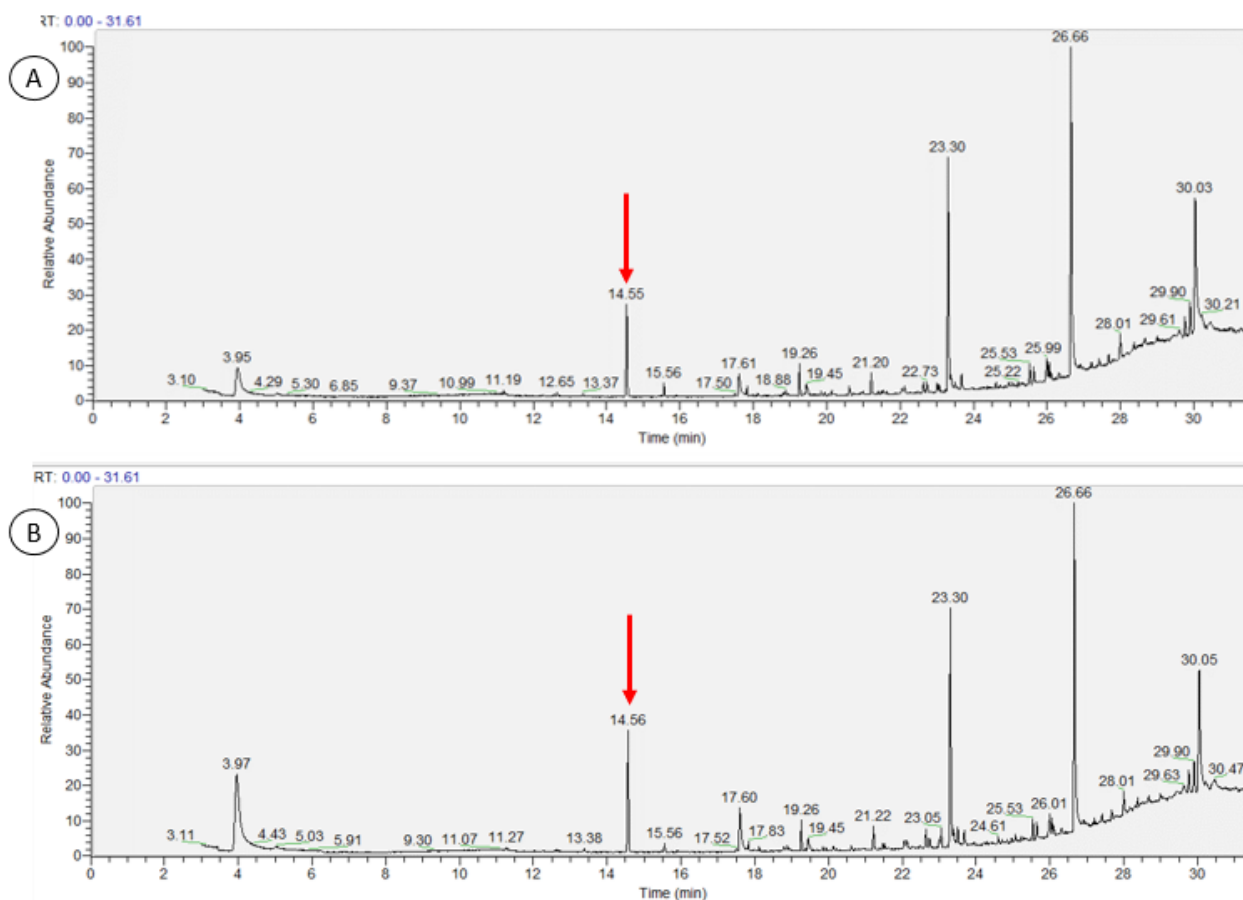


Figure 4.19: Gas chromatography-mass spectrometric analysis of 16 d old transgenic T_3 plants allowed to accumulate acetoin for 11 days. Whole 16 d old T_3 *Arabidopsis* plants of A6.8 and A8.5, respectively were placed in a SPME headspace vials (SU86009, 10 ml, Merck) with 2ml $\frac{1}{2}$ MS media for 11 days to estimate the amount of acetoin accumulated in containers during TGAS trial. Acetoin was detected in the **A)** A6.8 plants at 14.55 min and in the **B)** A8.5 plant at retention time of 14.56 min. (TGAS: Transgenic plant as acetoin source, Red arrow: Indicates acetoin peak)

4.4 Discussion

4.4.1 Detection of acetoin production *in planta*

Acetoin production was shown *in planta* for homozygous and heterozygous T₃ transgenic A-line plants possessing the *ALDC* transgene encoding the protein that is responsible for the conversion of α -acetolactate to acetoin (Figure 4.9). The successful detection of acetoin *in planta* supports the semi-quantitative analysis of the gene expression, by confirming that the *ALDC* gene was expressed and successfully translated to a functional protein. Furthermore, the GC-MS results revealed that the homozygous transgenic plants from the two independent lines produced different levels of acetoin, despite the fact that the relative transgene expression levels of the two lines obtained from RT-sqPCR were similar (Figure 4.10; Figure 4.11). Most likely the RT-sqPCR is insufficiently sensitive to detect any subtle differences in gene expression between the two homozygous lines which could have resulted in different protein levels, consequently causing the difference in acetoin levels.

The retention time for acetoin represents the time the analytes took to pass through the chromatographic column to reach the MS detector, which ranged from 14.50 and 14.85 min between different samples analysed. Retention time can be influenced by factors such as the flow rate, column used, and injection temperature, to name a few, which results in different retention times for the same analyte obtained by different machines and/or laboratories (Guiochon and Guillemin, 1988; Brevard *et al.*, 2011). Even the same conditions (same machine, same temperature etc.) will result in the retention time varying by seconds, consequently the peak obtained is also cross-referenced with an internal standard and the NIST11 mass spectral library of known compounds to ensure that the correct compound is identified (Addendum 2 Figure 5.5). The peak height or relative abundance can also be influenced by factors such as temperature, influencing repeatability and causing fluctuations in measured data points (Guiochon and Guillemin, 1988). However, the effects of temperature on the peak area are minute and comparisons based on peak area are generally more reliable than comparing relative abundance (peak height), particularly when paired together with standardised controls of known concentrations (Guiochon and Guillemin, 1988; Brevard *et al.*, 2011). In this study, the comparison of the volatile profiles for the plant growth stages analysed for both transgenic lines revealed that the 13 d old A8.5 plant showed an estimated concentration of 0.01% acetoin, based on the ratio of the acetoin peak to the total peak area of the chromatogram, compared to 0.22% calculated for the A6.8 plant at the same growth stage (Figure 4.10; Figure 4.11). However, the 21 d old plants for A8.5 and A6.8 had somewhat similar values of 0.8% and 0.7%, respectively. Wild-type plants showed no peak for acetoin. It is possible that the insertion site of the transgene is responsible for the delay in initial acetoin production seen for A8.5, but at 21 d of age the two lines produced a similar ratio of acetoin to other compounds in their respective volatile profiles. The A8.5 plant appeared to produce an estimated higher concentration of acetoin as it aged, whereas the A6.8

plant produced slightly less acetoin at an older growth stage. Based solely on the estimated acetoin concentration for A8.5, the plant seemed to increase acetoin production from 13 d to 30 d, which is the growth period regarded as the vegetative growth stage, whereafter the acetoin concentration slightly decreased when measured at the start of the reproductive stage (52 d; Figure 4.11). This slight decrease might correlate to the pressure of changes in hormones and carbohydrate assimilates to facilitate the transition from the vegetative to reproductive stage (Huijser and Schmid, 2011). At this stage, nutrient and energy sources would be redirected to fuel the reproductive systems, potentially reducing acetoin production.

4.4.2 Transgenic plant growth versus wild-type plant growth

Comparison of the *in vitro* growth parameters of WT plants versus the plants from the two independent A-lines showed no significant increase for any parameters for either of the transgenic lines (Figure 4.13). Moreover, the A6.8 plants had a significant decrease in average dry mass compared to WT plants. However, the A6.8 plants showed a significant increase in average fresh mass and dry mass compared to WT plants when grown *ex vitro* (Figure 4.16). In both *in vitro* and *ex vitro* conditions, the A8.5 plants grew similarly to the WT plants.

The decrease for dry mass *in vitro* and increase in dry mass *ex vitro* seen for A6.8 can more likely be attributed to the environment of the plants rather than to plant age or developmental stage. The *in vitro* plants grew for 28 days from germination to the conclusion of the trial (13 d pre-trial, 14 d during trial), whilst the *ex vitro* plants grew from seed for 30 days until the conclusion of the trial, thus the *in vitro* plants and *ex vitro* plants were of a similar age. The comparison of average plant fresh mass and dry mass measurements of the wild-type plants *in vitro* and *ex vitro* indicate that *Arabidopsis* plants prefer *ex vitro* conditions above humid *in vitro* conditions (Figure 4.13; Figure 4.16). The wild-type plants had an average fresh mass of 4.5 mg *in vitro*, whereas *ex vitro* plants had a 7 times higher average fresh mass of 33.62 mg. The average dry mass difference between *in vitro* (1.16 mg) and *ex vitro* (1.92 mg) plants were less than 2 times higher for *ex vitro* plants. Most likely *Arabidopsis* do not perform at optimal levels and smaller plants meant less acetoin was produced as the cost of expressing the transgene and subsequently producing acetoin most probably outweighed the growth promoting benefit of the volatile. Furthermore, the fact that the *in vitro* plants were enclosed, while the *ex vitro* plants were exposed to the large growth room environment, could have resulted in acetoin build-up in the container that might be detrimental to plant growth. A study by Sharifi *et al.* (2020) observed phytotoxicity in the leaf margins of 2 d old *Arabidopsis* plants exposed to 2 ng synthetic acetoin for 14 days *in vitro*, whereas Dempers (2015) showed significant increase in the leaf surface area for 14 d old *Arabidopsis* plants exposed to 2 ng acetoin for 10 days *in vitro*. It can thus be argued that the effect of acetoin on plant growth will be dependent on the plant age, concentration of acetoin, exposure period, and environmental

conditions. The plants grown *ex vitro* were not in an enclosed container and theoretically plants could use the necessary acetoin *in planta* and release any excess amounts into the environment. This could result in plants having an optimal concentration of acetoin present to elicit dry mass promotion, as seen for *ex vitro* A6.8 plants.

The A8.5 plants did not differ from the WT plants *in vitro* or *ex vitro*, regardless of relatively similar transgene expression to A6.8 plants and acetoin production being detected via GC-MS. A possible reason is that the site of insertion of the transgene affected an endogenous gene. Furthermore, *in vitro* A8.5 plants did not seem to be affected positively or negatively by the possible build-up of acetoin in the container as growth parameters were similar to WT plants (Figure 4.13). Based on the GC-MS analysis at different growth stages, the A8.5 plant in each consecutive growth stage (13 d to 30 d) had an increased proportion of acetoin in relation to the total peak area of the chromatogram (0.01% to 0.49%). Different transgenic lines can exhibit differences in growth and metabolism, presumably due to positional effects from the site of insertion of the transgene. Moreover, it is possible that in A8.5 plants the potential strain of producing acetoin might have affected growth by depleting α -acetolactate. AA consequence of such an event would be a depletion in the levels of, branched-chain amino acids (BCAA) as their biosynthesis is linked to the amount of α -acetolactate available (Xu *et al.*, 2011). In a previous study, BCAA analysis on an 8 week old transgenic A-line *Arabidopsis* plant showed no changes in amino acid levels (Dempers, 2015). However, plants in this study were 4 weeks old at their oldest and amino acid changes might have occurred at this particular age. Furthermore, the GC-MS analysis appears to indicate that the A8.5 plants started to produce acetoin later than the A6.8 plants, based on growth stages analysed with GC-MS (Figure 4.10; Figure 4.11). It is thus possible that A6.8 had a higher accumulation of acetoin from an earlier stage than A8.5, resulting in the significant decrease in dry mass and rosette diameter seen for A6.8 compared to WT plants. Furthermore, the ALDC protein produced by A8.5 may have posttranslational changes not present in the A6.8-produced protein due to effect of the particular genome context. The A8.5 plants might have exhibited similar effects if the trial was prolonged or conducted under different photoperiods. A similar study on the effects of acetoin production *in planta* on *Arabidopsis* found that at 16 h:8 h (day:night) photoperiod, a 14 d old T₃ transgenic plant (A line) had significantly higher measurement for growth parameters (fresh mass, dry mass, and leaf surface area) compared to WT plants (Dempers, 2015). The results from Dempers (2015) indicate that *in planta* production of acetoin can be beneficial and further optimization and investigation is required to determine the effect of different factors on the system. Furthermore, the plant age in this study was based on DAS (Days after sowing) and not DAG (Days after germination), which could skew the results if seeds from the different treatments did not germinate at exactly the same time.

4.4.3 Trials with transgenic plants as acetoin source

As novel investigation, it was tested whether the transgenic A-line plants could enhance the growth of other plants in their surroundings. It is hypothesized that if the transgenic *Arabidopsis* can achieve this, it could lead to the possible use these plants to enhance growth of other plants that could not be genetically altered. The potential for transgenic lines to act as an acetoin source for WT plants was tested *in vitro*, and wild type plants exposed to A8.5 transgenic plants did not differ significantly from the untreated control plants (Figure 4.18). On the contrary, the plants exposed to A6.8 showed significant decreases in all growth parameters compared to the WT plants. As trials were in an enclosed container, it is a possibility that the humid environment *in vitro* resulted in smaller plants, as evidenced by a comparison of the growth differences between wild-type plants grown *in vitro* and *ex vitro*. Furthermore, the possible build-up of acetoin in the container could be detrimental to plants as mentioned previously. A 16 d old plant for each transgenic line was placed in a SPME vial for 11 days to estimate the acetoin accumulation for each transgenic line for the period similar to the trial conducted (Figure 4.19). Interestingly, the A8.5 had an estimated acetoin concentration of 0.24%, while A6.8 had a 0.17% estimated acetoin concentration. As these concentrations are only an estimate and require a known concentration curve to validate, the cause and effect can only be speculated. Two studies exposing differently aged plants to 2 ng synthetic acetoin observed phytotoxicity in leaf margins of 2 d old plants and significant increase in leaf surface area for 14 d old plants, respectively (Dempers, 2015; Sharifi *et al.*, 2020). Thus, it is possible that different outcome could be observed at different plant growth stages (age), exposure period, and environmental conditions. It could also point to changes in acetoin concentration affecting the ability of plants to detect the volatile and would explain why A8.5 plants did not result in any increase or decrease in any growth parameter measured in the different trials. Due to time constraints, the system could not be optimised, tested for IST abilities or in *ex vitro* environment.

4.5 Conclusion

The previous research conducted by Dempers (2015) was unable to show that the single transgenic A-line *Arabidopsis* investigated with enhanced growth compared to WT *Arabidopsis* did indeed produce acetoin *in planta*. The current study improved on previous research by generating new recombinant vectors containing the *ALDC* transgene and transgenic plant material that resulted in two independent homozygous A-line *Arabidopsis* that did not exhibit gene silencing. Furthermore, this study successfully detected the *in planta* acetoin production that supports the hypothesis that *Arabidopsis* can produce acetoin *in planta* while maintaining growth similar or better than WT plants. Moreover, the current study included salinity stress tolerance in addition to growth promotion, as well as investigated the potential of the transgenic plants to enhance growth of other plants in their vicinity, not previously done.

Two independent transgenic *Arabidopsis thaliana* lines were successfully established with the ability to produce acetoin *in planta*. Dempers (2015) showed enhanced growth and a preliminary increase in salinity stress tolerance (not shown in thesis) for a single homozygous A-line plant *in vitro*, previously. It was expected to observe similar results in this study. However, the presence of the transgene did not enhance plant growth compared to WT *Arabidopsis thaliana* under the *in vitro* conditions tested as would have been expected. Furthermore, neither of the two lines showed enhanced salinity stress tolerance *in vitro*. As previously discussed, the most likely reason for this is the humid environment negatively influencing *Arabidopsis* growth, as the A6.8 line significantly outperformed the WT plants in both fresh and dry biomass when grown *ex vitro*. The A8.5 line had growth that was similar to the WT. Based on the GC-MS analysis, the two homozygous lines produced acetoin at different concentrations depending on plant developmental stage, and the trend of acetoin production analysed over developmental stages differed for each line. The results indicated that the effects of acetoin production *in planta* was not conserved between the independent homozygous lines.

Further analysis would be required to determine differences in the transgene expression for A6.8 and A8.5, as the RT-sqPCR method used is probably not sufficiently sensitive and RT-qPCR would be better suited for this purpose. Furthermore, *in vitro* conditions appear to not be ideal for *Arabidopsis* growth analysis and as lines are homozygous, there is no need for a selection step which would require such *in vitro* conditions. Thus, it is suggested that future work should focus on *ex vitro* trials. Further analysis could also investigate whether the levels of acetoin produced were detrimental to plant growth or if the insertion site or posttranslational modifications are responsible for the lack of growth promotion and IST observed *in vitro*. In future, additional homozygous lines should be generated to determine whether similar effects will be observed to either of the two lines investigated in this study, in order to more accurately conclude that observations were due to

presence of acetoin. The simple internal normalization method used to estimate acetoin concentrations in chromatograms is not ideal and other methods utilizing known concentration standards to determine specific peak concentrations would be advised. Moreover, future trials with the transgenic A-lines should be conducted at different photoperiods (including 10 h:14 h, 14 h:10 h, and 16 h:8 h day:night) as the research described in Chapter 2 has indicated the influence of the photoperiod on acetoin's ability to elicit plant growth promotion. As seen in GC-MS analysis at different developmental stages, it is suggested that plant developmental stage will affect the amount of acetoin produced. It has also been observed that different studies investigated different periods of time when conducting volatile studies, which might have different results (Ryu *et al.*, 2003; Dempers, 2015; Sharifi *et al.*, 2020). Thus, it would be advisable to study the effect of acetoin production *in planta* on growth parameters at different plant developmental stages, for different periods of time, and determining the age of plants according to DAG rather than DAS to ensure uniformity amongst plants employed in trials.

Conclusion

The effect of acetoin was tested through applications of the synthetic compound, and as a volatile produced by transgenic *E. coli* and transgenic *Arabidopsis thaliana*. Each chapter resulted in variable results, making it difficult to compare the effects of synthetic acetoin to those of acetoin produced by either the bacteria or plants.

Even though the ALDC protein could not be detected through the protein expression analysis, acetoin was detected from the transgenic *E. coli* BL21-CodonPlus(DE3)-RIPL through GC-MS. Thus, the aim to generate a transformed *Escherichia coli* strain that can produce the volatile acetoin was successful. The presence of the transgenic bacteria in growth and salinity tolerance trials resulted in a significant increase of plant fresh mass compared to plants exposed to the wild-type *E. coli* BL21-CodonPlus(DE3)-RIPL. No significant increase was, however, seen for dry mass. The results suggest that the transgenic *E. coli* BL21-CodonPlus(DE3)-RIPL have the potential to elicit plant growth promotion (fresh mass) and salinity stress tolerance, but this requires further investigation described below. Moreover, the acetoin-producing *E. coli* have the potential to address the shortcomings of utilising the pure compound or a bacterial strain releasing a complex blend of volatile compounds, as described in Chapter 3. This transgenic bacterium will allow for continuous exposure to acetoin, overcoming the issues of depletion observed when using a set amount of the pure compound, whilst allowing the study of the effect of a single volatile. The analysis of single volatile enables an accurate assessment of the growth promotion ability of that specific volatile, rather than a blend of several different compounds potentially affecting the phenotype.

Future studies would be advised to generate a transgenic *E. coli* BL21-CodonPlus(DE3)-RIPL overexpressing both *ALS* and *ALDC*, as the low levels of acetoin observed by the Voges-Proskauer test and GC-MS analysis are probably due to a lack of sufficient α -acetolactate (the precursor to acetoin) being produced by the endogenous *E. coli* *ALS*. Overexpression of *ALS* will most likely result in more α -acetolactate being available for acetoin production to enhance the potential effect on plant growth and stress resistance. Once clear growth promotion and IST is observed, further investigation on bacterial-treated plants at transcriptomic level is also recommended to determine the exact mechanism by which acetoin exerts its effects on plant growth. Preliminary data on root development indicated its potential as another growth parameter affected by acetoin and future analysis of root development during growth trials would be advised.

The main aim of this study was to enhance *Arabidopsis thaliana* growth and salinity stress tolerance by overexpressing the *ALDC* and *BDH1* genes, isolated from fungi and yeast respectively, that are

responsible for the production of acetoin and 2,3-butanediol *in planta*. The generation of transgenic plants able to produce acetoin were successful and two independent homozygous T₃ A-line plants were established. Due to plant death, double transformants (AB-line) with both genes for acetoin and 2,3-butanediol could unfortunately not be generated. However, the overexpression of the transgene *ALDC* and *in planta* production of acetoin in *Arabidopsis* was shown in two independent homozygous A-line plants (A6.8 and A8.5). The presence of the transgene enhanced plant growth for the A6.8 plants grown *ex vitro* compared to the WT *Arabidopsis thaliana*. Neither of the two lines showed enhance growth or salinity tolerance *in vitro*.

Future research should aim to generate additional homozygous lines to further support the effect of acetoin *in planta*. The GC-MS analysis at different growth stages of transgenic plants has the potential to give great insight into the relationship between acetoin production, effects on plant growth, and the developmental stage of plant. However, the lack of a standard curve for acetoin concentration in this study meant that the acetoin concentration had to be estimated through an internal normalization method. This method is not very sensitive or accurate and the development of a protocol to generate a concentration standard to determine specific peak concentrations would be of considerable benefit to future research.

All trials conducted in this study, including with transgenic *E. coli* and *Arabidopsis*, were influenced to some extent by plant age, which was determined by DAS instead of DAG, the latter being more accurate in representation of plant age. The use of DAG would exclude the possible late germination of certain seeds which could skew the results. Most of the trials were conducted with 13 d old (DAS) plants and it was necessary to pool plants for accurate dry mass measurement, which decreased the statistical strength of the experiments by reducing the number of replicate values used to determine significance. Furthermore, the small size of the plants in the *in vitro* trials resulted in the data points being in a narrow range and natural variation is thus likely to have an undue effect on the statistical significance of the results. The small size of the plants was mostly probably due to the *in vitro* conditions and potentially resulted in sub-optimal levels of acetoin being produced. Thus, future studies, including salinity stress tolerance, should focus on *ex vitro* trials, as A6.8 plants resulted in a significant increase in average fresh mass and dry mass compared to WT plants in such studies. Moreover, future trials should be conducted under different photoperiods (including 10 h:14 h, 14 h:10 h, and 16 h:8 h day:night) as photoperiod can influence the ability of acetoin to elicit plant growth promotion and IST. Additionally, the testing of a wider range of concentrations of acetoin, different plant developmental stages, determining age of plants with DAG rather than DAS, and different trial periods should also be considered in future trials.

Overall, the exposure to the transgenic acetoin-producing bacteria was more successful in increasing growth parameters and eliciting salinity tolerance compared to the *in planta* acetoin

production *in vitro*. Based on the observation that *Arabidopsis* in this study did not grow optimally *in vitro*, it suggests that the transgenic bacteria could have a greater effect in *ex vitro* trials in which roots could be exposed to acetoin instead of aerial parts of the plant. Furthermore, acetoin was detected in both the transgenic bacteria and transgenic plants, which could not be achieved with transgenic acetoin-producing plants in previous research by Dempers (2015). Finally, the significant increase in average fresh and dry mass for the *ex vitro* A6.8 plants strongly suggests that with further optimization, the *in planta* production of acetoin will have great potential to enhance plant growth and salinity stress tolerance.

This study has conclusively shown that overexpressing *ALDC* *in planta* in *Arabidopsis thaliana* did result in the production of acetoin and functional plants for at least one of the A-lines that performed similar or better than WT plants. The result, furthermore, suggests that the enhanced growth seen in the single A-line *Arabidopsis* by Dempers (2015) and ISR found by van der Merwe (2016) was most probably due to *in planta* acetoin production, although their method did not detect acetoin at the time. Due to the Covid-19 pandemic resulting in time constraints, trials and systems could not be optimised and thus, this study is regarded as groundwork for subsequent studies to build on with recommendation mentioned above and in individual conclusions. The determination of the effect of *in planta* acetoin production on different age *Arabidopsis* plants and for different periods of time in *ex vitro* conditions, will make it clear if this system will have a potential as method to ultimately enhance growth and adapt to stress situations in crop plants.

Literature cited

- Acosta-Motos JR, Ortuno MF, Bernal-Vicente A, Diaz-Vivancos P, Sanchez-Blanco MJ, Hernandez JA** (2017) Plant responses to salt stress: Adaptive mechanisms. *Agronomy* **7**: 1 - 38. doi:10.3390/agronomy7010018
- Adams SR, Langton FA** (2005) Photoperiod and plant growth: a review. *The Journal of Horticultural Science and Biotechnology* **80**: 2-10. doi:10.1080/14620316.2005.11511882
- Amtmann A** (2009) Learning from evolution: *Thellungiella* generates new knowledge on essential and critical components of abiotic stress tolerance in plants. *Molecular Plant* **2**: 3-12. doi: 10.1093/mp/ssn094
- Arakaki AK, Ceccarelli EA, Carrillo N** (1997) Plant-type ferredoxin-NADP⁺ reductases: A basal structural framework and a multiplicity of functions. *The FASEB Journal* **11**: 133-140. doi: 10.1096/fasebj.11.2.9039955
- Ashraf M** (2004) Some important physiological selection criteria for salt tolerance in plants. *Flora* **199**: 361-376. doi:10.1078/0367-2530-00165
- Assaha DVM, Ueda A, Saneoka H, Al-Yahyai R, Yaish MW** (2017) The role of Na⁺ and K⁺ transporters in salt stress adaptation in glycophytes. *Frontiers in Physiology* **8**: 1-19. doi: 10.3389/fphys.2017.00509
- Baerenfaller K, Massonnet C, Hennig L, Russenberger D, Sulpice R, Walsh S, Stitt M, Granier C, Grisse W** (2015) A long photoperiod relaxes energy management in *Arabidopsis* leaf six. *Current Plant Biology* **2**: 34–45. doi: 10.1016/j.cpb.2015.07.001
- Bailly A, Weisskopf L** (2012) The modulating effect of bacterial volatiles on plant growth. *Plant Signal Behaviour* **7**:79-8. doi: 10.4161/psb.7.1.18418
- Bakka K, Challabathula D** (2020) Amelioration of salt stress tolerance in plants by plant growth-promoting rhizobacteria: Insights from “omics” approaches. *Plant Microbe Symbiosis*. Springer Nature, Switzerland AG. doi: 10.1007/978-3-030-36248-5_16
- Bakker PAHM, Pieterse CMJ, De Jonge R, Berendsen RL** (2018) The soil-borne legacy. *Cell* **172**: 1178-1180. doi: 10.1016/j.cell.2018.02.024
- Barry AL, Feeney KL** (1967) Two quick methods for Voges-Proskauer test. *Applied Microbiology* **15**:1138-1141.

- Beneduzi A, Ambrosini A, Passaglia LMP** (2012) Plant growth-promoting rhizobacteria (PGPR): Their potential as antagonists and biocontrol agents. *Genetics and Molecular Biology* **35**: 1044-1051. doi: 10.1590/s1415-47572012000600020
- Bradford MM** (1976) A rapid and sensitive method for the quantitation of microgram quantities of protein utilizing the principle of protein-dye binding. *Analytical Biochemistry* **72**: 248–254. doi: 10.1016/0003-2697(76)90527-3
- Brevard H, Cantergiani E, Cachet T, Chaintreau A, Demyttenaere J, French L, Gassenmeier K, Joulain D, Koenig T, Leijs H** (2011) Guidelines for the quantitative gas chromatography of volatile flavouring substances. *Flavour and Fragrance Journal* **26**:297–299. doi: 10.1002/ffj.2061
- Brilli F, Loreto F, Baccelli I** (2019) Exploiting plant volatile organic compounds (VOCs) in agriculture to improve sustainable defense strategies and productivity of crops. *Frontiers in Plant Science* **10**: 1 – 5. doi:10.3389/fpls.2019.00264
- Cappellari LDR, Banchio E** (2020) Microbial volatile organic compounds produced by *Bacillus amyloliquefaciens* GB03 ameliorate the effects of salt stress in *Mentha piperita* principally through acetoin emission. *Journal of Plant Growth Regulation* **39**: 764–775. doi: 10.1007/s00344-019-10020-3
- Carrasco KBR, Fornasiero RB, Tassoni A, Bagni N** (2007) Identification of two phenotypes of *Arabidopsis thaliana* under in vitro salt stress conditions. *Biologia Plantarum* **51**: 436-442. doi: 10.1016/j.plaphy.2008.02.005
- Chang AY, Chau VWY, Landas JA, Pang Y** (2017) Preparation of calcium competent *Escherichia coli* and heat-shock transformation. *JEMI methods* **1**: 22-25.
- Chen GC, Jordan F** (1984) Brewers' yeast pyruvate decarboxylase produces acetoin from acetaldehyde: A novel tool to study the mechanism of steps subsequent to carbon dioxide loss. *Biochemistry*. **23**:3576-3582. doi: 10.1021/bi00311a002
- Cho SM, Kang BR, Han SH, Anderson AJ, Park JY, Lee YH, Cho BH, Yang KY, Ryu CM, Kim YC** (2008) 2R,3R-Butanediol, a bacterial volatile produced by *Pseudomonas chlororaphis* O6, is involved in induction of systemic tolerance to drought in *Arabidopsis thaliana*. *Molecular Plant-Microbe Interactions* **21**: 1067–1075. doi: 10.1094/MPMI -21-8-1067
- Choi SK, Jeong H, Kloepper JW, Ryu CM** (2014) Genome sequence of *Bacillus amyloliquefaciens* GB03, an active ingredient of the first commercial biological control product. *Genome Announcements* **2**: e01092-14. doi: 10.1128/genomeA.01092-14

- Chung JH, Song GC, Ryu CM** (2016) Sweet scents from good bacteria: Case studies on bacterial volatile compounds for plant growth and immunity. *Plant Molecular Biology* **90**: 677-687. doi: 10.1007/s11103-015-0344-8
- Clough SJ, Bent AF** (1998) Floral dip: a simplified method for *Agrobacterium* mediated transformation of *Arabidopsis thaliana*. *Plant Journal* **16**: 735–743. doi: 10.1046/j.1365-313x.1998.00343.x
- Cookson SJ, Chenu K, Granier C** (2007) Day length affects the dynamics of leaf expansion and cellular development in *Arabidopsis thaliana* partially through floral transition timing. *Annals of Botany* **99**: 703-711. doi: 10.1093/aob/mcm005
- Coolen S, Proietti S, Hickman R, Olivás NHD, Huang PP, Van Verk MC, Van Pelt JA, Wittenberg AHJ, De Vos M, Prins M, Van Loon JJA, Aarts MGM, Dicke M, Pieterse CMJ, Van Wees SCM** (2016) Transcriptome dynamics of *Arabidopsis* during sequential biotic and abiotic stresses. *The Plant Journal* **86**: 249-267. doi: 10.1111/tpj.13167
- Cosgrove D** (1987) Wall relaxation and the driving forces for cell expansive growth. *Plant Physiology* **84**: 561-564. doi: 10.1104/pp.84.3.561
- Davies ME** (1964) Acetolactate and acetoin synthesis in ripening peas. *Plant Physiology*. **39**: 53-59. doi: 10.1104/pp.39.1.53
- Dempers D** (2015) Overexpression of α -acetolactate decarboxylase and acetoin reductase / 2,3-butanediol dehydrogenase in *Arabidopsis thaliana*. MSc dissertation, Stellenbosch University
- Devaraj H, Pook C, Swift S, Aw KC, McDaid AJ** (2018) Profiling of headspace volatiles from *Escherichia coli* cultures using silicone-based sorptive media and thermal desorption-GC/MS. doi: 10.1002/jssc.201800684
- Dotaniya ML, Meena VD** (2015) Rhizosphere effect on nutrient availability in soil and its uptake by plants: A review. *Proceedings of the National Academy of Sciences, India Section B - Biological Sciences* **85**:1-12. doi: 10.1007/s40011-013-0297-0
- Farag MA, Ryu CM, Sumner LW, Paré PW** (2006) GC-MS SPME profiling of rhizobacterial volatiles reveals prospective inducers of growth promotion and induced systemic resistance in plants. *Phytochemistry* **67**:2262-2268. doi: 10.1016/j.phytochem.2006.07.021
- Farag MA, Zhang H, Ryu CM** (2013) Dynamic chemical communication between plants and bacteria through airborne signals: Induced resistance by bacterial volatiles. *Journal of Chemical Ecology* **39**: 1007-1018. doi: 10.1007/s10886-013-0317-9
- Fincheira P, Quiroz A** (2018) Microbial volatiles as plant growth inducers. *Microbiological Research* **208**: 63-75. doi: 10.1016/j.micres.2018.01.002

- Forlani G** (1998) Purification and properties of pyruvate carboxylase from *Zea mays* cultured cells. *Photochemistry* **50**: 1305-1310
- Forlani G, Mantelli M, Nielsen E** (1999) Biochemical evidence for multiple acetoin-forming enzymes in cultured plant cells. *Phytochemistry* **50**: 255-262
- Forni C, Duca D, Glick BR** (2017) Mechanisms of plant response to salt and drought stress and their alteration by rhizobacteria. *Plant and Soil* **410**: 335-356. doi: 10.1007/s11104-016-3007-x
- Fouda A, Hassan SED, Eid AM, Ewais EED** (2019) The interaction between plants and bacterial endophytes under salinity stress: Endophytes and secondary metabolites. *Phytochemistry* **1** – 17. doi: 10.1007/978-3-319-76900-4_15-1
- Gase K, Weinhold A, Bozorov T, Schuck S, Baldwin IT** (2011) Efficient screening of transgenic plant lines for ecological research. *Molecular Ecology Resources* **11**: 890-902. doi: 10.1111/j.1755-0998.2011.03017.x
- Ghosh R, Gilda JE, Gomes AV** (2014) The necessity of and strategies for improving confidence in the accuracy of western blots. *Expert Review of Proteomics* **11**: 549–560. doi: 10.1586/14789450.2014.939635
- Giakountis A, Cremer F, Sim S, Reymond M, Schmitt J, Coupland G** (2010) Distinct patterns of genetic variation alter flowering responses of *Arabidopsis* accessions to different daylengths. *Plant Physiology* **152**: 177-191. doi: 10.1104/pp.109.140772
- Goelling D, Stahl U** (1988) Cloning and expression of an α -acetolactate decarboxylase gene from *Streptococcus lactis* subsp. *diacetylactis* in *Escherichia coli*. *Applied and Environmental Microbiology* **54**: 1889-1891.
- Guiochon G, Guillemin CL** (1988) Quantitative analysis by gas chromatography measurement of peak area and derivation of sample composition. *Journal of Chromatography Library* **42**: 629-659. doi: 10.1016/S0301-4770(08)70087-3.
- Hashem A, Tabassum B, Abd-Allah EF** (2019) *Bacillus subtilis*: A plant-growth promoting rhizobacterium that also impacts biotic stress. *Saudi Journal of Biological Sciences* **26**: 1291-1297. doi: 10.1016/j.sjbs.2019.05.004
- Hase S, Van Pelt JA, Van Loon LC, Pieterse CMJ** (2003) Colonization of *Arabidopsis* roots by *Pseudomonas fluorescens* primes the plant to produce higher levels of ethylene upon pathogen infection. *Physiological and Molecular Plant Pathology* **62**: 219–226. doi: 10.1016/S0885-5765(03)00059-6

- Hassan MK, McInroy JA, Kloepper JW** (2019) The interactions of rhizodeposits with plant growth-promoting rhizobacteria in the rhizosphere: A review. *Agriculture* **9**: 1-13. doi: 10.3390/agriculture9070142
- Huijser P, Schmid M** (2011) The control of developmental phase transitions in plants. *Development* **138**:4117-4129. doi:10.1242/dev.063511
- Hwang I, Sheen J, Müller B** (2012) Cytokinin signaling networks. *Annual Review of Plant Biology* **63**: 353–380.
- Ilangumaran G, Smith DL** (2017) Plant growth promoting rhizobacteria in amelioration of salinity stress: A systems biology perspective. *Frontiers in Plant Sciences* **8**: 1-14. doi: 10.3389/fpls.2017.01768
- Imaizumi T** (2010) *Arabidopsis* circadian clock and photoperiodism: Time to think about location. *Current Opinion in Plant Biology* **13**: 83-89. doi: 10.1016/j.pbi.2009.09.007
- Joseph BC, Pichaimuthu S, Srimeenakshi S, Murthy M, Selvakumar K, M G, Manjunath SR** (2015) An overview of the parameters for recombinant protein expression in *Escherichia coli*. *Cell Science & Therapy* **6**: 1-7. doi: 10.4172/2217-7013.1000221
- Kashyap BK, Solanki MK, Pandey AK, Prabha S, Kumar P, Kumari B** (2019) *Bacillus* as plant growth promoting rhizobacteria (PGPR): A promising green agriculture technology. *Plant Health Under Biotic Stress* 219-239. doi: 10.1007/978-981-13-6040-4_11
- Kaushal M, Wani SP** (2016) Rhizobacterial-plant interactions: Strategies ensuring plant growth promotion under drought and salinity stress. *Agriculture, Ecosystems and Environment* **231**: 68-78. doi: 10.1016/j.agee.2016.06.031
- Kay J, Jewett MC** (2015) Lysate of engineered *Escherichia coli* supports high-level conversion of glucose to 2,3-butanediol. *Metabolic Engineering* **32**: 133-142. doi: 10.1016/j.ymben.2015.09.015
- Kwon YS, Ryu CM, Lee S, Park HB, Han KS, Lee JH, Lee K, Chung WS, Jeong MJ, Kim HK** (2010) Proteome analysis of *Arabidopsis* seedlings exposed to bacterial volatiles. *Planta* **232**: 1355–1370. doi:10.1007/s00425-010-1259-x
- Lee B, Farag M, Park HB, Kloepper JW, Lee SH, Ryu CM** (2012) Induced resistance by a long-chain bacterial volatile: Elicitation of plant systemic defense by a C13 volatile produced by *Paenibacillus polymyxa*. *PLoS One* **7**: 1–11. doi:10.1371/journal.pone.0048744
- Lee K, Seo PJ** (2014) Airborne signals from salt-stressed *Arabidopsis* plants trigger salinity tolerance in neighboring plants. *Plant Signaling & Behaviour* **9**: 1-5. doi: 10.4161/psb.28392

- Lindsey BE, Rivero L, Calhoun CS, Grotewold E, Brkljacic J** (2017) standardized method for high-throughput sterilization of *Arabidopsis* seeds. *Journal of Visualized Experiments* 128. doi: 10.3791/56587
- Liu XM, Zhang H** (2015) The effects of bacterial volatile emissions on plant abiotic stress tolerance. *Frontiers in Plant Science* 6: 1 – 6. doi: 10.3389/fpls.2015.00774
- Low LY, Yang SK, Kok DXA, Ong-Abdullah J, Tan NP, Lai KS** (2018) Transgenic plants: Gene constructs, vector and transformation method. *New Visions in Plant Science* 41 - 61. doi: 10.5772/intechopen.79369
- Lu, Y** (2011). Extract genomic DNA from *Arabidopsis* leaves (can be used for other tissues as well). *BIO-PROTOCOL* 1. doi: 10.21769/BioProtoc.90
- Mauchline TH, Malone JG** (2017) Life in earth – the root microbiome to the rescue? *Current Opinion in Microbiology* 37: 23-28. doi: 10.1016/j.mib.2017.03.005
- Mifflin BJ** (1974) The location of nitrate reductase and other enzymes related to amino acid biosynthesis in the plastids of root and leaves. *Plant Physiology*. 54: 550-555.
- Mulo, P** (2010) Chloroplast-targeted ferredoxin-NADP⁺ oxidoreductase (FNR): Structure, function and location. *Biochimica et Biophysica Acta* 1807: 927-934. doi: 10.1016/j.bbabi
- Munns R** (2002a) Comparative physiology of salt and water stress. *Plant, Cell and Environment* 25: 239–250. doi: 10.1046/j.0016-8025.2001.00808.x
- Munns R** (2002b) Salinity, growth and phytohormones. *Salinity: Environment - Plants - Molecules*. Kluwer Academic Publishers, Netherlands. doi: 10.1007/0-306-48155-3_13
- Munns R, Tester M** (2008) Mechanisms of salinity tolerance. *Annual Review of Plant Biology* 59: 651 – 681. doi: 10.1146/annurev.arplant.59.032607.092911
- Murashige T, Skoog F** (1962) A revised medium for rapid growth and bioassays with tobacco tissue cultures. *Physiologia Plantarum* 15:473-497. doi: 10.1111/j.1399-3054.1962.tb08052.x
- Nadeem SM, Naveed M, Zahir ZA, Asghar HN** (2013) Plant–microbe interactions for sustainable agriculture: Fundamentals and recent advances. *Plant Microbe Symbiosis: Fundamentals and Advances* 51-103. doi: 10.1007/978-81-322-1287-4_2
- Narusaka M, Shiraishi T, Iwabuchi M, Narusaka Y** (2010) The floral inoculating protocol: A simplified *Arabidopsis thaliana* transformation method modified from floral dipping. *Plant Biotechnology* 27: 349-351.
- Nielsen D, Yoon SH, Yuan CJ, Prather KLJ** (2010) Engineering Acetoin and meso-2,3-Butanediol Biosynthesis in *E. coli*. *Biotechnology Journal* 5:274-284. doi: 10.1002/biot.200900279

- Niu SQ, Li HR, Parè PW, Aziz M, Wang SM, Shi H, Li J, Han QQ, Guo SQ, Li J, Guo Q, Ma Q, Zhang JL** (2016) Induced growth promotion and higher salt tolerance in the halophyte grass *Puccinellia tenuiflora* by beneficial rhizobacteria. *Plant Soil* **407**: 217-230. doi: 10.1007/s11104-015-2767-z
- Numan M, Bashir S, Khan Y, Mumtaz R, Shinwari ZK, Khan AL, Khan A, Al-Harrasi A** (2018) Plant growth promoting bacteria as an alternative strategy for salt tolerance in plants: A review. *Microbiological Research* **209**: 21-32. doi: 10.1016/j.micres.2018.02.003
- Olanrewaju OS, Glick BR, Babalola OO** (2017) Mechanisms of action of plant growth promoting bacteria. *World Journal of Microbiological Biotechnology* **33**: 1-16. doi: 10.1007/s11274-017-2364-9
- Passricha N, Saifi S, Khatodia S, Tuteja N** (2016) Assessing zygoty in progeny of transgenic plants: current methods and perspectives. *Journal of Biological Methods* **3**: e46. doi: 10.14440/jbm.2016.114
- Per TS, Khan NA, Reddy PS, Masood A, Hasanuzzaman M, Khan MIR, Anjum NA** (2017) Approaches in modulating proline metabolism in plants for salt and drought stress tolerance: Phytohormones, mineral nutrients and transgenics. *Plant Physiology and Biochemistry* **115**: 126 – 140. doi: 10.1016/j.plaphy.2017.03.018
- Rasool S, Hameed A, Azooz MM, Rehman M, Siddiqi TO, Ahmad P** (2013) Salt stress: Causes, types and responses of plants. *Ecophysiology and response of plants under salt stress*. Springer Science and Business Media, LLC. doi: 10.1007/978-1-4614-4747-4_1
- Rudrappa T, Biedrzycki ML, Kunjeti SG, Donofrio NM, Czymmek KJ, Parè PW, Bais HP** (2010) The rhizobacterial elicitor acetoin induces systemic resistance in *Arabidopsis thaliana*. *Communicative and Integrative Biology* **3**: 130-138. doi: 10.4161/cib.3.2.10584
- Rosier A, Medeiros FHV, Bais HP** (2018) Defining plant growth promoting rhizobacteria molecular and biochemical networks in beneficial plant-microbe interactions. *Plant and Soil* **428**: 35–55. doi: 10.1007/s11104-018-3679-5
- Rosmarin M** (2020) Enhancing drought and osmotic stress tolerance by overexpressing α -acetolactate decarboxylase and acetoin reductase/2,3-butanediol dehydrogenase in planta. MSc dissertation, Stellenbosch University
- Ryu CM, Farag MA, Hu CH, Reddy MS, Wei HX, Pare PW, Kloepper JW** (2003) Bacterial volatiles promote growth in *Arabidopsis*. *Proceedings of the National Academy of Sciences* **100**: 4927-4932. doi: 10.1073/pnas.0730845100

- Sasse J, Martinoia E, Northen T** (2017) Feed your friends: do plant exudates shape the root microbiome? *Trends in Plant Science* **23** : 25-41. doi: 10.1016/j.tplants.2017.09.003
- Sanders D** (2000) Plant biology: The salty tale of *Arabidopsis*. *Current Biology* **10**: 486-488.
- Shafi J, Tian H, Ji M** (2017) *Bacillus* species as versatile weapons for plant pathogens: A review. *Biotechnology & Biotechnological Equipment* **31**: 445-459. doi: 10.1080/13102818.2017.1286950
- Sharifi R, Kiani H, Ahmadzadeh M, Behboudi K** (2020) Optimization of acetoin production by biological control strain *Bacillus Subtilis* GB03 using statistical experimental design. *Biological Journal of Microorganism* **8**: 47-57. doi: 10.22108/BJM.2018.110315.1120
- Sharifi R, Ryu CM** (2018) Revisiting bacterial volatile-mediated plant growth promotion: Lessons from the past and objectives for the future. *Annals of Botany* **20**: 1-10. doi: 10.1093/aob/mcy108
- Shen BR, Zhu CH, Yao Z, Cui LL, Zhang JJ, Yang CW, He ZH, Peng XX** (2017) An optimized transit peptide for effective targeting of diverse foreign proteins into chloroplasts in rice. *Scientific Reports* **7**:46231. doi: 10.1038/srep46231
- Shrivastava P, Kumar R** (2015) Soil salinity: A serious environmental issue and plant growth promoting bacteria as one of the tools for its alleviation. *Saudi Journal of Biological Sciences* **22**: 123–131. doi: 10.1016/j.sjbs.2014.12.001
- Singer TP, Pensky J** (1952) Mechanism of acetoin synthesis by α -carboxylase. *Biochimica et Biophysica Acta* **9**: 316-327. doi: 10.1016/0006-3002(52)90167-4
- Sulpice R, Flis A, Ivakov AA, Apelt F, Krohn N, Encke B, Abel C, Feil R, Lunn JE, Stitt M** (2014) *Arabidopsis* coordinates the diurnal regulation of carbon allocation and growth across a wide range of photoperiods. *Molecular Plant* **7**: 137-155. doi: 10.1093/mp/sst127
- Sun Y, Kong X, Li C, Liu Y, Ding Z** (2015) Potassium retention under salt stress is associated with natural variation in salinity tolerance among *Arabidopsis* accessions. *PLoS One* **10**: 1-25. doi:10.1371/journal.pone.0124032
- Tahir HAS, Gu Q, Wu H, Raza W, Hanif A, Wu L, Colman MV, Gao X** (2017a) Plant growth promotion by volatile organic compounds produced by *Bacillus subtilis* SYST2. *Frontiers in Microbiology* **8**:1-11. doi: 10.3389/fmicb.2017.00171
- Tahir HAS, Gu Q, Wu H, Raza W, Safdar A, Huang Z, Rajer FU, Gao X** (2017b) Effect of volatile compounds produced by *Ralstonia solanacearum* on plant growth promoting and systemic resistance inducing potential of *Bacillus* volatiles. *BMC Plant Biology* **17**:133-149. doi:10.1186/s12870-017-1083-6

- Taiz L, Zeiger E, Moller IM, Murphy A** (2015) Plant Physiology and Development. 6th Edition. Sinauer Associates. Sunderland, CT.
- Tassoni A, Franceschetti M, Bagni N** (2008) Polyamines and salt stress response and tolerance in *Arabidopsis thaliana* flowers. Plant Physiology and Biochemistry **46**: 607-613. doi:10.1016/j.plaphy.2008.02.005
- Tsukanova KA, Chebotar VK, Meyer JJM, Bibikova TN** (2017) Effect of plant growth-promoting Rhizobacteria on plant hormone homeostasis. South African Journal of Botany **113**: 91-102. doi: 10.1016/j.sajb.2017.07.007
- Van der Merwe S** (2016) Attempting to enhance sugarcane growth through genetic modification. MSc dissertation, Stellenbosch University
- Xie SS, Wu HJ, Zang HY, Wu LM, Zhu QQ, Gao XW** (2014) Plant growth promotion by spermidine-producing *Bacillus subtilis* OKB105. Molecular Plant-Microbe Interactions **27**: 655–663. doi:10.1094/MPMI-01-14-0010-R.
- Xie X, Zhang H, Paré PW** (2009) Sustained growth promotion in *Arabidopsis* with long-term exposure to the beneficial soil bacterium *Bacillus subtilis* (GB03). Plant Signaling and Behavior **4**: 948-953. doi: 10.4161/psb.4.10.9709
- Xu H, Jia S, Liu J** (2011) Development of a mutant strain of *Bacillus subtilis* showing enhanced production of acetoin. African Journal of Biotechnology **105**: 779-788. doi: 10.5897/AJB10.1455
- Xu Q, Xie L, Li Y, Lin H, Sun S, Guan X, Hu K, Shen Y, Zhang L** (2015) Metabolic engineering of *Escherichia coli* for efficient production of (3R)-acetoin. Journal of Chemical Technology and Biotechnology **90**: 93-100. doi: 10.1002/jctb.4293
- Xu Y, Chu H, Gao C, Tao F, Zhou Z, Li K, Li L, Ma C, Xu P** (2014) Systematic metabolic engineering of *Escherichia coli* for high-yield production of fuel bio-chemical 2,3-butanediol. Metabolic Engineering **23**: 22-33. doi: 10.1016/j.ymben.2014.02.004
- Zhang H, Kim MS, Krishnamachari V, Payton P, Sun Y, Grimson M, Farag MA, Ryu CM, Allen R, Melo IS, Paré PW** (2007) Rhizobacterial volatile emissions regulate auxin homeostasis and cell expansion in *Arabidopsis*. Planta **226**: 839-851. doi: 10.1007/s00425-007-0530-2
- Zhang R, Vivanco JM, Shen Q** (2017) The unseen rhizosphere root–soil–microbe interactions for crop production. Current Opinion in Microbiology **37**: 8-14. doi: 10.1016/j.mib.2017.03.008
- Zhang X, Rao Z, Li J, Zhou J, Yang T, Xu M, Bao T, Zhao X** (2015) Improving the acidic stability of *Staphylococcus aureus* α -acetolactate decarboxylase in *Bacillus subtilis* by changing basic residues to acidic residues. Amino Acids **47**: 707-717. doi: 10.1007/s00726-014-1898-5

Zhao C, Zhang H, Song C, Zhu JK, Shabala S (2020) Mechanisms of Plant Responses and Adaptation to Soil Salinity. Cell – The innovation 1 – 41. doi: 10.1016/j.xinn.2020.100017

Addendum 1

Vectors and alignments

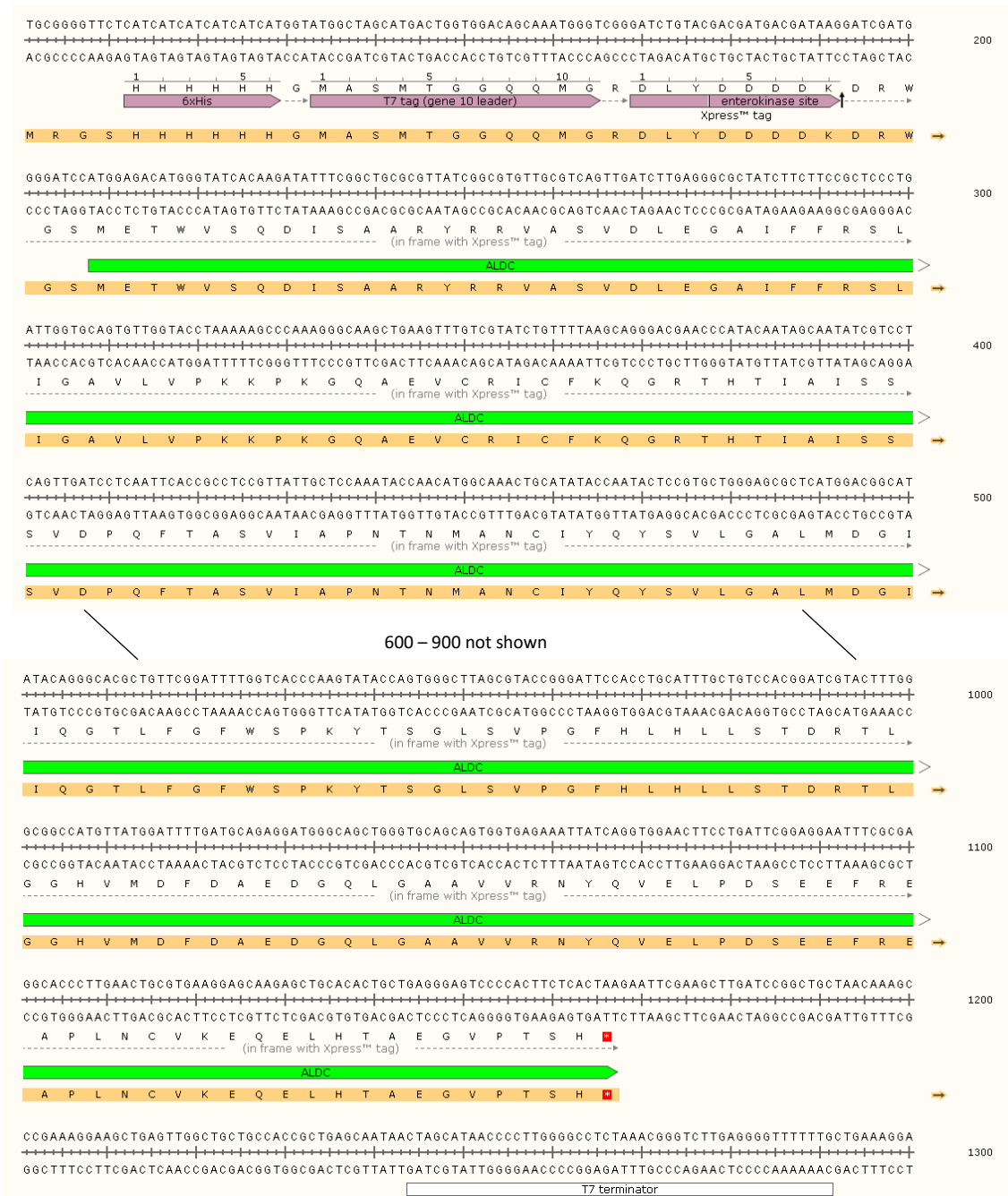


Figure 5.1: Alignment of transgene *ALDC* with Xpress tag in pRSETA vector. *α*-Acetolactate decarboxylase was transformed into pRSETA in frame with Xpress tag to ensure expression of protein with His-tag. The alignment shows that the gene in frame with the 6 × His-tag, T7 tag and enterokinase site, as well as the T7 terminator.

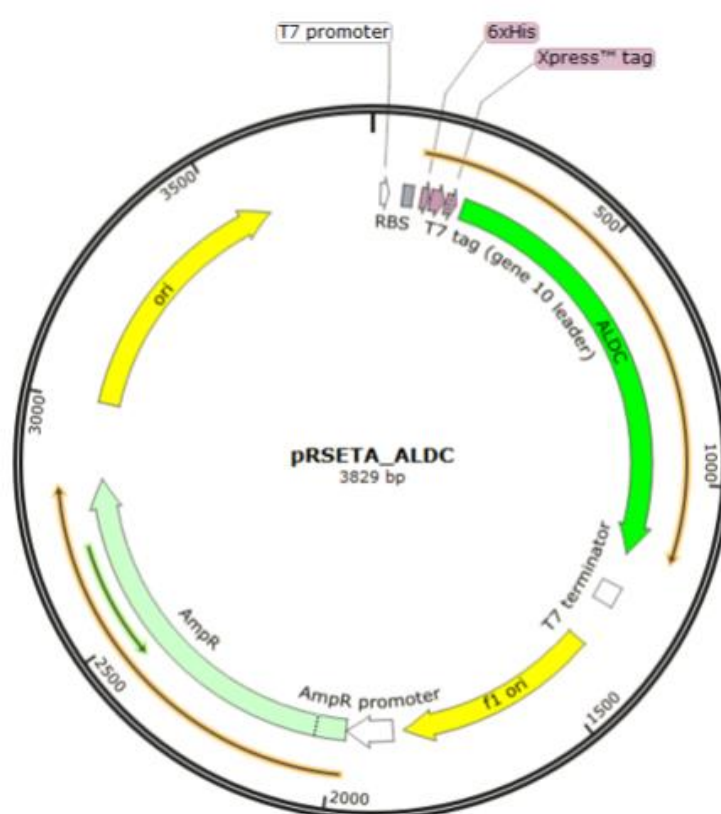


Figure 5.2: Protein expression vector construct for ALDC. α -Acetolactate decarboxylase was transformed into pRSETA via ligation with T4 DNA Ligase in frame with Xpress tag to ensure expression of protein with His-tag.

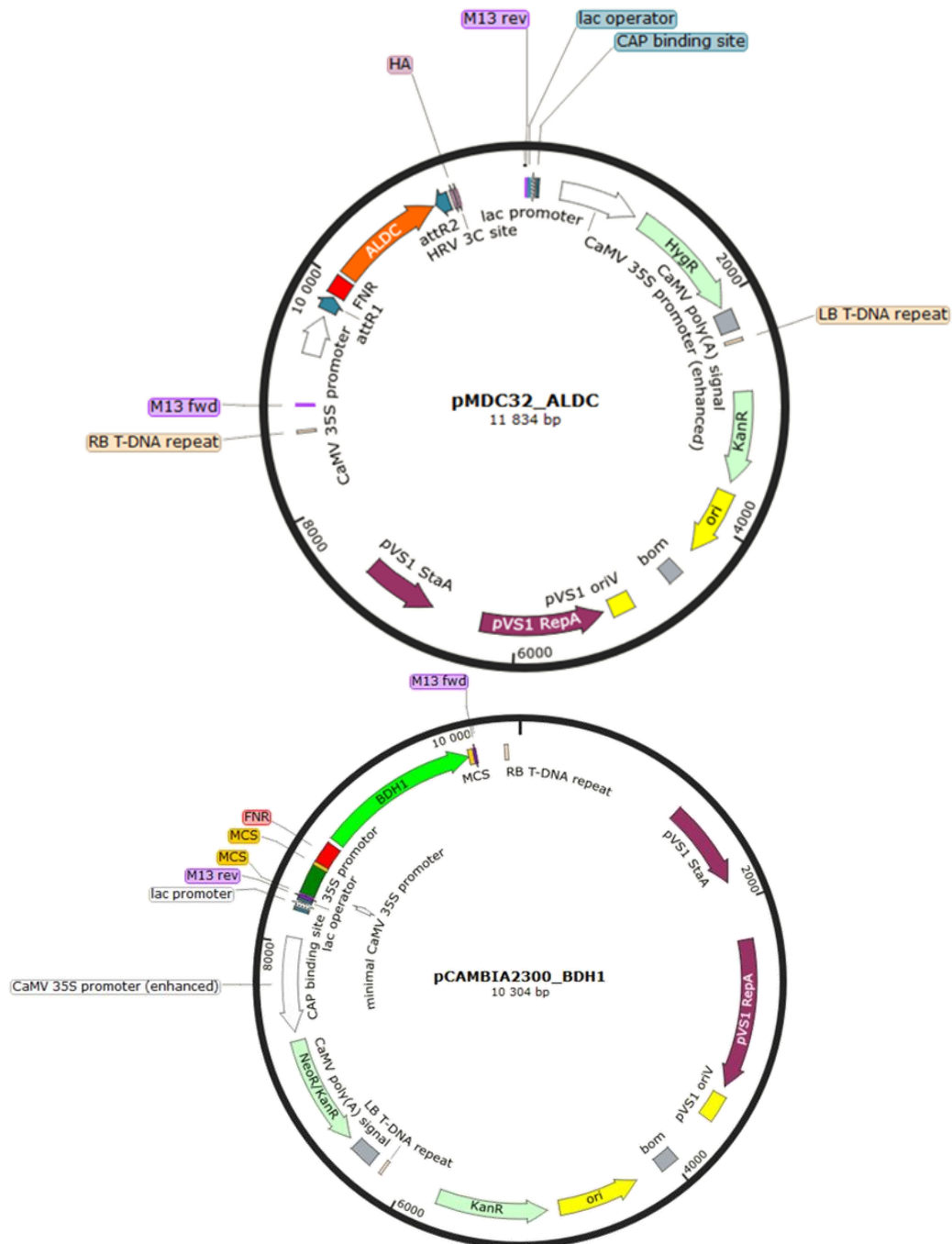


Figure 5.3: Vector constructs for *ALDC* and *BDH1*. *α*-Acetolactate decarboxylase was transformed into pMDC32 via Gateway cloning, while *acetoin reductase/2,3-butanediol dehydrogenase* was transformed into pCAMBIA2300 through ligation with T4 DNA Ligase. Both genes were inserted in frame with a CaMV 35S promoter and flanked by a ferredoxin-NADP⁺ reductase (FNR) chloroplastic transit peptide.

Addendum 2

Graphs and data

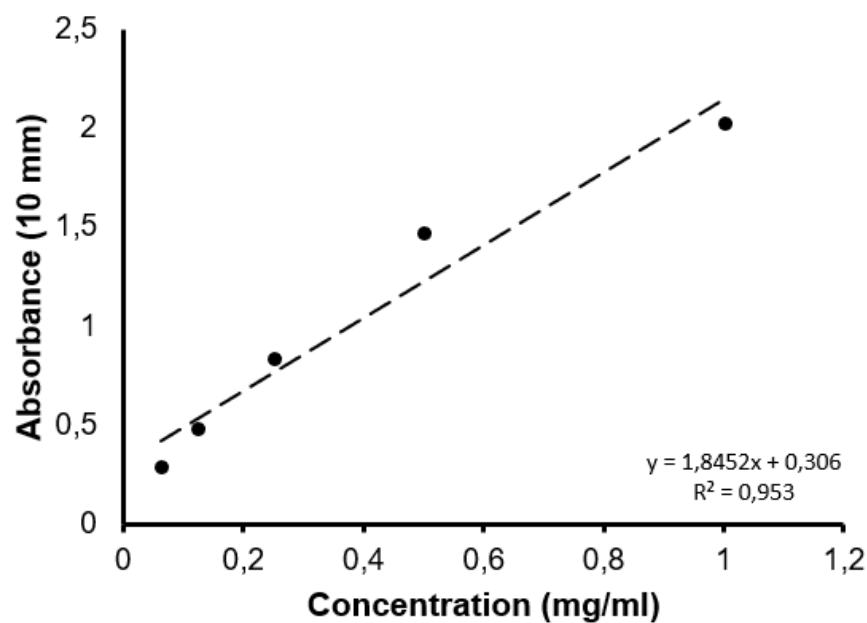


Figure 5.4: BSA standard curve at 595 nm. Standard curve was determined using a range of BSA from 0,0625 mg/mL to 1 mg/mL. The absorbance (10 mm) was measured at 595 nm and the standard curve obtained had a regression (R^2) of 0.953.

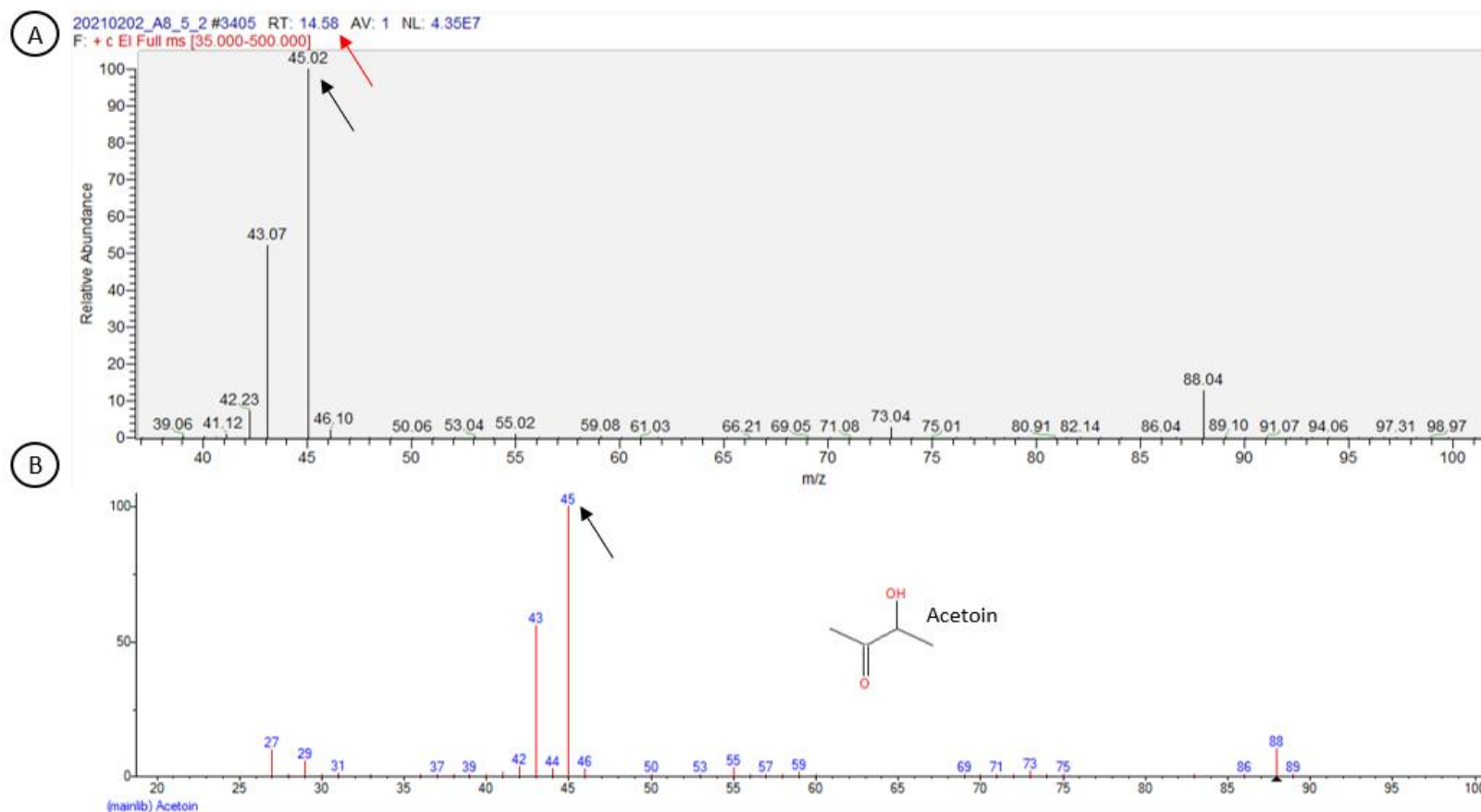


Figure 5.5: Identification of acetoin in gas chromatography-mass spectrometric analysis. Compounds were tentatively identified by comparison of retention times (T_R) and, by comparison with NIST11 mass spectral library. In order to identify the compound at specific peak on the chromatogram (Relative abundance vs retention time), **A**) the mass-to-charge (m/z) ratio for the peak at specific retention time is used (Relative abundance vs m/z). In this specific case, acetoin was detected in the sample at a retention time of 14,58 min with a m/z of 45,02. **B**) The m/z value is used to identify the compound in the NIST11 mass spectral library, and acetoin is known to have a m/z of 45. Indicated by red arrow is the retention time for sample; and black arrow indicates mass-to-charge ratio for acetoin.



Figure 5.6: Roots of plants exposed to bacterial strains. Identically-sized 13 d old seedlings were used to set up the experiment. After two weeks of exposure to the respective *E. coli* BL21-CodonPlus (DE3)-RIPL strains, the plants were photographed. Growth trials were conducted at long-day-length (14 h:10 h photoperiod) conditions. Indicated are *E. coli* BL21 wild-type strain (WT); *E. coli* BL21 strain with pRSETA empty vector (EV); *E. coli* BL21 strain with pRSETA vector containing *ALDC* gene (AA).

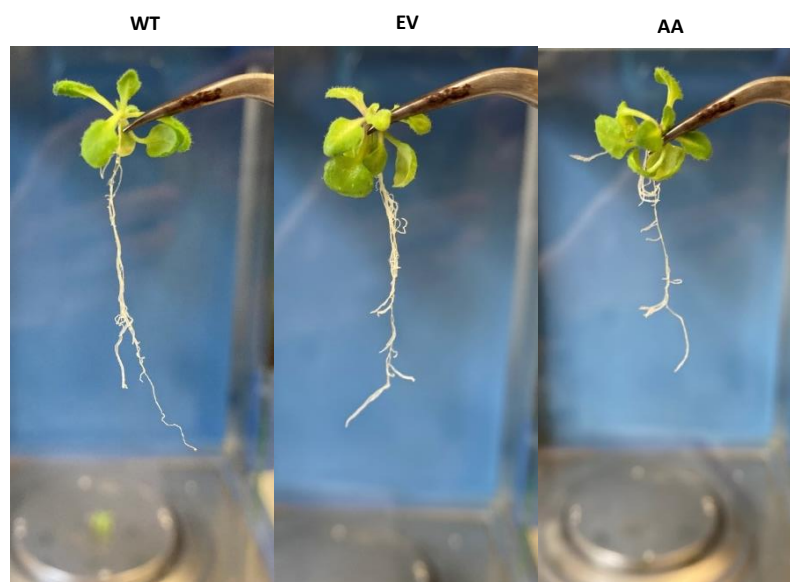


Figure 5.7: Roots of plants exposed to bacterial strains and salinity. Identically-sized 13 d old seedlings were used to set up the experiment. After two weeks of exposure to the respective *E. coli* BL21-CodonPlus (DE3)-RIPL strains and 100 mM NaCl, the plants were photographed. Growth trials were conducted at long-day-length (14 h:10 h photoperiod) conditions. Indicated are *E. coli* BL21 wild-type strain (WT); *E. coli* BL21 strain with pRSETA empty vector (EV); *E. coli* BL21 strain with pRSETA vector containing *ALDC* gene (AA).

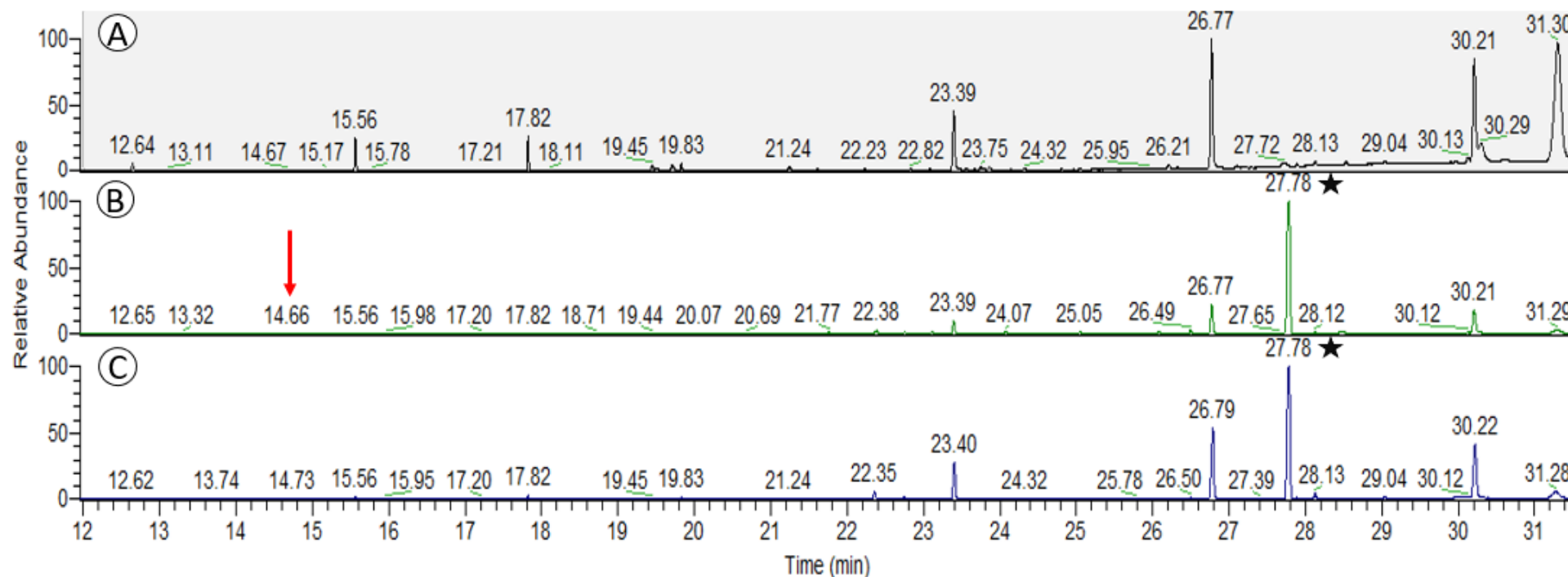


Figure 5.8: Gas chromatography-mass spectrometric analysis of *Escherichia coli* bacteria and wild-type *Arabidopsis thaliana*. The volatile profile of WT *Arabidopsis thaliana* and both *E. coli* BL21-CodonPlus(DE3)-RIPL strains containing the *ALDC* gene and empty vector were compared. All three volatile profiles showed the presence of ethylene glycerol isomers (at T_R of ± 23.39 , 26.77 , 30.31 and 31.3 min). Indicated are **A)** WT *Arabidopsis thaliana*, **B)** *E. coli* BL21-CodonPlus(DE3)-RIPL strain containing the *ALDC* gene, **C)** *E. coli* BL21-CodonPlus(DE3)-RIPL strain containing empty vector, acetoin by red arrow, and indole by black star.